5-20-2011

Complexation of Organic Guests and Coordination of Metal Ions by Cyclodextrins: Role of Cyclodextrins in Metal-Guest Interactions

Curtis William Jarand
University of New Orleans

Complexation of Organic Guests and Coordination of Metal Ions by Cyclodextrins: Role of Cyclodextrins in Metal-Guest Interactions

A Dissertation

Submitted to the Graduate Faculty of the
University of New Orleans
in partial fulfillment of the
requirements for the degree of

Doctor of Philosophy
in
Chemistry

by

Curtis William Jarand

B.S. Southern Illinois University at Carbondale, 1995
M.S. New Mexico State University, 2000

May, 2010

Table of Contents

List of Figures

List of Tables

Abstract

Nitroaromatic explosives, such as trinitrotoluene (TNT), are of particular environmental concern due to their recalcitrance in soils and their potent toxicity and mutagenicity to both aquatic and mammalian species. TNT was the most widely used military explosive through the era encompassing both the First and Second World Wars. As a result, there is widespread contamination of soils by TNT around weapons manufacture, testing, and disposal facilities. Fenton chemistry (ferrous ion catalyzed generation of hydroxyl radicals) has shown utility in the remediation of TNT in soils but it suffers from non-specificity and the need for acidic conditions to prevent loss of iron as iron hydroxides. Cyclodextrins (CDs) have demonstrated the ability to increase the efficiency of Fenton degradation of aromatic pollutant species. The increase in degradation efficiency observed in the CD Fenton reaction systems has been credited to the formation of a pollutant/CD/ferrous ion ternary complex which has the ability to produce hydroxyl radicals at the site of bound ferrous ions during Fenton reactions. This results in an increase in hydroxyl radical concentration near the target guest molecule relative to the bulk solution, leading to a targeted degradation of the complexed guest molecule. In order to assess the viability of CD assisted Fenton reactions for the remediation of TNT, a thorough knowledge of the kinetics, degradation products, and role of binary and ternary complexes is required. Research presented in this dissertation examined the role of CDs in the Fenton oxidation of TNT, specifically: 1) the kinetics of TNT degradation in the presence of CDs for a Fenton reaction system, 2) the products of these reactions through chromatographic and mass spectrometric methods, and 3) NMR and binding studies of binary and ternary complexes.

Keywords: TNT, Nitroaromatic, Cyclodextrin, Fenton, Remediation

CHAPTER 1

FENTON CHEMISTRY AND APPLICATIONS FOR TARGETED POLLUTANT DESTRUCTION

Introduction

The search for inexpensive, effective, and safe methods to remediate polluted soils and waters has long been a major goal of researchers and workers involved in environmental cleanup and remediation. Techniques such as bioremediation, phytoremediation, soil composting, incineration and soil flushing have been used with varying degrees of success for different environmental contaminants and matrices in soils. In aqueous matrices, typical remediation procedures include bioremediation through aerobic or anaerobic digesters, air sparging, and ozonation. Many of the above methods can be expensive and difficult to apply, and many of the above procedures require removal and ex-situ treatment of the contaminated matrix.

In recent years, treatments using advanced oxidative processes (AOPs) have received a great deal of interest as an effective means to treat systems containing oxidizable pollutants. AOPs consist of a variety of different techniques capable of generating radical species which act as the oxidant in these systems. These processes have shown application for the remediation of pollutants in a variety of matrices and many of the methods can be performed in-situ. Of the AOPs studied for application in environmental remediation, the Fenton reaction and closely associated methods such as photo-Fenton and Fenton-like reactions have garnered a great deal of interest due to the low cost, availability and safety of needed reagents and the strength of the oxidizing agent, the hydroxyl radical, that is produced (1).

Despite the interest in Fenton reactions for environmental applications, the method is not without a number of complications that must be dealt with in order to successfully apply it in most matrices. Firstly, the hydroxyl radical is an aggressive and non-selective oxidant. In matrices with a high total organic content (TOC), scavenging of the hydroxyl radical occurs through interactions with other components of the matrix besides the target compound (2). This is particularly problematic in most soils, but can also be a significant hurdle to overcome in heavily contaminated water. Additionally, the Fenton reaction requires conditions of low pH to be most effective (1). This is problematic for environmental remediation in soils and water systems. Due to the aggressive and non-selective nature of the hydroxyl radical oxidant generated in the Fenton reaction, numerous reaction products are commonly observed for target pollutants. Therefore, a comprehensive understanding of the reaction products occurring from the application of Fenton and other AOP reaction systems is required in order to assure that the generated waste products pose less of an environmental and health threat than the target compound being treated. Additionally, the product distribution and identity can vary greatly with changes in the composition or conditions of the reaction matrix. The complexity and variability of the generated products is therefore another factor that can complicate the use of Fenton chemistry for environmental remediation.

In this and later chapters, detailed discussions of the applications of Fenton and related reactions for targeted pollutant destruction in industrial, agricultural, and particularly, environmental applications, are given. Methods were developed and studied that have the potential to help overcome difficulties in the environmental application of Fenton chemistry through the use complexation of contaminants and chelation of the iron catalyst through the use of environmentally benign cyclodextrins. The majority of these studies involved the application

of Fenton chemistry to degrade the environmentally recalcitrant pollutant, 2,4,6-trinitrotoluene (TNT). The application of Fenton chemistry and the use of cyclodextrins (CDs) to assist the degradation of TNT are thoroughly described in terms of kinetics and product distribution.

The Fenton Reaction

The Fenton reaction uses a mixture of Fe^{2+} and hydrogen peroxide (H_2O_2) to generate hydroxyl radicals (·OH) which are capable of reacting at or near diffusion controlled rates (10^8-10^{10} M^{-1} s^{-1}) with both organic and inorganic oxidizable species (3). The generated ·OH is an extremely powerful oxidant, second only to fluorine, with an oxidation potential of approximately 2.8 V versus a normal hydrogen electrode (NHE) at pH 7.0 (4). The first description of the use of Fe^{2+} and H_2O_2 to create an oxidizing environment was reported by Henry J. Fenton in 1894, when he noted that a solution of ferrous salts and H_2O_2 could be utilized to oxidize tartaric acid (5). In this study he also recognized that only catalytic amounts of Fe^{2+} were required, and that Fe^{3+} was less effective at initiating the reaction. Since this first description, the reaction bearing his name has been extensively studied and detailed descriptions of the reaction mechanisms, kinetics, and applications have been detailed.

The first description of the mechanism underlying the Fenton reaction was given by Haber and Weiss in 1934 when they proposed that the active oxidant species in the reaction was ·OH (6). Haber and Weiss were also the first to lay out in some detail that a Fe^{2+}/Fe^{3+} redox cycle was involved in the generation of the hydroxyl radicals. The Fe^{2+}/Fe^{3+} redox cycle explains the earlier observation by Henry J. Fenton that Fe^{3+} could be used to initiate the reaction, albeit at a slower initial rate. Barb *et al.* further expanded the mechanism leading to ·OH generation in a series of papers in which they proposed a 7 step sequence of reactions (7-9):

$$Fe^{2+} + H_2O_2 \rightarrow Fe^{3+} + OH^- + \cdot OH \quad (1.1)$$

$$Fe^{3+} + H_2O_2 \rightarrow Fe^{2+} + \cdot O_2H + H^+ \quad (1.2)$$

$$\cdot OH + H_2O_2 \rightarrow \cdot O_2H + H_2O \quad (1.3)$$

$$\cdot OH + Fe^{2+} \rightarrow Fe^{3+} + OH^- \quad (1.4)$$

$$Fe^{3+} + \cdot O_2H \rightarrow Fe^{2+} + O_2H^+ \quad (1.5)$$

$$Fe^{2+} + \cdot O_2H + H^+ \rightarrow Fe^{3+} + H_2O_2 \quad (1.6)$$

$$\cdot O_2H + \cdot O_2H \rightarrow H_2O_2 + O_2 \quad (1.7)$$

Equations 1.1 through 1.7 have been extensively examined since first being proposed and are well understood and accepted for systems in which no other redox species or strongly coordinating ligands are present (1).

Overall, reactions 1.1 through 1.7 sum to yield:

$$2\ H_2O_2 \rightarrow O_2 + H_2O \quad (1.8)$$

As can be readily seen through the summed reactions of the Fenton system, the end products of the reaction are benign. In addition to the O_2 and H_2O produced, $Fe^{2+/3+}$ is typically converted to ferric iron hydroxides, which are also benign, and will precipitate from the reaction medium unless the matrix is highly acidic.

A number of other reactions beyond those in equations 1.1-1.7 have been proposed and some evidence has been given that suggests the presence of an aquo or organocomplex of high valence iron capable of acting as an oxidant in some environments (10-12). The evidence

proposed for the existence of a high valence iron species, such as a ferryl ion (FeO^{2+}), acting as the oxidizing species during Fenton reactions has been difficult to prove since the observed products have not differed from those that would be expected through oxidation by ·OH (1). Therefore, the 7 reactions proposed by Barb *et al.* are generally accepted as an accurate description of the Fenton reaction in typical applications and have been heavily referenced since they were first described.

The reactions shown in equations 1.1 and 1.2 are the initiating steps involved in the Fenton reaction, yielding the ·OH oxidant and allowing the redox cycling of Fe^{2+} to Fe^{3+}, and back, in order to regenerate the Fe^{2+} catalyst need to initiate the Fenton reaction. Equation 1.2 has a rate constant of 0.001 to 0.1 $M^{-1}s^{-1}$ at pH 3 which is several orders of magnitude slower than equation 1.1, with a rate constant of 70 $M^{-1}s^{-1}$ (13). The remaining equations 1.3-1.7 have rate constants on the order of 10^6-10^8 $M^{-1}s^{-1}$, significantly faster than the initiating reactions (13). Therefore, the reduction of Fe^{3+} to Fe^{2+} in reaction 1.2 forms the rate limiting step for production of ·OH by the Fenton reaction. The differences in rates between the initiating reaction and second reaction can be readily observed during the application of Fenton reactions. The use of Fe^{2+} will lead to a rapid buildup of ·OH in solution which quickly initiates the reaction with target compounds. The use of Fe^{3+} gives a lag phase until sufficient Fe^{2+} is generated to initiate ·OH production, at which point the reaction system will then proceed identically to an Fe^{2+} initiated system (1).

Oxidation of organic compounds by ·OH produced during the Fenton reaction generally proceeds through hydrogen abstraction, addition across double bonds or through addition to an aromatic ring (equations 1.9-1.11) (14):

$$\cdot OH + R\text{-}H \rightarrow H_2O + \cdot R \quad (1.9)$$

$$\cdot OH + C{=}C \rightarrow \cdot C\text{-}C\text{-}OH \quad (1.10)$$

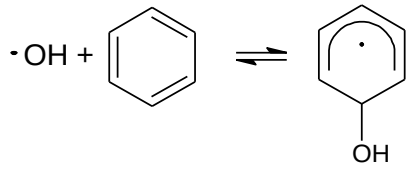

(1.11)

The carbon-centered radical species that are formed are themselves reactive and will proceed through further processes with other components of the sample matrix, as well as components of the Fenton reaction, potentially yielding a wide variety of products. It is worth noting that reactions 1.9 and 1.10 are irreversible, while reaction 1.11 is reversible in some situations (15). In aerobic environments, where oxygen is present in the reaction medium, the carbon-centered radicals can also react with O_2 in the matrix to yield hydroperoxyl ($HO_2\cdot$), organo-peroxyl (R-OO·) or organo-oxyl (R-O·) radicals. These oxygen containing radicals have rate constants on the same order as those of the hydroxyl radical and are capable of analogous reactions to those shown in 1.1 through 1.7 (1). The incorporation of these oxygen containing radicals into the reaction system increases the complexity of the overall reaction and makes prediction of the final products an even more difficult task.

While the Fenton reaction is typically considered as an oxidative process, the coexistence of both an oxidative and a reductive pathway has been demonstrated in several different studies using very aggressive Fenton conditions (16, 17). The addition of a reductive pathway was proposed in these systems due to the Fenton reaction kinetics having occurred well above the expected ·OH mediated reaction rate. The increased kinetic rates were credited to the formation of superoxide radical, $\cdot O_2^-$, and hydroperoxide anions, HO_2^-, shown in reactions 1.13 and 1.14 respectively. Both $\cdot O_2^-$ and HO_2^- are strong reducing agents capable of reacting at near diffusion

controlled rates (16, 17). The formation of these reducing agents can occur when high concentrations of H_2O_2 (> 0.3 M) are used according to the following proposed steps (16):

$$H_2O_2 + \cdot OH \rightarrow \cdot O_2H + H_2O \quad (1.12)$$

$$\cdot O_2H \rightleftharpoons H^+ + \cdot O_2^- \quad pK_a = 4.8 \quad (1.13)$$

$$\cdot O_2H + \cdot O_2^- \rightarrow HO_2^- + O_2 \quad (1.14)$$

However, the conditions used in these studies are atypical of most applications. Under the conditions typically used, oxidation of organic species by the Fenton generated radicals, particularly ·OH, is the dominant mechanism leading to pollutant destruction.

Industrial. Agricultural and Environmental Applications of Fenton and Related Reactions

While hydroxyl radicals are powerful and effective oxidants, they are also non-selective and will react readily react with any accessible and oxidizable components of the matrix undergoing Fenton treatment (2). The rate constants for the reaction of ·OH with oxidizable organic compounds are on the order of 10^7-10^{10} $M^{-1}s^{-1}$ (18). The rapid and non-selective reaction of ·OH in the reaction matrix can lead to a greatly reduced effectiveness in treating target pollutants due to scavenging of ·OH by non-target species. This scavenging leads to increasing the reagent demands, reduced efficiency, and higher expense for the treatment process. Additionally, the Fenton reaction is most effective only under conditions of low pH (less than pH 4) in order to prevent the loss of iron as insoluble iron hydroxides, halting the generation of ·OH by stopping the Fe^{2+}/Fe^{3+} redox cycle (19). The precipitated iron hydroxide sludge is also undesirable in many environmental and industrial applications from a mechanical viewpoint,

where its ability to clog filtration systems and prevent the free movement of liquid in equipment and soils is problematic. Conversely, the requirement of low pH to prevent iron hydroxide formation is often difficult in many applications and typically requires neutralization as an end step in the remediation process. This is particularly true in soils where acidification can be extremely difficult or impractical to accomplish and typically leads to sterilization of the treated soils (1, 14).

The problems surrounding the use of Fenton chemistry in industrial, agricultural and environmental applications long limited the method and very few studies on the use of Fenton and Fenton-like systems for targeted pollutant destruction can be found in the literature before the 1990's. However, starting in the early 1990's a number of researchers began to examine approaches to overcome the issues of ·OH scavenging, precipitation of iron, and the requirements of acidifying large volumes of soil or water. These approaches have included soil flushing to extract pollutants into an aqueous matrix for treatment to reduce ·OH scavenging by soil components, chelation of the iron, incorporation of iron into solid supports or utilization of iron bearing minerals to reduce or stop losses of iron as iron hydroxides, and through complexation of target pollutants to increase selectivity (20-23).

The use of Fenton and Fenton-like systems as well as a number of other AOPs for use in industrial and environmental remediation processes has received a great deal of attention since the early investigations in the 1990's and now forms a significant area of research. A large number of studies have been described in the literature and these methods are now widely regarded as a practical and effective remediation method for many applications (1). To date, the pollutants examined in these studies have included phenols, polycyclic aromatic hydrocarbons (PAHs), petroleum waste and by-products, pesticides, chlorinated aliphatic and aromatic

compounds, anilines, explosives, solvents, and a wide variety of other readily oxidizable compounds (1, 2, 4, 10, 14, 16, 19, 20, 22, 24, 25).

The sample matrices studied for targeted pollutant destruction by Fenton processes have ranged from bench-scale reactions in waters and soils to pilot-scale studies in soils, soil slurries, aquifer systems and waste water streams to large scale remediation sites listed under the USEPA's Comprehensive Environmental Response, Compensation, and Liability Act (CERCLA), more commonly known as Superfund sites. Fenton applications have also been examined at waste sites under the jurisdiction of the US Department of Energy (USDOE) and the US Department of Defense (USDOD). Additionally, a number of companies, such as In-Situ Oxidative Technologies, Inc. (ISOTEC, http://www.insituoxidation.com/), Cedar Creek Engineering (http://www.cedarcreekengineering.com/), and US Peroxide (http://www.h2o2.com/) have also been formed that use Fenton or Fenton-like procedures for in-situ remediation of sites with readily oxidizable and accessible contaminants, such as leaking underground petroleum storage tanks.

Fenton Processes for Treating Aqueous Wastes

Most studies on the use of Fenton and other AOPs have focused on their application for the oxidation of contaminants in water and waste water streams. The relative ease of using these methods in an aqueous matrix compared to a soil matrix is a likely reason for the larger number of studies in water systems. The large number of studies examining Fenton and other AOPs in water and waste water streams has led to numerous successful applications for industrial, environmental, and agricultural wastes. In many applications, the strong oxidizing environment

generated by these reactions lead to complete or near complete mineralization of the contaminant species, yielding small organic acids such as formic and oxalic acids (1).

Chlorinated organic compounds have been extensively examined as candidates for Fenton remediation in aqueous wastes. Numerous studies involving Fenton remediation of chlorinated organics have been conducted by J. J. Pignatello and coworkers at the Connecticut Agricultural Experiment Station. Pignatello and coworkers focused primarily on chlorophenoxy herbicides such as 2,4-dichlorophenoxyacetic acid (2,4-D) and 2,4,5-trichlorophenoxyacetic acid (2,4,5-T), which are extensively used worldwide in agricultural applications for the control of broadleaf weeds (26-30). Chlorinated organic compounds examined by other researchers have included chlorinated biphenyls, polychlorinated ethenes and methanes, and chlorinated solvents (31-34).

In studies by Pignatello and Sun examining oxidation of 2,4-D and 2,4,5-T by Fenton systems, they found that complete destruction of the herbicides at 0.1 mM was achievable. The presence of chloride was found to decrease the efficiency of the process. The optimal pH ranges were found to be in the range of 2.7-3.0 for reactions with free iron (26). However, another study by Pignatello and Sun found that the effective pH range for 2,4-D removal could be extended to near neutral (pH 6) through chelation of Fe^{3+} by a variety of chelators before initiation of the reaction (27). While complete mineralization was not observed, up to 80% removal of 2,4-D was achieved at a starting concentration of 1 mM was observed within 4 hours for a number of the chelators examined. The observed rates of loss varied inversely with the concentration of chelator examined, giving indirect evidence that the decreased rates occurred through $\cdot OH$ scavenging by the chelators.

In another study by Pignatello and Sun, they found that illuminating the reaction vessels with UV light during the Fenton process increased the reaction rates and the degree of mineralization of 2,4-D compared to reactions conducted without illumination (28). The use of UV light for increasing the efficiency of Fenton reactions is a commonly used procedure, typically referred to as a photo-Fenton reaction while Fenton reactions conducted without illumination are referred to as the somewhat confusing name, thermal Fenton reactions (1). Despite the name, thermal Fenton reactions do not require heating.

The increased efficiency observed during the photo-Fenton process in the Sun and Pignatello studies was credited to several potential mechanisms (29). The proposed mechanisms include photolysis of $FeOH^{2+}$ to yield Fe^{2+} and ·OH, UV catalyzed decarboxylation of Fe/2,4-D complexes to free Fe^{2+} and generate a carbon-centered radical capable of further reactions, or through other potential photochemical processes that could photolyze ferric-peroxy, Fe/O_2H^{2+}, complexes. Direct photolysis of of H_2O_2 may also have contributed to the increased reaction efficiency (35). The proposed mechanisms work through either increasing the Fe^{2+} concentration, rapidly increasing the concentration of ·OH in the system via reaction 1.1, or through directly increasing the free radical concentration in solution.

Fenton reactions have been used in drinking water to remove or prevent by-products which occur during the disinfection of the water through chlorination procedures, such as tri-halomethanes (THMs) (33, 34). In a study by Tang and Tassos, removal of bromoform could be achieved with 65-85% overall efficiency across a concentration range of 49-295 ppb of bromoform at pH 3.5. However, trichloromethane was resistant to oxidation via Fenton reaction and no significant degradation was observed.

Murray and Parsons examined the possibility of preventing the formation of THMs through the elimination of natural organic matter (NOM) prior to disinfection procedures. They determined that reduction of NOM by 90% or greater was possible using Fenton methods, bringing NOM concentrations below the USEPA mandated limit of 10 ppb for typical water treatment applications. This reduction in NOM significantly reduces the availability of organic components need to form THMs during the chlorination process.

Other applications of Fenton chemistry in drinking water have included the reduction arsenic concentrations through oxidation and co-precipitation with iron hydroxides generated by the reaction (36). However, the iron hydroxide precipitates are undesirable products and can be problematic in many drinking water purification plants if the precipitates are not properly flocculated prior to entering filtration systems, and the viability of this method for commercial applications seems unlikely.

The application of Fenton methods for the treatment of aqueous waste streams generated from the use of dyes during textile manufacturing have been examined in a number of studies. Dye waste streams contain large amounts of organic waste materials, are typically highly colored, and have a very high chemical oxygen demand (COD). Fenton processes have been shown to be highly effective at decolorizing dye wastes and have demonstrated COD removal efficiencies as high as 90% in some applications and up to 97% decolorization (32, 37).

The degradation of phenols and polyphenols found in wastes from vineyards and olive processing has been demonstrated in several studies using either a combined biological and Fenton treatment process or a photo-Fenton process (38-40). In studies by Mosteo and coworkers examining the treatment of vineyard wastes by combined biological/Fenton and photo-Fenton systems, a reduction in the TOC of aqueous wastes streams was as high as 50%

after the initial Fenton or photo-Fenton treatment. Subsequent bioremediation (activated sludge) treatment brought TOC levels to less than 10% of their initial value. In a study by Khoufi and coworkers examining Fenton treatment of aqueous wastes from olive pressing and milling, a 68% reduction in the total polyphenols was observed. Additionally, a reduction in the overall toxicity of the waste stream was observed, which improved the performance of subsequent bioremediation by anaerobic digesters.

Fenton treatment of waste streams from paper pulp production has shown to be highly effective at reducing the concentration of halogenated organic wastes which are commonly present as well reducing the overall toxicity of the streams (41). Reductions in COD of 83% as well as significant reduction in color have been reported for Fenton treatment of paper pulp wastes (42). The Fenton process examined in this study proved more effective, as well as more cost efficient, than the more commonly used ozonation procedure.

Fenton processes have been successfully applied to remove di- and trinitrotoluenes (DNT and TNT, respectively) from spent acid streams occurring from the commercial process of toluene nitration (43). In this process, sulfuric and nitric acids are used in the nitration process, resulting in a highly acidic waste stream which readily amenable to Fenton treatment. In this study, Chen and coworkers utilized very aggressive conditions, with H_2O_2 concentrations as high as 7.6 mM and H_2SO_4 comprising ~75% of the volume of the waste stream. Under these conditions, they observed complete removal of TOC from the waste stream with no detectable nitrotoluenes post reaction.

Fenton Reactions for Treating Soil Pollutants

The application of Fenton and other AOPs for use in soil remediation has proven to be a much more difficult task than their use in water applications, for reasons previously mentioned. However, common soil remediation methods such as incineration or landfilling are expensive and highly labor intensive, so there is a desire among researchers in the field to develop alternative methods. The use of Fenton remediation systems in soils has therefore generated a great deal of interest among a number of many researchers as well as government agencies such as the USEPA, the USDOD and the USDOE due to the low cost, safety, and availability of the reagents as well as the possibility of *in situ* treatment.

Studies on the effectiveness of Fenton's reagents for remediating soil contaminants have examined pollutants such as chlorinated solvents and polychlorinated aromatics, (31, 44) polycyclic aromatic hydrocarbons, (14, 45) petroleum wastes, (46-48) pesticides (49, 50) and explosives, which will be examined in a later chapter.

Watts and coworkers examined the application of a modified Fenton reaction to degrade pentachloroethane in a silty loam soil matrix (16). They demonstrated that the reaction system was able to completely remove pentachloroethane under the conditions used in the study. Additionally, they found reaction products which were indicative that a reductive process was occurring alongside the oxidation by ·OH. The authors proposed that under the conditions high H_2O_2 concentration used in the study, up to 2 M, that $\cdot O_2^-$ and HO_2^- were being generated in the reaction mixture, occurring via reactions 1.12-1.14. They credited the reductive pathway to the presence of these two components. Further evidence of a reductive pathway was observed after addition of chloroform, a reductive scavenger, significantly reduced pentrachloroethane removal.

In another study, Watts and coworkers examined the use of Fenton methods to remove perchloroethylene (PCE) and polychlorinated biphenyls (PCBs) from a model soil matrix, using sand as their surrogate matrix (31). In the study, they were able to reduce PCE and PCB levels by 90% and 70%, respectively. The rate constants were also determined and PCE loss was shown to follow first-order kinetics while PCB followed a zero-order scheme. While the results of this work appear promising for PCE and PCB removal, sand is poorly representative of typical soil matrices because of its very low TOC. Therefore, translating results conducted in sand to actual soil samples is difficult due to scavenging of Fenton generated radicals in soils.

Martens and Frankenberger examined the use Fenton reagents to degrade polycyclic aromatic hydrocarbons (PAHs) in soil resulting from crude oil contamination (45). The ability of the Fenton reagents to degrade the PAHs showed a strong correlation to the molecular weight of the PAH, with lighter PAHs such as naphthalene and phenanthrene showing significant decreases in concentration while concentrations of heavier PAHs such as pyrene and chrysene showing very little change. The addition of a surfactant, sodium dodecyl sulfate (SDS), increased PAH degradation and at a concentration of 5-10 mM, promoting the removal of the otherwise recalcitrant heavier PAHs. However, the results of this study should be viewed with some caution due to the extremely high PAH spike level use, 400 mg per 30 g of soil. Additionally, losses of PAHs were also observed over the course of the 56 day treatment period in soils without Fenton treatment. For the lighter PAHs examined in the study, losses from treated and non-treated soils gave similar results at the end of the treatment period, indicating that other processes such as volatilization or biotic degradation were occurring in the soils.

A later study by Lundstedt and co-workers examined PAH removal from contaminated soils at a defunct gasworks facility by Fenton reagents with and without pretreatment of the soil

with an ethanol wash (14). PAH levels in the soils examined by this study ranged from 2-275 ppm, much lower than the study by Martens and Frankenberger and more representative of typically observed contamination levels. The residual concentrations of the PAHs detected after the ethanol/Fenton treatment ranged from approximately 30% for naphthalene and methylnaphthalenes to 80-90% for larger PAHs such as pyrenes and fluoranthenes. These results agree with the general conclusion of increasing resistance to oxidation as the number of rings in the PAH increased, as seen by Martens and Frankenberger. The effect of ethanol pre-treatment facilitated a marginally higher contaminant removal from the soil, under the laboratory scale conditions of this study. For *in situ* remediation, this pre-treatment would be much more difficult to accomplish and residual ethanol would prove problematic, as it readily scavenges ·OH (51).

Watts and coworkers examined the Fenton treatment of a Palouse loess soil sample contaminated with diesel fuel (48). The study examined the effectiveness of a number of different naturally occurring iron-bearing minerals to catalyze ·OH production in laboratory scale reactors. $Fe(ClO_4)_3$ and $Fe(NO_3)_3$ were found to be the most effective catalysts and reactions utilizing them along with 1.5 M H_2O_2 were capable of removing over 99% of diesel at a starting concentration of 1000 ppm. Ferric minerals were determined to be more effective than ferrous minerals at diesel removal and this was credited to the rapid loss of H_2O_2 in the reaction system from the conversion of Fe^{2+} to Fe^{3+} via reaction 1.1. The ability of the anionic counter-ions in the iron-bearing minerals to quench the generated radicals also correlated with decreasing efficiency in diesel removal for the studied systems.

Peters and coworkers studied the Fenton treatment of laboratory scale sand and soil columns spiked with gasoline over a wide range of Fe and H_2O_2 concentrations as well as

examining the impact of the H_2O_2 to gasoline ratios (47). Flow-through columns with an approximate volume of 375 ml were packed with either sand or soil and control reactions were conducted under the same conditions, using an aqueous gasoline solution. The concentration of Fe in the form of $Fe(NO_3)_3 \cdot 9\ H_2O$ was added as an aqueous solution at 0-500 mg/L of the Fenton reaction solution and approximately 600 ml of H_2O_2 was passed through the column at a concentration range of 3.5-35% (1.5-15 M). The ratios of H_2O_2 to gasoline were varied from 5:1 to 50:1. The aqueous control study demonstrated complete removal of gasoline in the control solutions under Fe^{3+} concentrations of 200 mg/L and 1.5 M H_2O_2 at a 5:1 ratio of H_2O_2 to gasoline. Comparison of the aqueous control data to the sand and soil column data is difficult to interpret for this study. The aqueous samples were prepared by mixing the aqueous gasoline solution and Fenton reagents in a reaction vessel and allowing them to stand for two hours, while the sand and soil samples reacted in flow through columns and no information on flow rate or residence times for the columns was provided. Additionally, the sand and soil column reactions utilized high peroxide concentrations, 7.5 and 15 mM, which created conditions of excessive heating which could have readily volatized gasoline in the sample matrix. For columns reacted under these peroxide concentrations, temperatures reached 80-100 °C in the columns, forcing the termination of Fenton reagent flow to allow the reactions to cool.

More recently Lu and Zhang conducted a well designed study of petroleum waste reduction in soil slurries using ethylenediaminetetraacetic acid (EDTA) chelated Fe^{3+} as the Fe catalyst during Fenton treatment (46). They concluded that an 85% reduction in total methylene chloride extractables, from a starting concentration of 14,800 mg/kg of soil, was possible. The optimal conditions found for the study utilized neutral pH and approximately 2.5 moles of H_2O_2 per kg of treated soil. The excellent results obtained using EDTA chelated Fe^{3+} at neutral pH are

encouraging for other researchers examining methods of soil treatment where acidification is not practical.

Two studies by Pignatello and co-workers examined the Fenton treatment of 2,4-D, metalochlor (2-chloro-N-[2-ethyl-6-methylphenyl]-N-[2-methoxy-1-methylethyl]acetamide) and methyl parathion (O,O-dimethyl O-(4-nitrophenyl) phosphorothioate) in soil slurries using chelated Fe^{3+} (49, 50). The chelating agents used in the studies were nitrilotriacetate (NTA) and N-(2-hydroxyethyl)iminodiacetate (HEIDA) and were found to effectively solubilize Fe^{3+} at pH 6. Reactions were carried out in 1:1 soil slurries of a topsoil containing 1.57% TOC with a pH of 5.7. The impact of reaction temperature was examined, with temperatures varied from 10 to 60 °C. The total contact time for the Fenton reagents was 5 hours. The optimal reaction conditions for the herbicides examined were determined to be at 35 °, with the Fe^{3+}/ligand complex added at 0.01 mg/kg of soil and the H_2O_2 was added at 100 times the concentration of the Fe complex. Under these conditions, up to a 90% reductions in the herbicide concentrations in the soils were observed.

Summary

The Fenton reaction and related AOPs have shown significant utility in the treatment of waters and soils with a variety of industrial, agricultural and environmental pollutants. The application of these methods has been spurred by the low cost, relative safety, and wide availability of the required materials. However, difficulties arising from the need to reduce pH or effectively chelate Fe to reduce catalyst losses, scavenging of generated radicals in high TOC matrices, and the complexity and distribution of potentially harmful reaction products occurring during incomplete mineralization of pollutants continue to pose obstacles in the application of

these methods in many situations. There is a real need for research aimed at increasing the efficiencies of these type reactions through increasing the availability of the Fe catalyst, increasing the selectivity of the reaction through targeted complexation of organic species, and thoroughly detailing the reaction products of incompletely oxidized pollutants, particularly when the toxicity of these reaction by-products may be greater than the parent materials.

CHAPTER 2

2,4,6-TRINITROTOLUENE: HISTORY, ENVIRONMENTAL IMPACT, FATE, AND TOXICOLOGY AND THE POTENTIAL FOR USE OF CYCLODEXTRINS IN REMEDIATION

Introduction

2,4,6-Trinitrotoluene (TNT) is a crystalline solid originally synthesized by the German chemist Joseph Wilbrand in 1863. Wilbrand's synthesis consisted of refluxing toluene with fuming nitric and sulphuric acids then adding water to precipitate the TNT crystals (52). The initial use of TNT was as a yellow dye in the textile industry, but the primary application of TNT was not realized until the beginning of the 20th century when the explosive ability of this compound was utilized and weaponization of the material began by the German and British militaries (53).

TNT became the major explosive for military munitions starting with the First World War and continuing throughout much of the 20th century, and is still used a component of many munitions and explosives. The utility of TNT as a military explosive comes from a number of the compound's properties. First, TNT is a secondary explosive requiring an ignition source to initiate the explosive reaction (54). This gave TNT a significant advantage over other known explosives at the beginning of the 20th century, such as nitroglycerin and nitrocellulose. Both nitroglycerin and nitrocellulose are shock sensitive which makes them extremely dangerous and impractical for weaponization. Another advantage of a secondary explosive is that munitions containing the explosive can penetrate targets before detonation, making them capable of doing

significantly more damage to the structure being attacked. This property of TNT was realized at the beginning of the 20th century when German and British Navies found that TNT based munitions were capable of doing significantly more damage to the hulls of vessels. This was due to the fact that the detonation could be triggered after the shell penetrated the hull of an enemy vessel, as opposed to detonating on the surface of the hull which dissipated much of the explosive power of the shell. TNT also has a low melting point of 80.35 ºC, well below its ignition point of 240 ºC, which allows it to be safely poured and molded into shell and munitions casings (55). In addition to these other advantages, TNT has a high explosive velocity of 6900 m/s with a total energy of 4.6 megajoules/kg, making it a very powerful and effective explosive for munitions. In fact, the explosive power of TNT forms the basis for the standard by which other explosives are compared, a 'TNT equivalent'. The TNT equivalent is commonly used by the military to reference the explosive power of materials as being equivalent 'x kilotons of TNT'.

TNT is still used in large quantities by the military and modern applications typically consist of mixing it with other secondary explosives, such as the nitramines 1,3,5-trinitrohexahydro-1,3,5-triazine (RDX) and 1,3,5,7-tetranitro-1,3,5,7-tetraazocyclooctane (HMX). One the most commonly used explosive mixtures, Composition B, consists of 60% RDX and 40% TNT mixed with a small amount of wax binder and has been in use since the Second World War. TNT and TNT mixtures are used in a wide variety of munitions, ranging from small explosives such as grenades and mortar shells to larger weapons such as rockets and bombs. The U.S. military halted production of TNT at their munitions facilities during the 1980s but the recent wars in Iraq and Afghanistan have drastically increased the need for explosives, and production was restarted at several facilities in 2005 (56).

Toxicology of TNT

The toxicity of TNT was first realized during the beginning of the First World War when numerous cases of fatal toxic hepatitis were observed occurring in workers at munitions plants in England. In addition to hepatitis, cases of severe and sometimes fatal aplastic anemia were often observed. In the U.S., it was estimated that 475 workers died and 17,000 cases of severe TNT poisoning occurred during the First World War (53). By the Second World War, the incidence of severe health effects on workers began to decline, due to a better understanding of exposure routes and improving workplace practices (57). Studies of TNT exposure have focused primarily on the analysis of hepatic, hematologic and ocular function in workers exposed to high levels of TNT. Some incidence of dermatological, gastric and nervous system disorders have also been linked to TNT exposure (53). However, very little data exists from controlled clinical studies of TNT exposure in humans.

Several animal studies have been conducted using rats, mice and beagle dogs, focusing on oral administration of TNT (58). In rats and mice administered TNT oral lavage, the dose level leading to death in 50% or greater of the population (LD50) ranged between 660-1320 mg/kg/day. Female rats and mice were significantly more sensitive than males by factor of about 1.5 for rats and 2 for mice. Symptoms occurring before death were tremors and mild convulsions (58). In beagle dogs, an oral dose of 32 mg/kg/day was found to lead to the death of 2 of 6 females by week 14 of the study. No deaths occurred in male dogs (58). Target organs and symptoms in rats and mice exposed to TNT show many of the same clinical signs as humans exposed to high levels of TNT.

More recently, concern about the toxicity of TNT has shifted to the examination of its impact on the environment and species likely to be affected by soil and aquatic contamination.

Since little clinical data on TNT exposure in humans exists, these studies have also been used in combination with the limited number of animal studies to model the potential for human exposure, establish regulatory limits, and to assess the risk posed by TNT contamination in soil and groundwater systems. In addition to the toxicity of TNT, consideration must also be given to the metabolites of TNT in soils systems as well numerous other nitroaromatic compounds that can be found in the soils near production facilities. The wide variety of nitroaromatic compounds around production facilities results from compounds that are formed as impurities during the production process, which are removed and disposed of (59). Soil contamination by these impurities are particularly problematic at older ordnance production facilities which lacked proper disposal procedures (60).

The large number of nitroaromatic materials which must be considered when evaluating the toxicological impact of TNT production and use adds a significant degree of complexity to studies examining their impact on soil and water systems. Table 2.1 lists the most common nitroaromatic contaminants found at contaminated sites and these compounds comprise the list of materials evaluated by Neuwoehner and coworkers in a comprehensive toxicological assay in 2007 (59).

Table 2.1. Typical composition and concentration ranges of nitroaromatics found at TNT contaminated sites (adapted from Neuwoehner et al., 2007).

Compound	Typical concentration in soil (mg/kg)	Typical concentration in water (µg/L)
2,4,6-trinitrotoluene	<0.05-5524.8	4-3,400
2,4-dinitrotoluene	0-9.5	4.8-340
2,6-dinitrotoluene		24-64
2-amino-4,6-dinitrotoluene	0.1-37.6	12-370
4-amino-2,6-dinitrotoluene		4.4-210
1,3,5-trinitrobenzene	<0.05-39.5	0.1-220
3,5-dinitrophenol		12-210
3,5-dinitroaniline	0.08-0.67	
2,4,6-trinitrobenzoic acid	0.4-0.9	2-63
2,4-dinitro-5-sulfonic acid		400-500
2,4-diamino-6-nitrotoluene		ND-83,000
2,6-diamino-4-nitrotoluene		ND-35,000

Work by Neuwoehner and coworkers utilized four ecotoxicological assays (algae growth inhibition, daphnids immobilization, luminescence inhibition, and cell growth inhibition), three genotoxicological assays (umu test, NM2009 test, and SOS Chromotest) and the Ames test for mutagenicity to examine TNT and a variety of compounds commonly found at sites contaminated by TNT. In the ecotoxicological assays, effective concentrations in 50% of the population tested (EC50) were as low as 170-200 ppb in several of the assays. The genotoxicological assays gave the lowest observable effective concentrations (LOECs) for TNT and TNB as 6.3 and 8.3 ppm, respectively. TNB showed the strongest potential for mutagenic effects with an LOEC of 1 ppm for *Salmonella typhimurium* strain TA100. TNT, 3,5-dinitrophenol and 3,5-dinitroaniline gave LOECs in the range of 8-12 ppm for mutagenic effects. Overall their work is in agreement a number of smaller earlier studies and demonstrated that TNT and TNB pose the most serious risk for ecological impact, followed by 3,5-dinitrophenol, 3,5-dinitroaniline and 4-amino-2-nitrotoluene (61-63). Initial products of TNT degradation in

soils, such as dinitrotoluenes and amino-dinitrotoluenes were found to be less toxic than the TNT and this also held true for products produced during more complete remediation, such a nitrobenzoic acids and diamino-nitrotoluenes.

A study by Maeda and co-workers examined the mutagenicity of TNT as well as many of the same products in the study by Neuwoehner and coworkers by umu test, using the luminescent bacterium *Salmonella typhimurium* strain TA1535/pTL210, and came to similar conclusions on the relative mutagenicity of the studied compounds (64). Maeda and co-workers posit that the mutagenicity of nitroaromatic compounds positively correlate with the number of nitro groups present on the target molecule. Their conclusions would indicate that reduced TNT products typically found at contaminated sites would pose less threat than the parent compounds. However, reduced amino products are more water soluble than the nitro pre-cursors and can pose more of a threat in certain soil environments with either low humic content or high water content (65).

Environmental Impact of TNT

The global production of TNT over the last century, and its use in numerous armed conflicts, has led to significant contamination of soils and groundwater in a vast number of locations. In the United States, the U.S. army reports that at least 1.2 million tons of soils at various facilities exceed the established remediation goal of 17.2 mg/kg of TNT in soils set by the U.S. Environmental Protection Agency (USEPA) for the Nebraska Ordnance Plant (NOP) (60, 66). The NOP was one of a number of US Army ordnance plants to produce TNT and was the first ordnance facility to be listed under the USEPA's national priority listing (NPL), more commonly referred to as 'superfund' sites (67). The U.S. Agency for Toxic Substances and

Disease Registry (ATSDR) lists 23 US Army munitions facilities responsible for TNT production and storage with TNT contamination (55). Figure 2.1 shows a map of states with NPL sites, listed by the ATSDR, containing TNT above the established USEPA remediation goal.

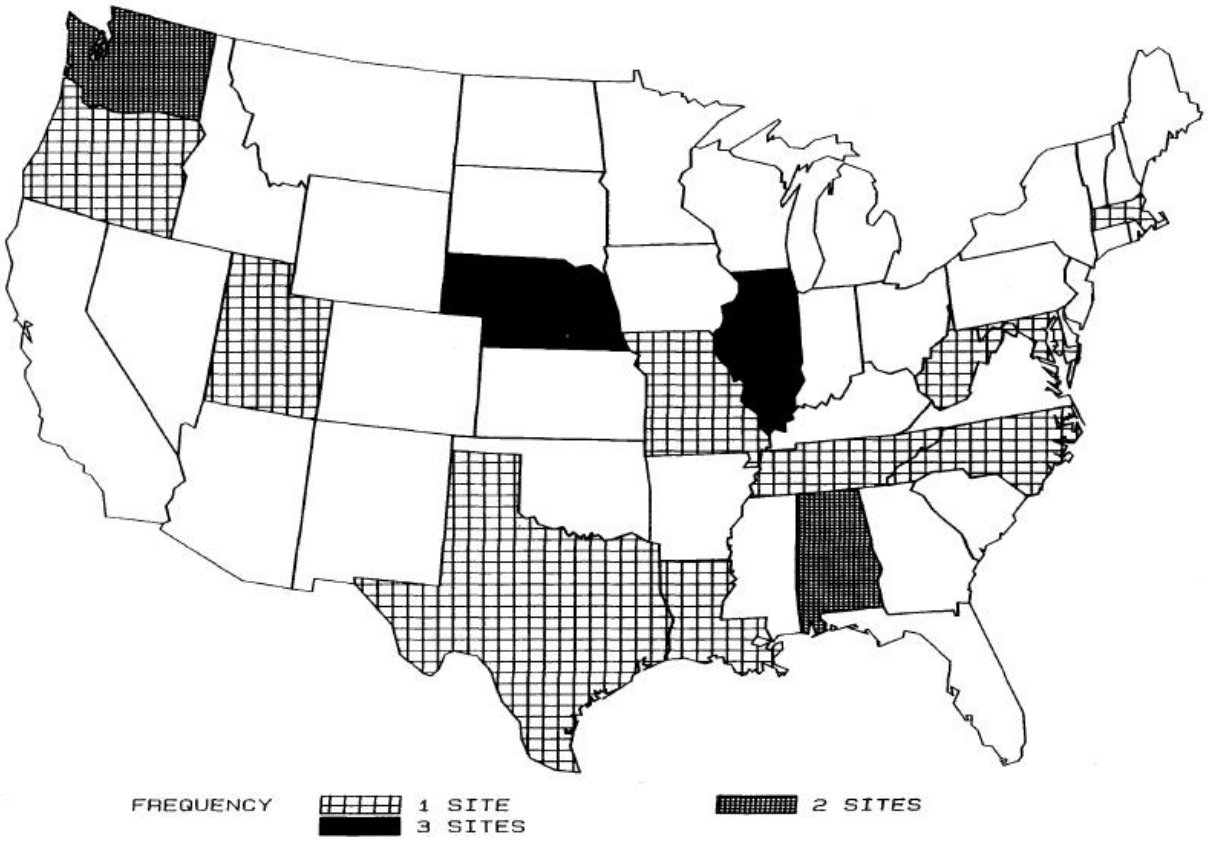

Figure 2.1. Frequency and distribution of NPL (superfund) sites containing TNT above the USEPA mandated limit (55).

In addition to production and storage facilities, numerous training and live-fire ranges have considerable levels of TNT contamination from low-order (incomplete) detonations and unexploded ordinances (UXOs) (56, 68). A recent study of 23 live fire ranges in the United States and Canada found widespread contamination of soils by TNT and other energetic materials and these 23 sites represent only a fraction of the total number of live-fire ranges

operated by the United States and Canada (69, 70). In total, the United States Department of Defense (USDOD) has identified over 1000 sites with significant levels of contamination by explosives (60). Significant levels of TNT contamination from low-order detonations and UXOs can also be expected in areas of the world which have suffered from serious armed conflict over the last several decades, such as many parts of the Middle East, Africa, and South Asia. Another potentially serious problem with UXO contamination in many parts of the world is the uptake of TNT and its metabolites by plants in contaminated soils (71). Uptake of TNT and its metabolites by plants can have a broad-ranging impact on agriculture through direct ingestion of food crops by humans and through livestock exposure in feed produced from contaminated grains and grasses. In addition to the impact on humans and domesticated animals, TNT poses a threat to wildlife feeding on contaminated crops and plants.

Contamination of soils by TNT can pose a threat to groundwater, and serious concerns exist about the movement of TNT and its various metabolites into the water table, and ultimately, into drinking water supplies. The USEPA has established a limit of 2 μg/L of TNT in residential water supplies, based on lifetime risk factor for chronic oral dosing (72). Other studies have recommended even lower levels, in the 0.1-0.2 μg/L range, based on extrapolated risk from no-observed-effect levels/lowest-observed-adverse-effect levels (NOAELs/LOAELs) in a number of animal studies (73). Of the sites identified by the USDOD as having significant levels of explosives contamination, over 95% of the sites contained TNT above permissible levels in soil and 87% contained TNT levels above permissible levels in groundwater (74).

Fate of TNT in the Environment

The fate of TNT varies greatly between contaminated soils, groundwater and surface waters. TNT has very low water solubility (approximately 80 mg/L at 25 ºC), though migration of TNT into groundwater can occur and is highly dependent on soil and groundwater conditions, pH, organic content of the soils, the presence or lack of nitro reducing bacterium, as well as the concentration of TNT in the soils (65, 75-78). In surface waters, TNT can undergo photolytic reduction to yield a variety of compounds. The rate of the photolytic reduction is heavily dependent on the biological content of the water as well as the water chemistry (79). In general, contamination of soils by TNT is considered to pose the most significant threat due to its recalcitrance and potential for migration into groundwater, and remediation efforts have primarily focused on soils.

A number of studies have examined the fate of TNT in soil and groundwater through either direct analysis of the materials present at contaminated sites or through lab-scale studies modeling different site conditions. Under most conditions, transformation of TNT occurs slowly and typically proceeds along a reductive pathway, yielding amino substituted and azoxy products. The reductive pathway typically occurs due to the presence of nitrogen reducing bacteria or fungi in the soils or through the presence of iron containing minerals (65, 77, 80).

Bradley and Chapelle examined microbial remediation of TNT by indigenous microorganisms at the Weldon Spring, MO munitions facility which was decommissioned in 1945 (81). They found that the microorganisms present at several of the sampling sites were capable of completely removing TNT from the collected soils in 22 days, under controlled conditions in the laboratory. However, significant contamination of the site by TNT still existed at the time of this study which was conducted 50 years after decommissioning. The continuing

presence of TNT indicates that other factors, besides the presence of the microorganisms, must play a role in the effectiveness of these soil components to degrade TNT. The study examined a number of these potential factors such as soil moisture content, presence of less recalcitrant nitrogen sources, oxygen content in soil headspace, and TNT concentration. The results of their study showed that low soil moisture content and TNT concentrations above 100 μmol/kg of soil were the primary factors that inhibited degradation. Either of these factors proved capable of completely inhibiting TNT degradation in the soil matrix.

Daun and colleagues have examined the cometabolic reduction of TNT under anaerobic conditions, using small amounts of glucose (20 mM in soil) as an auxiliary substrate for the TNT reducing microorganisms (82). They found that the reductive process takes place through multiple 2 electron transfers leading to formation of nitroso then hydroxylamino, and finally, amino groups on the ring. Figure 2.2 shows the successive 2 electron reduction steps leading to the formation of 4-amino-2,6-dinitrotoluene, typical of the process described by Daun et al. This sequence of product formation has also been described in other studies examining biological and non-biological reduction of aromatic nitro groups (83, 84).

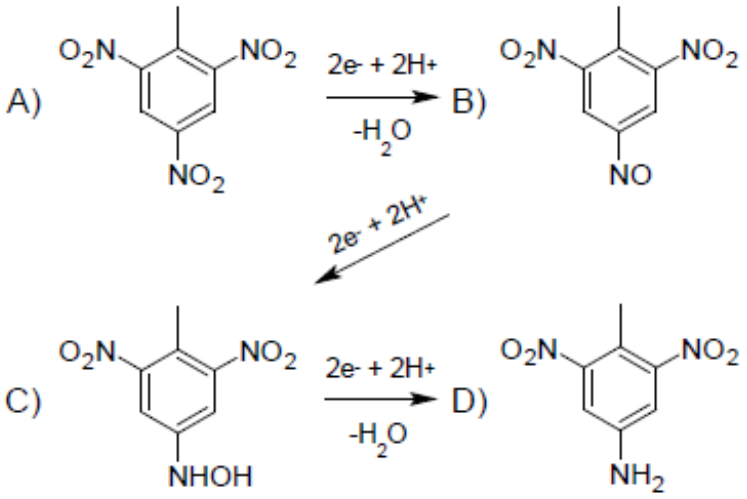

Figure 2.2. Six electron reductive pathway for the transformation of a) TNT to d) 4-amino-2,6-dinitrotoluene. Also shown are the intermediates b) 4-nitroso-2,6-dinitrotoluene and c) 4-hydroxylamino-2,6-dinitrotoluene (82).

Hofstetter and co-workers examined the reduction of TNT and a number of other (poly)nitroaromatic compounds under conditions deigned to model the movement of these compounds in a soil and aquifer system with iron-reducing subsurface conditions (83). The authors studied the role of reactive Fe^{2+} surface species on TNT reduction and product formation. These studies were conducted using FeO(OH) (goethite) coated sand in the presence of the iron reducing bacterium *Geobacter metallireducens* or ferrogenic aquifier sediments. Reduction of TNT in the presence of goethite was capable of completely reducing TNT to triaminotoluene (TAT) while the ferrogenic aquifer sediments, more representatives of actual environmental conditions, were incapable of complete reduction and left ca. 90% of the reduced TNT in the form of amino-dinitrotoluenes (ADNTs).

Achtnich and coworkers examined the stability of reduced radio-labeleled ^{14}C-TNT products in soils under a short-term (8 day) and long-term (51 day) anaerobic treatment (65). Both the short and long-term anaerobic treatments were followed by an aerobic treatment. In the

short-term anaerobic treatment, ADNTs were the dominant products while complete reduction to TAT was observed in the long-term study. Following aerobic treatment of the soils, it was found that 40% and 98% of the ^{14}C radio-label was bound to the soil matrix for the short-term and long-term studies, respectively. The authors credited the irreversible binding to cross-linking between the polar moieties of the reduced TNT products and humic fraction of the soil.

Thorn and colleagues have conducted several studies using ^{15}N solid-state cross polarization magic angle spinning (CP/MAS) and direct polarization magic angle spinning (DP/MAS) NMR to examine the products resulting from microbial degradation of ^{15}N radio-labeled TNT in soil composts (85-87). The results of their studies have shown that microbial degradation of TNT proceeds via a reductive pathway and can lead to a wide variety of products including mono-, di- and triamine products, reactive nitroso and hydroxylamino reductive intermediates, and azoxytoluenes formed from the nitroso and hydroxylamino intermediates. These studies have also shown that the reduction products are capable of binding to the organic fraction in soils through the formation of covalent bonds formed by aminohydroquinone, aminoquinone, heterocyclic and imine linkages. It was found that the covalently bound reductive components had the highest overall concentration in the lignocelloluse fraction of the composted soil. The formation of covalently bound reduced products has been indirectly observed in a number of other studies that have shown that complete degradation of TNT by reductive processes is possible, but that complete mineralization is not realized in reductive pathways in soils (65, 77, 82). The long-term threat posed by these bound reduction products is not well understood at this point in time. While the bound products are less likely to pose an environmental risk than potentially migratory compounds, weathering of soils and further

humification of the soil components has the potential for releasing transformed nitroaromatic species (87).

Weiß and colleagues examined the fate of ^{15}N and ^{14}C radio-labeled TNT in soil bioreactors in the presence of soils inoculated with a nitrogen reducing fungus, *Stropharia rugosoannulata* (88). The results of their work showed a number of reductive pathways occurring in the presence of *Stropharia rugosoannulata*, leading to a 60 to 85% reduction in radio-labeled TNT over the 6 month operation of the bioreactors (starting concentrations of 7.5 g of [^{14}C]TNT or [^{15}N]TNT per kg of soil). Similar to the studies by Thorn et al. and Achtnich et al., they found that a significant portion of the radio-labeled TNT that was degraded, 52 to 64%, was converted into non-extractable soil residues. Only 3% of the degraded TNT was extracted in the form amino-dinitrotoluenes.

Introduction to Cyclodextrin Chemistry and History

Cyclodextrins (CDs) are cyclic oligosaccharides typically composed of 6, 7, or 8 α-D-glucopyranose units joined through an α-1,4 glycosidic bond and are referred to as α-, β-, and γ-cyclodextrins, respectively (Figure 2.3). CDs are water soluble, yet the annulus of the ring provides a hydrophobic environment, giving CDs their ability to complex small non-polar molecules in aqueous environments. CDs are non-toxic, environmentally benign, inexpensive to produce and commercially available, and can be synthetically tailored with a variety of different functional groups attached to the CD ring. They are widely used in industrial, pharmaceutical, food, agricultural and environmental applications. The primary use of CDs in these diverse applications arises from their complexation properties and specific examples of these uses

include targeted chemical synthesis, drug delivery, use as emulsifiers, solubility enhancement of small organic molecules, and chromatographic applications (89, 90).

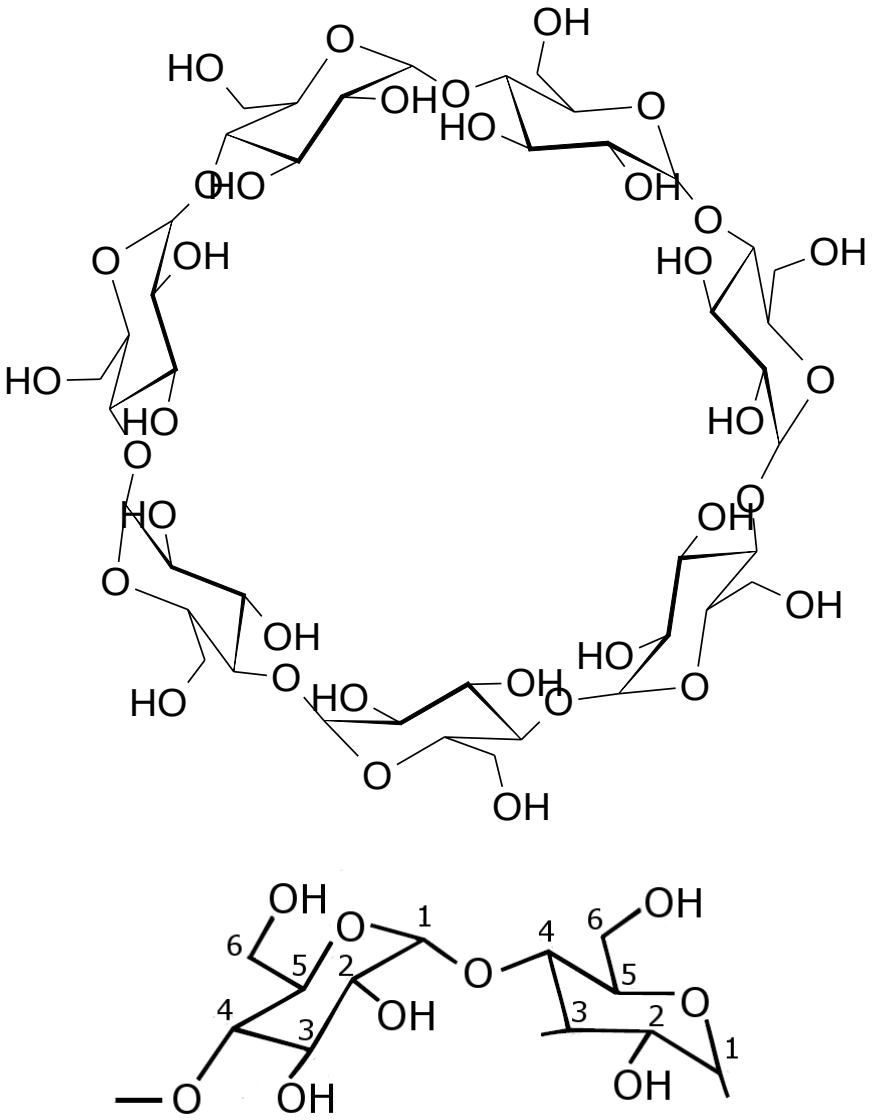

Figure 2.3. Structure of β-cyclodextrin, which consists of 7 α-D-glucopyranose units joined through α-1,4 glycosidic bonds (top). The α-1,4 glycosidic bonds are shown for two α-D-glucopyranose monomer units of a CD polymer (bottom).

While CDs are used in a diverse range of applications and industries, the fundamental physical property of these compounds that is typically utilized is their ability to complex small,

non-polar compounds. This ability to arises from the α-1,4 glycosidic bonds in CDs which orient the hydroxyl groups of the CD molecule along the edges of its torus-like structure (Figure 2.4). The primary hydroxyl groups orient along the larger rim of the torus, while the free rotation of the secondary hydroxyl groups creates a smaller effective diameter along the rim they are bonded to, relative to the primary hydroxyl rim. On the interior of the torus, the C3 and C5 protons of the α-D-glucopyranose units are oriented near the wider and narrower ends of the torus, respectively. This bonding arrangement yields a structure in which the interior of the torus provides a non-polar, hydrophobic environment while the exterior and rims are hydrophilic (91).

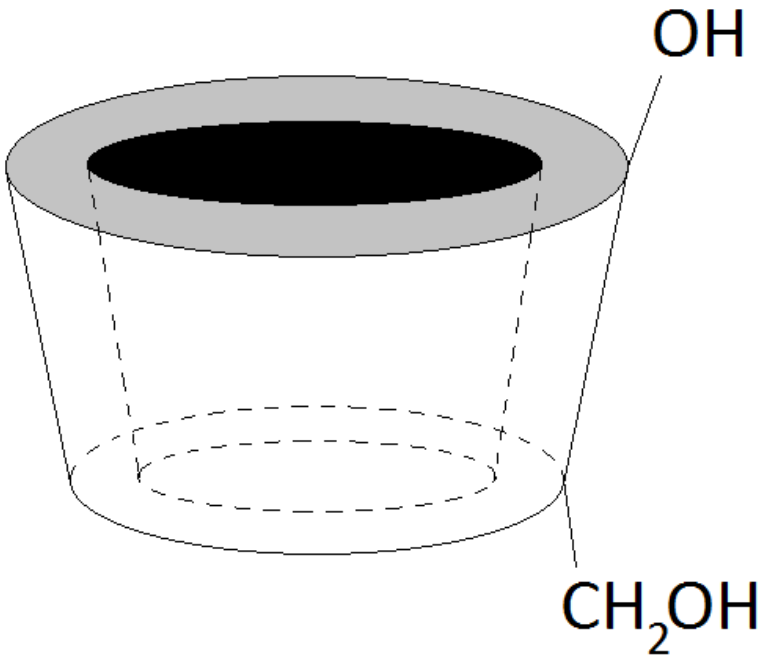

Figure 2.4. Torus-like structure of CDs, showing primary hydroxyl groups at the wider end of the CD torus, while secondary hydroxyl groups are bonded to the narrower end.

A number of physical properties of CDs are given in Table 2.2.

Table 2.2. Physical Properties of Cyclodextrins (89, 91, 92).

	α-CD	β-CD	γ-CD
number of α-D-glucopyranose units	6	7	8
molecular weight (g)	972	1135	1297
cavity diameter, Å	~5.2	~6.7	~8.4
cavity length, Å	8	8	8
cavity volume, ml/mol CD	104	157	256
water solubility, g/100 ml, 25°C	14.5	1.85	23.2

History of Cyclodextrins

The first reports of CDs in the literature occurred between the years of 1891 to 1911 in an initial study by Villiers which was later followed by a number of studies by Schardinger (93-96). Villiers examined the digestion of starch by the bacterium *Bacillus amylobacter* and discovered a small amount of crystalline material which he was able to isolate from the starch. Upon closer examination he proposed a chemical composition of $(C_6H_{10}O_5)_2 \cdot 3H_2O$ and named the material cellulosine. It has been suggested that the two crystalline forms observed by Villiers in this early work were actually α- and β-CDs (89).

Schardinger performed a number of studies examining heat resistant bacteria, particularly a bacterium he later named *Bacillus macerans*, as well as several other species which were believed to be pathogens able to survive the cooking process in food. While he discovered no evidence linking these bacteria to illness in humans, he did observe that *Bacillus macerans* was capable of producing crystalline isolates upon the digestion of starch as earlier observed by Villiers (95). Schardinger also developed a simple colorimetric test using iodine-iodide staining to distinguish between what would later be called α- and β-CDs (96). Schardinger established the fundamentals of CD chemistry and is given the primary credit with their discovery. In fact,

CDs were typically referred to as 'Schardinger dextrins' until the 1970s and most of the literature published until this time referred to them by this name.

A more in-depth understanding of the structure and an expansion in the understanding of the chemistry of CDs occurred through a series of studies from the mid-1930s through the early 1950s, primarily through studies by Freudenberg and coworkers (97-100). Freudenberg and co-workers were the first to demonstrate that CDs were composed of α-D-glucopyranose monomers with a linkage between the monomer units occurring through a α-1,4 glycosidic bridge (Figure 2.3) (99). Freudenberg was also the first to describe γ-CD and later determined its x-ray crystal structure (98, 101). Freudenberg's work greatly advanced the understanding of CD structure and chemistry and helped to pave the road for the development of their applications.

The first in-depth publications on the chemistry and application of CDs occurred in the 1950s in a book on inclusion complexes by Cramer as well as the first review article of CD literature by French (102, 103). Cramer's work on inclusion complexes established much of our modern understanding of the behavior of CDs during complexation and includes many details on the structure, cavity size, solubility and other physico-chemical properties and remains a commonly cited source to this day. French's review, 'The Schardinger Dextrins', covered synthesis and production of CDs by *Bacillus macerans*, fundamental physical, chemical, and structural properties as well what was understood about CD complexation with small organic molecules.

While French's review is still commonly cited, it has been noted that it contained a significant error which limited the application of CDs for a number of years (89). In the review, French states CDs appear to have a high toxicity based on a single study of rats fed a diet containing β-CD. In the cited study, rat mortality was 100% within a week of introducing β-CD

into the diet but the study appears to be poorly designed and without control subjects. Szejtli states that this statement by French deterred research into CD applications for human use for several decades, until later toxicity studies proved CDs to be non-toxic (89).

Research into the uses and applications of CDs remained limited until the 1970's, when advances in genetic engineering allowed the tailoring of cyclodextrin glycosyltransferases (CGTases) to increase activity and specificity towards different CDs (104). This advancement allowed the industrial scale production of CDs and had the dual effect of significantly decreasing cost as well as increasing the their availability (89). The decreased cost and increased availability spurred the growth of CD related research and the number of CD related research publications increased dramatically from the 1970's onward. Industrial, pharmaceutical, food, and agricultural applications were soon realized and the first International Symposium on Cyclodextrins was organized by József Szejtli held in Budapest, Hungary in 1981 (104).

Relevance of CDs in Environmental Applications

To date, the use of CDs in environmental applications has been limited. One application that has received some attention is as an additive in aqueous solutions used for soil washing. John McCray, Mark Brusseau and co-workers have published a number studies examining the effectiveness of CDs to aid in the solubilization of small hydrophobic pollutants to increase removal efficiency for ex-situ treatment (105-107). Brusseau and co-workers also studied the ability of CDs to increase the biodegradation of phenanthrene in soils through increased bioavailability due to solubility enhancement by CDs (108) as well as several studies have examining the simultaneous complexation of organic components along with metal and heavy metal contaminants in soils (109, 110). Of specific relevance to the studies presented in the

following chapters, studies have also examined the effectiveness of CDs for solubilization of TNT and its metabolites from soil matrices (92) and the utility of this method for ex-situ remediation of TNT by photo-Fenton and electro-Fenton methods (20, 23).

In the initial study by Brusseau and co-workers, an aqueous solution of hydroxypropyl-β-cylodextrin (hp-β-CD) was flushed through lab-scale soil columns containing two different soils with TOCs of 0.29% or 12.6%. The analytes examined included a number of low molecular weight PAHs and chlorinated aromatics of environmental concern which were applied to the soil columns at their aqueous solubility limit. The hp-β-CD solution was pumped through the soil columns and removal of analytes was monitored by UV and fluorescence detection. The results of their study showed that smaller, more hydrophobic compounds were more readily desorbed from the soil columns; that the soil with the higher TOC required either larger wash volumes or a higher concentration of hp-β-CD in the solution to achieve results similar to those in the low TOC soil; and that >99% extraction efficiency was feasible for some analytes.

Later studies by Brusseau and McCray began examining the pilot scale application of hp-β-CD solutions for soil washing of a site contaminated with very high levels of a non-aqueous phase organic liquid (NAPL) containing multiple components (105, 107). The initial saturation of NAPL in the soils was estimated to be 12.6%. Specific analytes included in the study consisted of poly-chlorinated hydrocarbons, benzene, toluene and xylenes (BTEXs), linear alkanes and PAHs. The washing solution consisted of 10% by weight of hp-β-CD applied to a 135 m^3 section of soil through the use of a horizontal flow field using 4 injection and three extraction wells. The total volume of wash solution applied was 65,500 L over a 14 day study period. NAPL removal was determined by periodic sampling of the extracted wash stream over the course of the study followed by GC-FID detection of target analytes. The total removal over

the course of the study was then calculated based on the results of soil-core sampling prior to soil washing. These results were then compared to a control study using only water to flush the test site. While the CD washing showed little impact on the concentrations of linear alkanes in the soils, significant removal of BTEXs, PAHs and poly-chlorinated hydrocarbons was achieved. The percent removal of these components ranged from around 40-44% for xylenes to 84% and 87% for trichloroethylene and benzene, respectively.

The first study of simultaneous metal and organic complexation was conducted by Wang and Brusseau when they examined the ability of carboxymethyl-β-CD (cm-β-CD) to form a ternary complex with anthracene, trichlorobenzene (TCB), biphenyl or dichlorodiphenyltrichloroethane (DDT) and Cd^{2+} (110). Complexation was monitored by UV-vis to determine the apparent solubility the organic components and by a cadmium-selective electrode to look at metal complexation. The apparently solubility of the organic components increased linearly with increasing cm-β-CD concentration, up to 10 g/L. The increase in solubility ranged from 4-fold for TCB to 75-fold for DDT at 10 g/L of cm-β-CD. Complexation of Cd^{2+} was also monitored at varying cm-β-CD concentrations and pH values. At a 10 ppm Cd^{2+} concentration, the free Cd^{2+} in solution for cm-β-CD concentrations of 2-10 g/L was between 10-20% and these values were stable in a pH range of 2-10. Additionally, simultaneous complexation of anthracene demonstrated no significant change in the ability of cm-β-CD to complex Cd^{2+}. The authors also proposed a structure for the ternary complex (Figure 2.5).

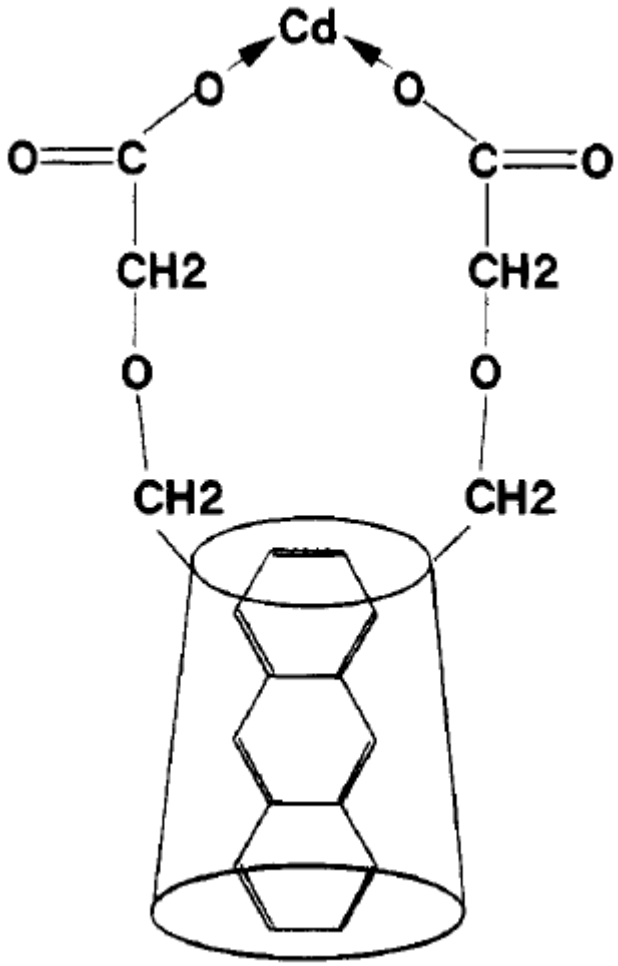

Figure 2.5. Proposed structure of Cd^{2+}/anthracene/cm-β-CD ternary complex (not to scale) (110).

A more recent study by McCray and co-workers again examined the ability of cm-β-CD to form ternary complexes with perchloroethylene (PCE) and Pb, Sr or Zn (109). They compared experimental data to that obtained using the geochemical modeling software, PHREEQC. They also found that the apparent solubility of the organic component increases linearly with increasing cm-β-CD concentration and that the presence of PCE had no discernible effect on metal complexation. Unlike PCE complexation, the concentration of complexed metal increased rapidly with initial addition of cm-β-CD up to approximately 20 g/L, but the slope the

plots of metal concentration versus cm-β-CD concentration followed that of an inverse exponential decay plot. The overall results of their study demonstrated good agreement between the experimental data and computational modeling and show cm-β-CD to be very effective at forming ternary complexes.

Sheremata and Hawari examined the ability of heptakis-2,6-di-O-methyl-β-cyclodextrin (dm-β-CD) and hp-β-CD to desorb TNT, 4-amino-2,6-dinitrotoluene (4-ADNT) and 2,4-diamino-4-nitrotoluene (2,4-DANT) from two different topsoils with low and high TOC, with the nitroaromatic compounds spiked into the soil samples (92). They performed an extensive examination of Freundlich sorption isotherms for nitroaromatic binding to the soils as well as desorption isotherms desorption into an aqueous medium as well as aqueous mediums containing the two CDs examined. Their study demonstrated that the CDs examined were able to effectively desorb the nitroaromatics from the high TOC soil in the order TNT > 4-ADNT > 2, 4-ADNT. The effective desorption order is expected based on hydrophobicity of the compounds as well as the fact that amino-nitroaromatics bind irreversibly with quinoidal moieties in the soil organic matter (87). For the low TOC soil, the opposite desorption order was observed and the authors credited this behavior to the formation of electron donor acceptor complexes between siloxane surfaces found on phyllosilicate minerals in the soil and the electron withdrawing nitro groups of TNT.

Yardin and Chiron conducted a laboratory scale study of the ability of methylated-β-CD (m- β-CD) and hp-β-CD to desorb TNT from a soil matrix followed by a subsequent photo-Fenton treatment of the soils to degrade the desorbed TNT (20). The study examined the TNT removal efficiency, degradation and mineralization rates subsequent to flushing with CDs, and proposed a degradation pathway for the TNT undergoing photo-Fenton treatment. The soil

examined in the study had a moderate TOC of 6.5% and was spiked with TNT at 200 mg/kg of soil and equilibrated for 2 months. TNT removal enhancement was calculated based on chromatographically determined association constants for the TNT:CD complexes, and m-β-CD was determined to be the more efficient of the two CDs at removing TNT. The calculated versus the observed enhancement factor for 5 mM m-β-CD was 2.7 versus 2.1, relative to soil flushing with nanopure water. Based on the enhancement factor, the authors chose to examine only m-β-CD for the remainder of the study. Photo-Fenton treatment of the desorbed TNT was performed and compared to the results obtained by performing an identical treatment of the soil extract obtained using only distilled water to flush the soil, as well as a water control spiked with TNT. An increase the apparent rate constant of 1.3 for TNT desorbed with cm-β-CD was reported, versus the water control. A nearly 2-fold increase the apparent rate constant versus the distilled water soil flushing was also observed. The authors credited the increase in apparent rate constants to the ability of the TNT:CD:Fe ternary complex to direct hydroxyl radical production towards the complexed TNT. The authors attempted an analysis of the products formed by LC-MS and LC-MS/MS and tentatively identified picric acid as the first step of the reaction followed by 2,4,6-trinitrobenzene-1,3-diol which then underwent ring opening to yield short chain carboxylic acids. However, a number of other ions were observed and not identified and the proposed pathway appears too simplistic for the variety of product ions observed.

Murati and co-workers examined the electro-Fenton degradation of TNT washed from soils using β-CD and cm-β-CD (23). The study demonstrated an enhanced removal efficiency of the TNT from treated soils but the electro-Fenton treatment offered results that contradicted several other studies examining the Fenton treatment of TNT in the presence of CDs (20, 111) as well as results presented in later chapters. In the study, the authors show a 90% removal rate for

TNT after 6 hours for a water control, without CDs present. In contrast, β-CD and cm-β-CD offer only 91% and 67% removal efficiency while other studies have clearly demonstrated an enhancement in TNT removal relative to water controls. The authors also performed an initial examination of reaction products by HPLC-UV and did not find evidence of 2,4,6-trinitrophenol, as observed by Yardin and Chiron (20).

Summary

TNT was the most widely used military explosive through the era encompassing both the First and Second World Wars and is still a major component of military explosives and munitions. As a result, contamination of soils by TNT around weapons manufacturing, testing, and disposal facilities poses serious environmental problems. TNT is of particular environmental concern due to its recalcitrance in soils and toxicity, mutagenicity and potential carcinogenicity to both aquatic and mammalian species. Biological and abiotic transformation of TNT follows a reductive pathway and leads to a wide variety of products. While these reduced products pose less of an environmental threat than TNT, many of them irreversibly bind to the soil matrix and their long-term impact is poorly understood.

The use of CDs in environmental remediation processes has shown promise in the solubilization and removal of small non-polar organic contaminants, like TNT, from soil matrices during soil flushing with CDs. Additionally, several studies have found that CDs can be used to accelerate the degradation of TNT during Fenton reactions. The use of soil flushing by CDs in combination with ex-situ remediation of TNT via Fenton chemistry could yield a viable soil remediation method. The use of CDs that can strongly chelate iron cations may also allow in-situ remediation of soils by limiting the need for pH adjustment.

CHAPTER 3

KINETICS AND INITIAL PATHWAY OF FENTON DEGRADATION OF TNT IN THE PRESENCE OF MODIFIED AND UNMODIFIED CYCLODEXTRINS

Introduction

Complexation of organic species and coordination of metal ions by cyclodextrins to form binary and ternary complexes is a well documented phenomenon. In environmental applications this complexation has been utilized in soil flushing with cyclodextrins to increase the pollutant water solubility and removal efficiency (105, 112) and to enhance Fenton degradation of organics (20, 21). It has been proposed that the enhancement of Fenton degradation rates of small organics is due to the formation of ternary complexes of pollutant/cyclodextrin/Fe^{2+} which initiate hydroxyl radical production near the pollutant/cyclodextrin complex (21, 23). However, previous studies have not addressed whether the enhancement occurs through promotion of the oxidative pathways, through reductive pathways initiated by secondary cyclodextrin radicals, or through some combination of these effects which leads to the higher overall reaction rates observed. In this study the effects of modified and unmodified cyclodextrins and glucose on the kinetics of 2,4,6-trinitrotoluene (TNT) degradation during a Fenton reaction were examined and mechanisms were proposed to explain the observed effects.

TNT was the most widely used military explosive through the era encompassing both the First and Second World Wars. As a result, there is widespread contamination of soils by TNT around weapons manufacture, testing, and disposal facilities (77). TNT in these soils poses a serious environmental threat and health risk since it is poorly biodegradable and is both toxic and mutagenic in mammalian and aquatic species (57, 113). While Fenton reactions have

demonstrated utility in TNT remediation in soils (25), the acidic (pH 3.0-3.5) conditions required to prevent formation of insoluble iron hydroxides is problematic and typically require stabilization of the iron catalyst through processes such as chelation (1). Cyclodextrins have shown some promise in the solubilization and ex-situ Fenton treatment of TNT in soils (20, 23) and modified cyclodextrins able to effectively chelate iron at near neutral pH may have application for in-situ remediation of TNT in soils.

Cyclodextrins are cyclic oligosaccharides containing six (αCD), seven (βCD) or eight (γCD) α-D-glucose units with a 1-4 linkage in the ring. In solution, CDs have been shown to form binary guest-CD complexes through encapsulation of the guest molecule into the hydrophobic cavity of the CD (92, 114, 115). Metal ions may be coordinated by cyclodextrins through interaction with the oxygens in the α-D-glucose units or by functional groups of modified cyclodextrins (110, 115, 116). The enhancement of the Fenton degradation in the presence of CDs has therefore been credited to the formation of ternary guest-CD-Fe^{2+} complexes which have the ability to produce hydroxyl radicals at the catalytic Fe^{2+} site during Fenton reactions (20, 21). The authors have proposed that this results in an increase in hydroxyl radical concentration near the target guest molecule relative to the bulk solution, leading to a targeted degradation of the complexed guest molecule through either direct oxidation or the action of secondary CD radicals.

In this study, the ability of the cyclodextrins 6^A-[bis(carboxylatomethyl)amino]-6^A-deoxy-β-cyclodextrin (6βCDidaH_2), 6^A-[tri(carboxylatomethyl)(2-aminoethyl)amino-6^A-deoxy-β-cyclodextrin (6βCDedtaH_3), structures given in Figure 3.1, β-cyclodextrin (βCD) and carboxymethyl-β-cyclodextrin (cmβCD) to enhance the degradation rate of TNT during a Fenton reaction have been examined. In addition to the CDs, the effect of D-glucose at varying

concentration was also examined to probe the impact of complexation of the organic species on the overall behavior of the reaction systems. The impact of iron chelation on the reaction rates was also examined using disodium ethylenediaminetetraacetate (Na_2EDTAH_2). Initial degradation pathways were examined through a combination of high performance liquid chromatography (HPLC), ion chromatography (IC) and mass spectrometry (MS). The pK_a values for 6βCDidaH$_2$ and the Fe^{2+} binding stoichiometry of the Fe^{2+} complexes formed with 6βCDida^{2-} and 6βCDidaH$^-$ complex were determined by collaborators.

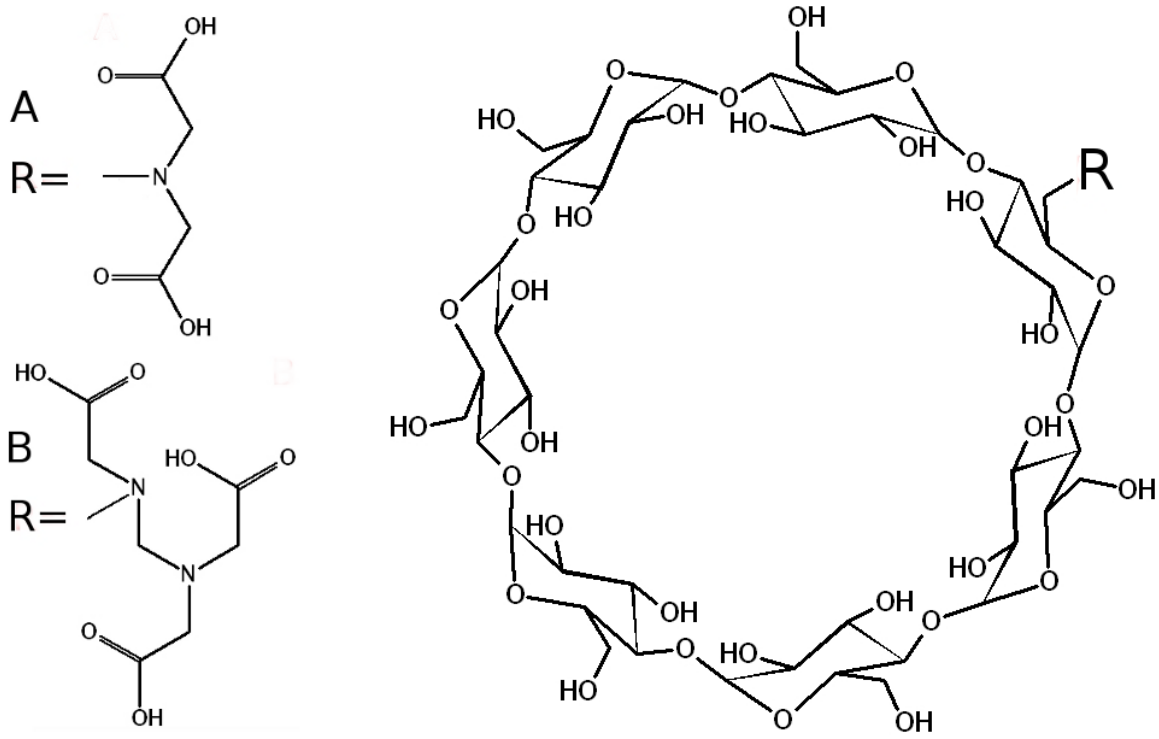

Figure 3.1. Structure of 6βCDidaH$_2$ (A) and 6βCDedtaH$_3$ (B).

Experimental Section

TNT (98%, min 30% H_2O) and 1,3,5-trinitrobenzene (TNB, 99%, min 30% H_2O were obtained from Chem Service. 2-amino-4,6-dinitrotoluene (2-ADNT) and 4-amino-2,6-dinitrotoluene (4-ADNT, analytical standard in 1:1 methanol:acetonitrile) were obtained from Accustandard. $FeSO_4 \cdot 7H_2O$ (A.C.S. grade) and disodium ethylenediaminetetraacetate (Na_2EDTAH_2, A.C.S. grade) were obtained from Fisher Scientific. D-glucose (A.C.S. grade) was obtained from Aldrich. Acetonitrile (ACN, HPLC grade) was obtained from EMD. βCD and cmβCD were obtained from Cerestar and 6βCDidaH_2 and 6βCDedtaH_3 were synthesized as previously reported (117, 118). All reagents containing H_2O were vacuum desiccated in small quantities prior to use in order to allow accurate mass measurement and all other reagents were used as received. All aqueous solutions were prepared using 18 mΩ water from a Barnstead NanopureUV or a Milli-Q-Reagent water purification system with a distilled water feed. All aqueous solutions of the nitroaromatics were prepared from aliquots of concentrated stock solutions in acetonitrile that were evaporated under a gentle stream of dry nitrogen before being reconstituted by overnight stirring in 18 mΩ water. All nitroaromatic solutions were stored in amber glass bottles and used within one month of preparation.

Potentiometric titrations were carried out by collaborators using a Metrohm Dosino 800 titrimator, a Metrohm Titrando 809 potentiometer and an Orion 81-03 combination electrode filled with aqueous 0.10 mol dM^{-3} $NaClO_4$ solution. The electrode was soaked in 0.10 mol dM^{-3} $NaClO_4$ solution for at least three days prior to use. Titrations were performed in a water-jacketed 2 cm^3 titration vessel held at 298.2 ± 0.1 K. During the titrations, a gentle stream of nitrogen bubbles (previously passed through both aqueous 0.10 mol dM^{-3} KOH to remove any CO_2 traces and then aqueous 0.10 mol dM^{-3} $NaClO_4$) was passed through the titration solutions,

which were magnetically stirred. The titration solutions were equilibrated in the titration vessel for 15 min before commencement of the titration to allow the solution to equilibrate to 298.2 K and become saturated with nitrogen. The electrode was calibrated every 24 hours by titration of a solution 0.01 mol dM^{-3} in $HClO_4$ and 0.09 mol dM^{-3} in $NaClO_4$. (The pK_w obtained from this electrode calibration was 13.77.) For each system, 0.10 mol dM^{-3} NaOH was titrated against 0.001 mol dM^{-3} 6βCDidaH_2 alone and either in the presence of 0.0005 or 0.001 mol dM^{-3} Fe^{2+} in solutions 0.010 mol dM^{-3} in $HClO_4$ and 0.09 mol dM^{-3} in $NaClO_4$. Deionized water produced with a Milli-Q-Reagent system was boiled to remove residual CO_2 for all solution preparations. The pK_as and stability constants for Fe^{2+} complexation were derived through fitting the appropriates algorithms to the titration data using the Hyperquad2003 program from Protonic Software (119) and speciation plots were generated using the Hyss2006 (120) program from the same source. The pK_a for $[Fe(OH_2)_6]^{2+}$ to give $[Fe(OH)_5(OH)]^{+}$ used in the fitting procedure was 7.10 (120).

Fenton reactions for TNT were conducted by preparing 10 mL aqueous solutions of 0.1 mM TNT and adding 1 mM CD and allowing to equilibrate for at least 30 minutes prior to initiation of reaction. Immediately before reaction, 5 mM $FeSO_4$•$7H_2O$ was added. For reactions requiring pH adjustment, H_2SO_4 was added prior to the addition of $FeSO_4$•$7H_2O$. Reactions were conducted in a round bottom flask with continuous magnetic stirring. Addition of H_2O_2 was accomplished via syringe pump using a 150 mM aqueous solution added at a flow rate of 2 mL h^{-1} for the TNT systems. The concentration of the stock H_2O_2 solution was determined by titration with sodium thiosulfate and potassium iodate. The Fenton reactions in the presence of D-glucose, and EDTA (used herein as generic abbreviation for $EDTAH_4$ irrespective of the state of protonation) were run under identical conditions to the CD-containing systems. Sampling

of the reaction was accomplished by removing a 300 μL aliquot of the reaction mixture and adding it to a sample vial containing 300 μL of 1% v:v 1-propanol in water to quench the Fenton reaction through hydroxyl radical scavenging by the 1-propanol. Samples were centrifuged and passed through 0.22 μm PTFE syringe filters to remove precipitated iron hydroxides prior to analysis by HPLC, IC or MS.

HPLC analysis was conducted on an Agilent 1100 HPLC system with a diode array absorbance detector operated with full spectral data collection from 200-400 nm. An Alltech Econosphere C18, 150 × 4.6 mm i.d., 5 μm particle size, reversed phase column was used in the studies of analysis of residual TNT concentration and for the initial determination of decomposition products. The mobile phase gradient for TNT analysis consisted of 30:70 ACN:water, isocratic from 0 to 3 minutes followed by a linear gradient from 3 to 13 minutes to 100% ACN and holding for 5 minutes at 100% ACN until 18 minutes, to insure all analytes had eluted. The column was then equilibrated under the initial run conditions 30:70 ACN:water for 5 minutes before performing the next sample injection. Quantitation of TNT was carried out based on absorbance at 230 nm with a 5 point calibration curve, performed daily. Calibration curves had an R^2 value of 0.99 or greater.

Identification of initial reaction products was performed through retention time and spectral matching using an in-house generated spectral library of nitroaromatic compounds utilizing Agilent Chemstation software. The spectral library was constructed by analyzing single component nitroaromatic compounds prepared and analyzed under identical conditions to the TNT analyzed in the study. Identification of initial products was verified by mass spectrometry using an Applied Biosystems 3200 Q Trap LC/MS/MS with direct sample introduction via

syringe pump at 8 μL/min. Samples were diluted in 1:1 methanol:water with 0.1 % formic acid for introduction into the electrospray ionization source of the mass spectrometer.

The production and concentration of nitrate and ammonium ions in the reaction samples were determined by IC using a Dionex DX500 ion chromatograph with a Dionex ED40 electrochemical detector. Nitrate analysis was conducted using a 4 mm i.d. Dionex IonPac AG14 column with a Dionex ASRS 300 suppressor. The mobile phase consisted of 3.5 mM Na_2CO_3 with 1 mM $NaHCO_3$ at a flow rate of 1 mL/min. Ammonium analysis was conducted using a 4 mm i.d. Dionex IonPac CG12A column with a Dionex CSRS 300 suppressor. The mobile phase was 22 mN H_2SO_4 at a flow rate of 1 mL/min. Ion detection was performed in conductivity mode. Quantitation of nitrate and ammonium was performed using a 4 point calibration curve, performed daily. Calibration curves had an R^2 value of 0.99 or greater.

Results and Discussion

The pK_a values of 6βCDidaH_2 and 6βCDedtaH_3 and the stoichiometry of their conjugate bases with Fe^{2+}.

Work by collaborators showed the measured pK_a values of 6βCDidaH_2 and 6βCDedtaH_3 (structures shown in Figure 3.1) to be different than the values for the free chelators, iminodiacetic acid (IDAH_2) (120) and EDTAH_4, (121) respectively. The data are reported in Table 3.1. For 6βCDidaH_2, pK_{a1} was too acidic to be measured by the technique utilized. For 6βCDedtaH_3, pK_{a1} and pK_{a2} were too acidic to be determined. Because 6βCDedtaH_3 has one fewer acidic groups than EDTAH_4, the third p*K*a of 6βCDedtaH_3 is compared to the fourth p*K*a of EDTAH_4. Similarly, the fourth p*K*a of 6βCDedtaH_3 is compared to the fifth p*K*a of EDTAH_4

and the fifth p*K*a of 6βCDedtaH$_3$ is compared to the sixth p*K*a of EDTAH$_4$. All pK_a values measured in this study were determined in aqueous $HClO_4$ 0.01 mol dM^{-3}/$NaClO_4$ 0.09 mol dM^{-3} by potentiometric titration with 0.10 mol dM^{-3} aqueous NaOH at 298.2 K. The p*K*a values for IDA were altered by covalent attachment of the IDA group to the cyclodextrin. Similarly, the p*K*a values for EDTA also change upon covalent attachment to the cyclodextrin. The changes in the pK_a values of the substituted βCDs compared to those of IDAH$_2$ and EDTAH$_4$ were attributable to changes induced in the electronic character of the substituents when bonded to βCDs. Furthermore, changes in hydration because of proximity to the hydroxyl groups of βCD also play a role in controlling the p*K*a values for these groups (122).

Table 3.1. Measured p*K*a values for 6βCDidaH$_2$ and 6βCDedtaH$_3$ and reported p*K*a values for IDAH$_2$ and EDTAH$_4$ (120, 121).

6βCDidaH$_2$	IDAH$_2$	6βCDedtaH$_3$	EDTAH$_4$
pK_{a2} = 4.08 ± 0.09	pK_{a2} = 2.61	pK_{a3} = 2.89 ± 0.08	pK_{a4} = 2.68
pK_{a3} = 8.75 ± 0.09	pK_{a3} = 9.35	pK_{a4} = 4.28 ± 0.05	pK_{a5} = 6.11
		pK_{a5} = 9.48 ± 0.03	pK_{a6} = 10.17

A comparison of formation constants shows the stability of [Fe(6βCDidaH)]$^+$ to be less than that of [Fe(6βCDida)] . The probable causes of the difference are the charge attraction between Fe^{2+} and 6βCDidaH$^-$ being less than that between Fe^{2+} and 6βCDida^{2-} and the decreased denticity of 6βCDidaH$^-$. This reasoning is in accord with the observation that ligand protonation usually decreases the stability of metal complexes (121). The complexation of Fe^{2+} by two 6βCDida^{2-} to give [Fe(6βCDida)$_2$]$^{2-}$ is characterized by log(β/dm^6 mol^{-2}) = 9.29 which is slightly

less than $\log(\beta/dm^6\ mol^{-2}) = 9.81$ for $[Fe(ida)_2]^{2-}$ (120). This result suggests that steric hindrance from the βCD entities in the formation of $[Fe(6\beta CDida)_2]^{2-}$ is small. The pK_a (6.64) of $[Fe(6\beta CDidaH)]^{+}$ is lower than that of $6\beta CDidaH^{-}$ ($pK_a = 8.75$), which is consistent with the positive charge of the $[Fe(6\beta CDidaH)]^{+}$ enhancing deprotonation. The formation of $[Fe(6\beta CDida)(OH)]^{-}$ and $[Fe(6\beta CDida)(OH)_2]^{2-}$ arising from water ligand deprotonations are characterized by increasing pK_as as the overall negative charge of the conjugate base increases.

The speciation of the Fe^{2+}-$6\beta CDida^{2-}$ system with respect to pH is shown in Figure 3.1. At pH <2 virtually all of the Fe^{2+} is in the fully hydrated state, $[Fe(OH_2)_6]^{2+}$. As pH increases and $6\beta CDidaH_2$ deprotonates, $[Fe(6\beta CDidaH)]^{-}$, $[Fe(6\beta CDida)]$ and $[Fe(6\beta CDida)_2]^{2-}$ form with subsequent formation of $[Fe(6\beta CDida)(OH)]^{-}$ and $[Fe(6\beta CDida)(OH)_2]^{2-}$ as one and two water ligands deprotonate, respectively as pH increases further.

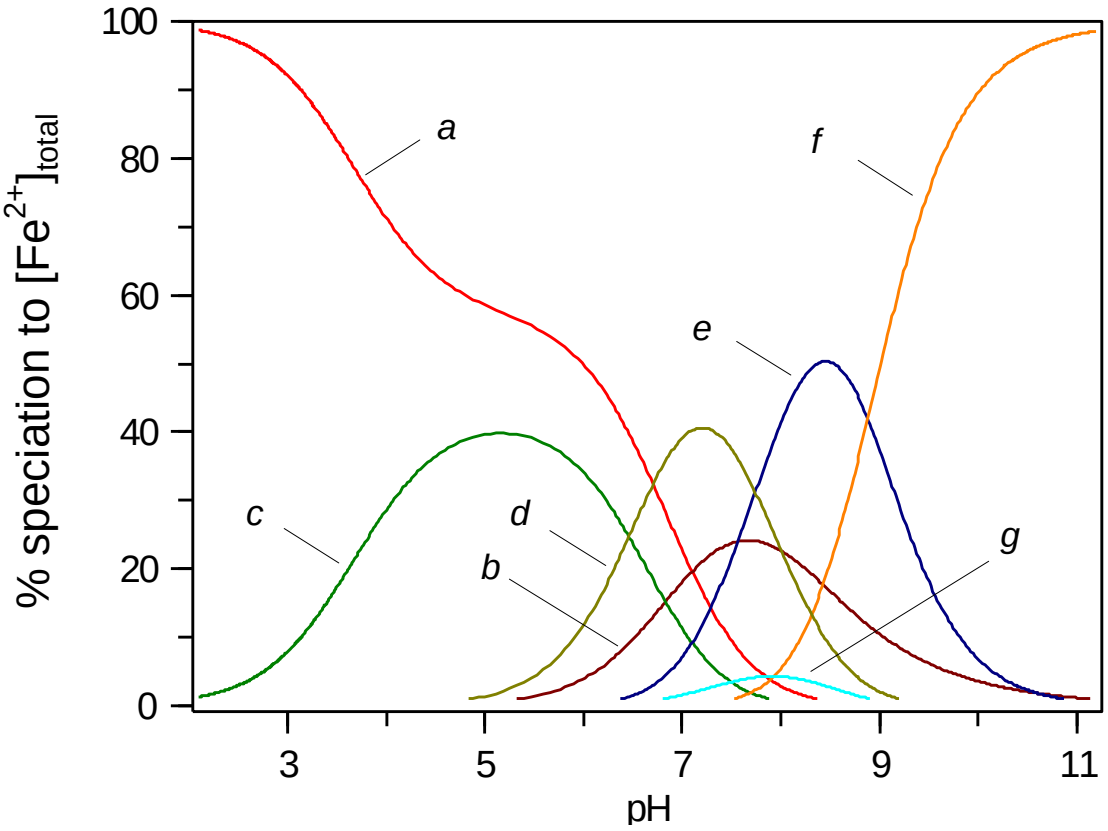

Figure 3.2. Speciation of 1:1 Fe^{2+}/6βCDida^{2-} complexes. Curve a = free Fe^{2+}, curve b = $Fe(OH)^{+}$, curve c = $[Fe(6\beta CDidaH)]^{+}$, curve d = [Fe(6βCDida)], curve e = $[Fe(6\beta CDida)(OH)]^{-}$, curve f = $[Fe(6\beta CDida)(OH)_2]^{2-}$ and curve g = $[Fe(6\beta CDida)_2]^{2-}$ for the complexation of the Fe^{2+}:6βCDida^{2-} systems at 298.2 K.

Fenton Degradation of TNT in the Presence of CDs

Fenton mediated degradation of TNT was examined in the presence of the four CDs, D-glucose, and EDTA. Control reactions were conducted in nanopure water, utilizing identical conditions of pH, Fe concentration and H_2O_2 addition rates. Reaction conditions were as previously stated in the experimental section and TNT loss was monitored by HPLC with UV absorbance detection at 230 nm.

The stability of TNT in the presence of Fe^{2+} and Fe^{3+}, H_2O_2 and several of the cyclodextrins used in the study was examined by preparing solutions of TNT and each of the

individual components to yield two component solutions. The concentrations of the components in the solutions were identical to those used in Fenton degradation studies. The stability of the TNT was determined by examining any decreases in TNT concentration after 72 hours of storage in the dark at room temperature. The TNT concentrations remained stable for all binary mixtures examined, indicating that Fe catalyzed reduction of TNT does not occur under these conditions. Degradation of TNT was observed only when both iron and peroxide were present in the system.

The Fenton reactions in this study were performed with the continuous addition of peroxide to generate a steady state concentration of hydroxyl radicals in solution (21, 123). Under these conditions plots of ln[TNT] vs. time yielded good linear regressions for the majority of the reaction systems studied, therefore a pseudo first-order kinetic model was deemed appropriate to apply to results (124). R-squared values for the linear regression of the TNT degradation rates ranged from 0.957 (pH 3.1 water, no CDs) to greater than 0.999 (pH 3.1 in presence of 6βCDidaH$_2$). βCD and cmβCD showed some deviation for linearity for plots of ln[TNT] vs. time but linear regressions were calculated for comparative purposes.

Table 3.2 reports the measured pseudo first-order rate constants (*k*') for TNT degradation for the reaction systems examined. At both pH 3.1 and 7.0, the relative rates of TNT degradation in the presence of cyclodextrins were found to follow the general trend of βCD > cmβCD > 6βCDidaH$_2$ ≈ 6βCDedtaH$_3$ > water control. The most substantial enhancement was for βCD at pH 3.1 which showed a seven fold increase in the observed first-order degradation rate of TNT. Both cmβCD and βCD demonstrated similar behavior, though cmβCD demonstrated a 20-45% smaller enhancement in TNT degradation rate depending on the pH. This smaller enhancement is likely due to differences in the TNT-cmβCD complex formation constants compared to TNT-βCD complexes, differences in the rates of cmβCD radical formation and/or reactivity of the

cmβCD radical towards TNT , or differences in Fe^{2+} activity (cmβCD weakly binds Fe^{2+}) (116). Despite the smaller enhancement, cmβCD also shows an increase in the TNT degradation rate throughout the time course of the experiment (Figure 3.3). The plots of ln[TNT] vs. time for both βCD and cmβCD indicate that the TNT degradation rate accelerates throughout the time course of the monitored reaction times (Figure 3.3). This acceleration is likely due to a secondary reaction process being initiated and is observed at both pH values studied. A more detailed discussion of this acceleration in TNT degradation rates is given later in this chapter.

Table 3.2. Measured pseudo first order rate constants for TNT degradation (100 μM starting concentration) during Fenton reactions in the presence of cyclodextrins, D-glucose, and EDTA. Relative rate constants (k/k_o) were obtained by normalizing to the rate constant observed for reaction in water with no additives (k_o).

	pH = 3.1		pH = 7.0	
	Measured *k*' (min^{-1})[a]	Enhancement over pure water (k/k_o)	Measured *k*' (min^{-1})[a]	Enhancement over pure water (k/k_o)
Pure Water	0.11 ± 0.01	-	0.12 ± 0.01	-
6βCDida^{2-} (1 mM)	0.229 ± 0.002	2.0 ± 0.2	0.170 ± 0.005	1.4 ± 0.1
6βCDedta^{3-} (1 mM)	0.164 ± 0.006	1.4 ± 0.2	ND	-
cmβCD (1 mM)	0.43 ± 0.03	3.8 ± 0.5	0.49 ± 0.05	4.1 ± 0.6
βCD (1 mM)	0.8 ± 0.2	7.0 ± 2.0	0.61 ± 0.09	5.1 ± 0.9
D-glucose (1 mM)	ND[b]	-	0.062 ± 0.004	0.51 ± 0.06
D-glucose (7 mM)	ND	-	0.155 ± 0.003	1.3 ± 0.1
EDTA (1 mM)	ND	-	0.033 ± 0.004	0.27 ± 0.04

[a] ± Standard Error
[b]Not determined

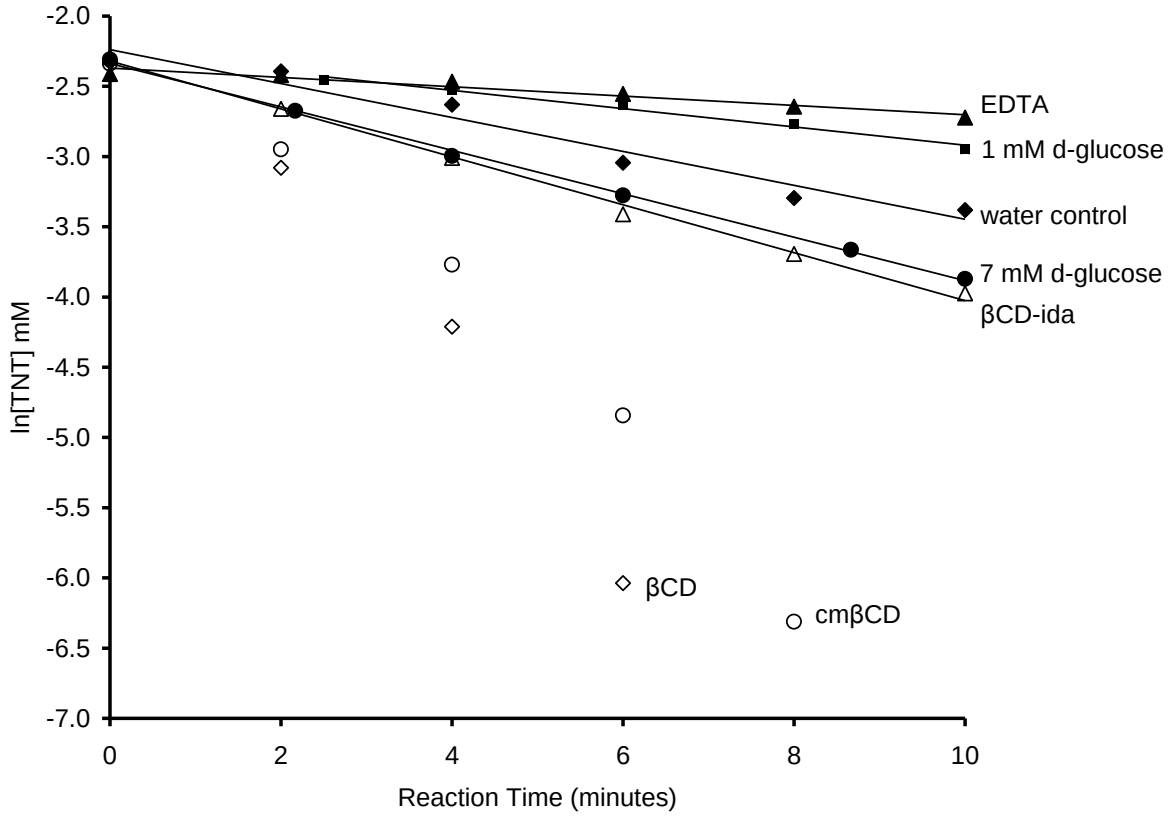

Figure 3.3. Plots of ln[TNT] vs. reaction time at pH 7.0 for reaction systems studied. Concentrations of EDTA and CDs are 1 mM, glucose concentrations are 1 or 7 mM. Similar trends are observed at pH 3.1.

Two of the cyclodextrins used in this study, 6βCDidaH_2 and 6βCDedtaH_3, were derivatized with a single metal chelating group attached to the narrow end of the cyclodextrin. A space filling model of 6βCDidaH_2 shows this and is given in Figure 3.4. Because these compounds bind Fe^{2+} strongly (see Figure 3.2), it was expected that they would yield increased TNT degradation rates caused by proximity of the Fe^{2+} to the TNT in ternary Fe^{2+}-cyclodextrin-TNT complexes. While Fenton reactions in the presence of these cyclodextrins did result in enhanced TNT degradation, the observed enhancements were smaller than those for βCD and cmβCD (see Table 3.2). The smaller enhancement of TNT degradation rates for the chelating

CDs relative to the non-chelating CDs was further probed by examining the impact of EDTA on the reaction.

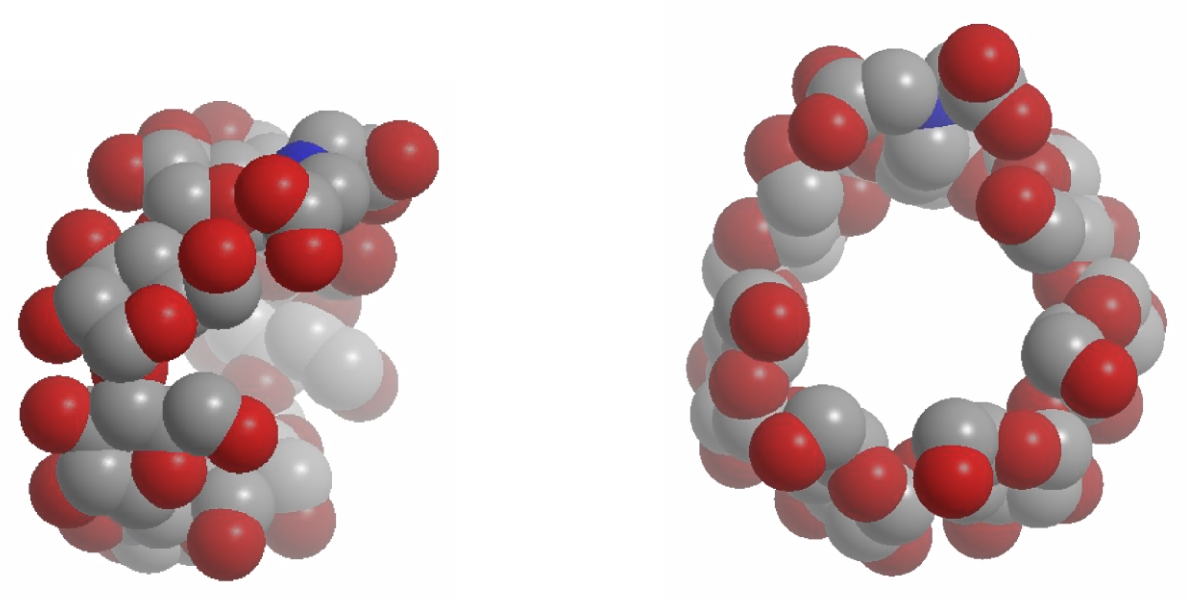

Figure 3.4. Space-filling model of 6βCDidaH$_2$. The nitrogen of the iminodiacetic acid group is shown in blue, carbon in grey and oxygen in red, hydrogen is not shown.

Degradation of TNT with 1 mM EDTA present resulted in a four-fold decrease in the observed TNT degradation rate constant (Table 3.2). This decrease was most likely caused by two factors: 1) competitive reactions where EDTA scavenges the hydroxyl radical and 2) changes in iron activity due to differing Fe^{2+}/Fe^{3+} binding constants with EDTA (125). For 6βCDidaH$_2$ and 6βCDedtaH$_3$, like EDTA, the effects of Fe^{2+} ligation would decrease iron activity which results in a decreased rate of hydroxyl radical production as well as providing a mechanism for competitive reactions which would scavenge hydroxyl radicals. The decreased hydroxyl radical production and scavenging effects readily explain the decreased TNT degradation rates observed for these cyclodextrins compared to βCD and cmβCD. However, despite these factors, an increase in the TNT degradation rates in the presence of 6βCDidaH$_2$ and 6βCDedtaH$_3$ is observed relative to the water controls by a factor of 1.4-2.0 and a 6 fold increase

in the rate for 6βCDidaH$_2$ relative to EDTA at pH 7.0 is observed. These results are a clear indication that complexation of TNT with the CD plays a role in accelerating the TNT degradation rates.

Another difference observed between the βCD and cmβCD reactions and the 6βCDidaH$_2$ and 6βCDedtaH$_3$ reactions is that reactions conducted with the former 2 CDs exhibit an increase in observed rate constants during the time frame of the study while the latter 2 CDs do not (Figure 3.3). This indicates that secondary radical mechanisms play more of a role in the reactions conducted with βCD and cmβCD compared to 6βCDidaH$_2$ and 6βCDedtaH$_3$. This type of behavior is typical of a lag phase occurring in which the secondary radicals of βCD and cmβCD have little impact on the reaction rates initially, but become more important in increasing TNT degradation rates as they increase in concentration. This type of lag phase and propagation is commonly observed in lipid peroxidation where the presence of secondary radicals occurring later in the reaction impact oxidation rates (126).

To examine the effect of other saccharides on the Fenton degradation of TNT, D-glucose was added at two different concentrations in the reactions in place of the CDs. When added at 1 mM, D-glucose resulted in a substantial decrease in the TNT degradation rate with a rate constant of about half that of pure water. This decrease in TNT degradation rate is most likely due to scavenging of hydroxyl radical by the glucose, thereby decreasing the hydroxyl radical concentration available to react with TNT. When D-glucose was added at 7 mM, a slight increase in TNT degradation rate was observed compared to reaction in pure water (k' increased 1.3-fold). Compared to 7 mM D-glucose, 1 mM βCD exhibited a much greater enhancement of TNT degradation (note the total number of moles of glucose units are equivalent since βCD is a 7-unit oligomer of D-glucose). This difference in extent of enhancement can be explained by

complexation of TNT with the CD. Such complexes would yield an environment where TNT would readily react with cyclodextrin radicals due to the proximity of the two species due to pre-association. For D-glucose, no pre-established TNT-glucose interaction exists, so D-glucose radicals would only react with TNT upon collision. Additionally, secondary radicals formed inside the CD cavity may be protected from further reactions until a reducible species enters the CD cavity. Since TNT is more likely associate with CDs than glucose, the inclusion of TNT after CD radical formation would increase the kinetics of TNT reduction relative to the glucose systems.

Previous studies using CD complexes in Fenton reactions have focused on acidified reaction systems since the optimal pH range for the Fenton reaction falls in the range of 3.0 to 3.5 to prevent oxidation of Fe^{2+} and precipitation as Fe^{3+} hydroxides (21, 24). In this study, the short time frame used for the Fenton reactions moderated Fe^{2+} loss and allowed reaction at pH 7. Additionally, both 6βCDidaH2 and 6βCDedtaH_3 strongly complex Fe^{2+} at neutral pH. A comparison of TNT degradation rates for Fenton reactions conducted in pH 3.1 or pH 7.0 water, with no cyclodextrins present, showed no significant difference in pseudo first-order rate constants. However, with the longer reaction times expected for in situ applications, near neutral pH values are not effective without Fe^{2+} chelation. Since the derivatized cyclodextrins are effective Fe^{2+} chelators at near neutral pH, they may eliminate the need for pH adjustment during in-situ applications.

Mechanism of Increased TNT Degradation Rates in the Presence of CDs

The increase in TNT degradation rates during the Fenton reaction in the presence of cyclodextrins is most likely due to a combination of several different factors. Firstly, increased

localized hydroxyl radical concentration near the ternary TNT/CD/Fe^{2+} complexes could lead to promotion of the oxidative mechanisms leading to degradation (21). Secondly, the generation of CD free radicals has been shown to readily occur through hydrogen abstraction in the presence of hydroxyl radicals (127), and the CD radicals formed would be efficient reducing agents. Hydroxyl radical reactions with CDs are rapid, $k = 4.2 \times 10^9$(L mol^{-1} s^{-1}) at pH ~7 for βCD (128), and demonstrate selectivity in the site of hydrogen abstraction, targeting protons on the C4, C5 and C6 carbons (129). NMR investigations of complexed molecules in the CD annuli have shown a strong interaction with the protons on the C3 and C5 carbons, since these protons reside on the interior of the annuli (Figure 3.5) (114). Selectivity in the site of hydrogen abstraction would be expected to produce an efficient reductive mechanism for molecules complexed in the annuli of the CD due to the proximity to the site of hydrogen abstraction on the C5 carbon of the CD radical species.

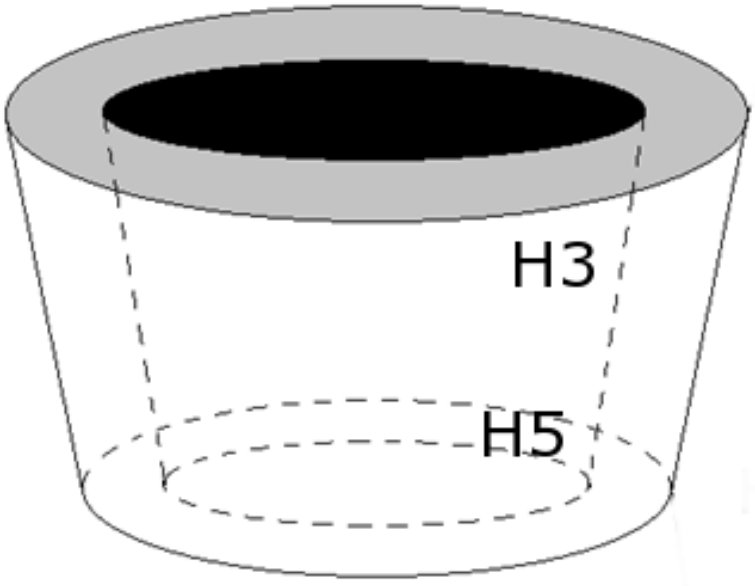

Figure 3.5. Location of the protons on the C3 carbon (H3) and the C5 carbon (H5) in the CD torus.

The Fenton reaction of TNT has been shown to yield TNB as a major initial oxidative product (130) and aminodinitrotoluenes have been shown to be the major products of TNT reduction in a variety of systems (65, 77, 83). These two compounds are the initial indicators of the presence of an oxidative or reductive pathway, respectively, and as such their presence in the reaction medium can be used as indicator of the mechanisms occurring. In the reaction systems in this study, the presence and concentration of TNB and aminodinitrotoluenes were determined initially by comparison with HPLC retention times and UV absorbance spectra of reference compounds. A spectral library of the reference compounds was constructed using Hewlett-Packard Chemstation Software and reference compounds were injected as single components and the retention time and absorbance spectra from 200-400 nm were stored in the library. Reactions were conducted for 10 minutes, with sampling and quenching of the reaction every two minutes.

For the HPLC analysis of the TNT Fenton reaction in nanopure water at pH 3.1 and pH 7.0 without CDs present, a number of minor transient UV-active products were observed to form during the time course of the reaction (Figure 3.6). However, the only major chromatographic peak observed for reaction in pure water that gave a spectral and retention time search match was identified as TNB at a 6.7 minute retention time (r.t.) and was confirmed by negative mode ESI-MS/MS analysis. Figure 3.7, top, shows the spectral match for TNB. The large peak which begins to form at a 1 minute retention time throughout the reaction is excess hydrogen peroxide in solution. Other early eluting peaks were not identified. All of the CD and d-glucose reaction systems examined showed the presence of TNB during the early stages of the Fenton reaction, with concentrations reaching a maximum by 2 minutes then decreasing throughout the time

course of the reaction. However, concentrations of TNB in the CD and d-glucose reactions were significantly lower than in reactions without CDs or d-glucose present.

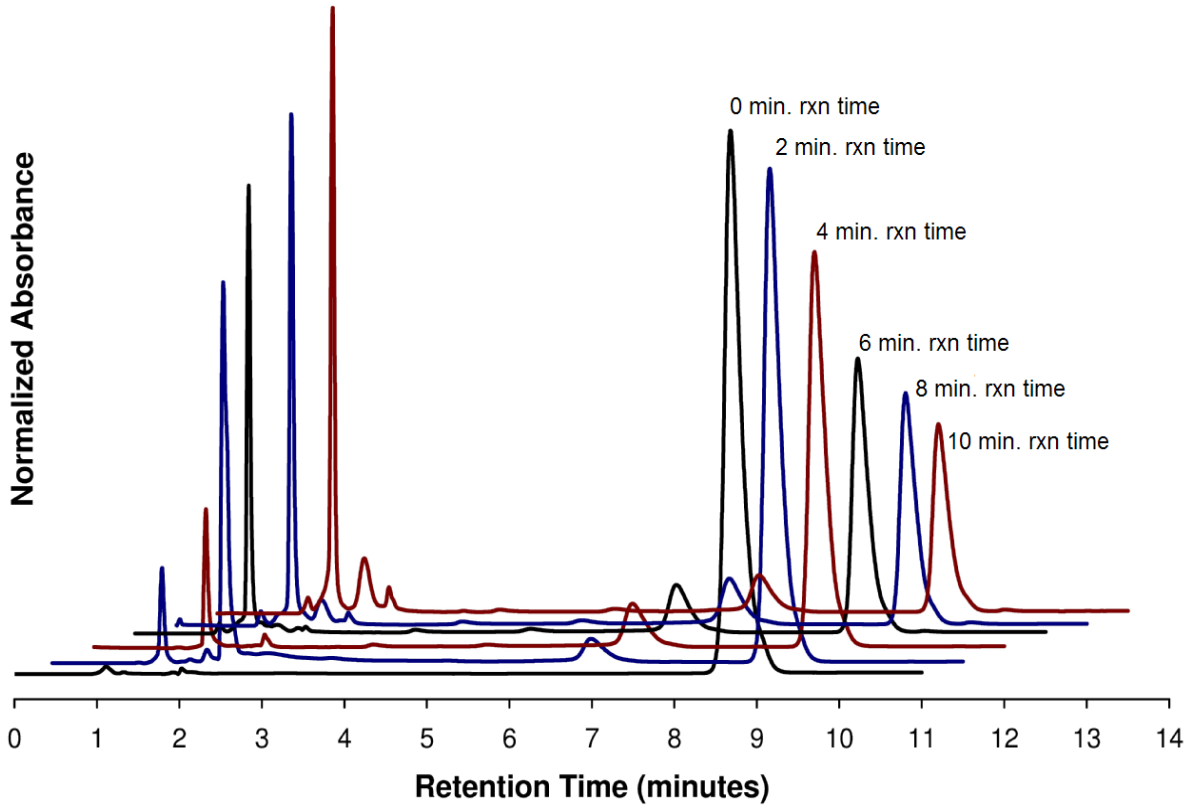

Figure 3.6. Overlay of chromatograms from 0 to 10 minute reaction times for nanopure water control, without dextrins present. TNT elutes at 8.6 minutes. The product eluting at 6.7 minutes was determined to be TNB.

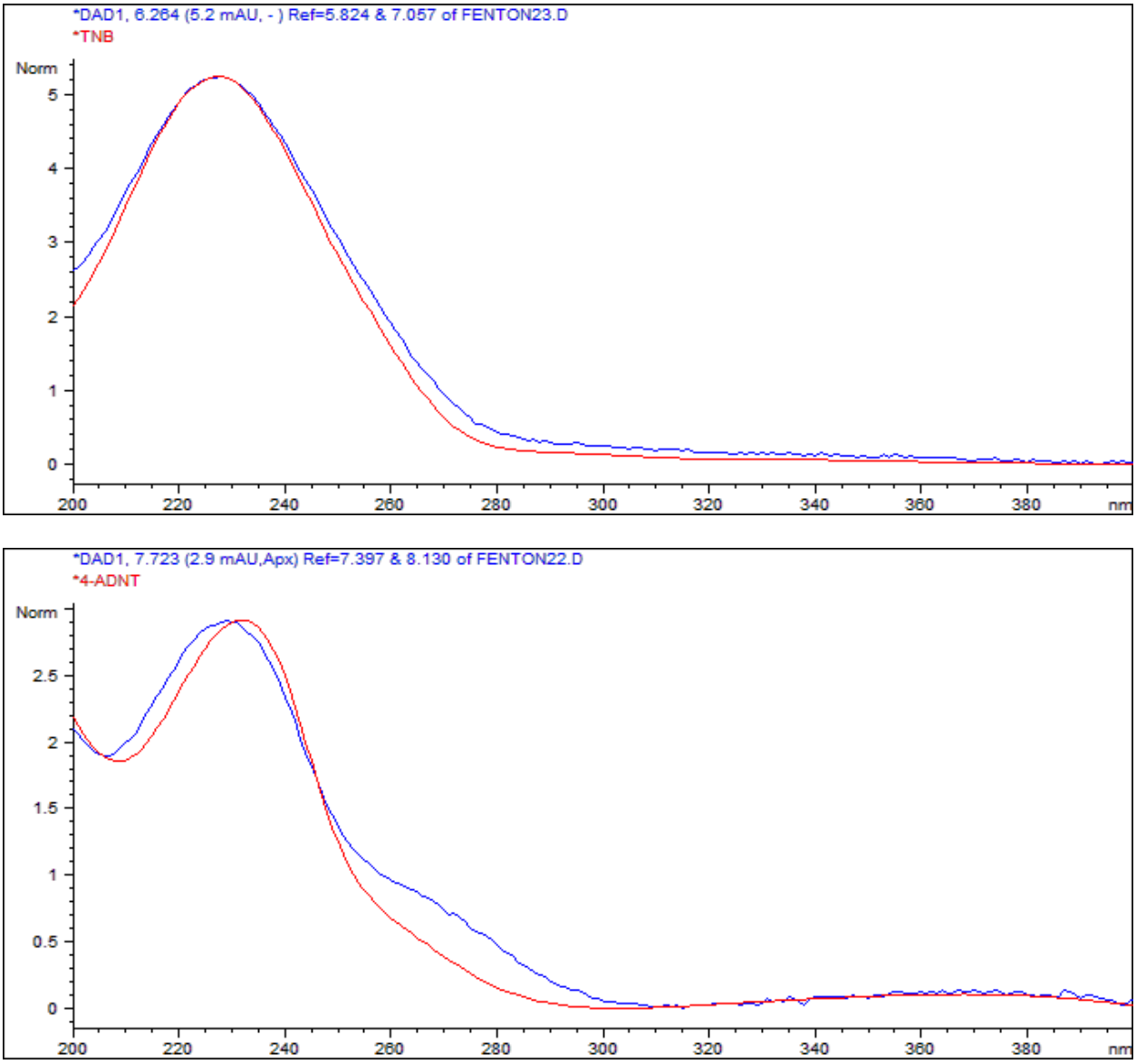

Figure 3.7. Representative r.t. and spectral search matches for TNB (top) and 4-ADNT (bottom).

Reactions conducted in the presence of CDs or d-glucose showed an additional major UV active product in the chromatograms a retention time of 7.6 minutes which was not observed in the reactions without dextrins present (Figure 3.8). The product was tentatively identified as 4-ADNT by retention time and UV spectral matching and confirmation was performed by positive

mode ESI-MS/MS analysis. Similar results were seen in the chromatograms of the other CDs examined, as well as D-glucose reactions.

Figure 3.9 a and b show a comparison of the relative concentrations of TNB and ADNT to the initial concentration of TNT in the reactions, calculated based on the response factor of TNT and 4-ADNT relative to TNT. For the data shown in Figure 3.9 b, 4-ADNT wasn't observed in the control reaction with without CDs or glucose present. For all of the CD reactions monitored, the maximum 4-ADNT concentration relative to the initial TNT concentration fell in the range of 1.25-2%. Reactions containing 7 mM d-glucose produced over twice the 4-ADNT concentration observed for CDs, at slightly over 4% despite having the slowest overall TNT degradation rate of any of the dextrin containing reactions. The data shown in figure 3.9 give a strong indication that the reductive pathway plays an important role in the Fenton degradation of TNT. The relative increase in 4-ADNT for d-glucose compared to CD containing shows that this pathway is particularly important for d-glucose containing systems. The increased relative concentration of 4-ADNT observed may be due to a combination of effects including an increase in the kinetics of the reductive pathway relative to the oxidative pathway pathway and an overall lower reaction rate which would degrade the 4-ADNT formed in the initial reaction more slowly than reactions containing CDs.

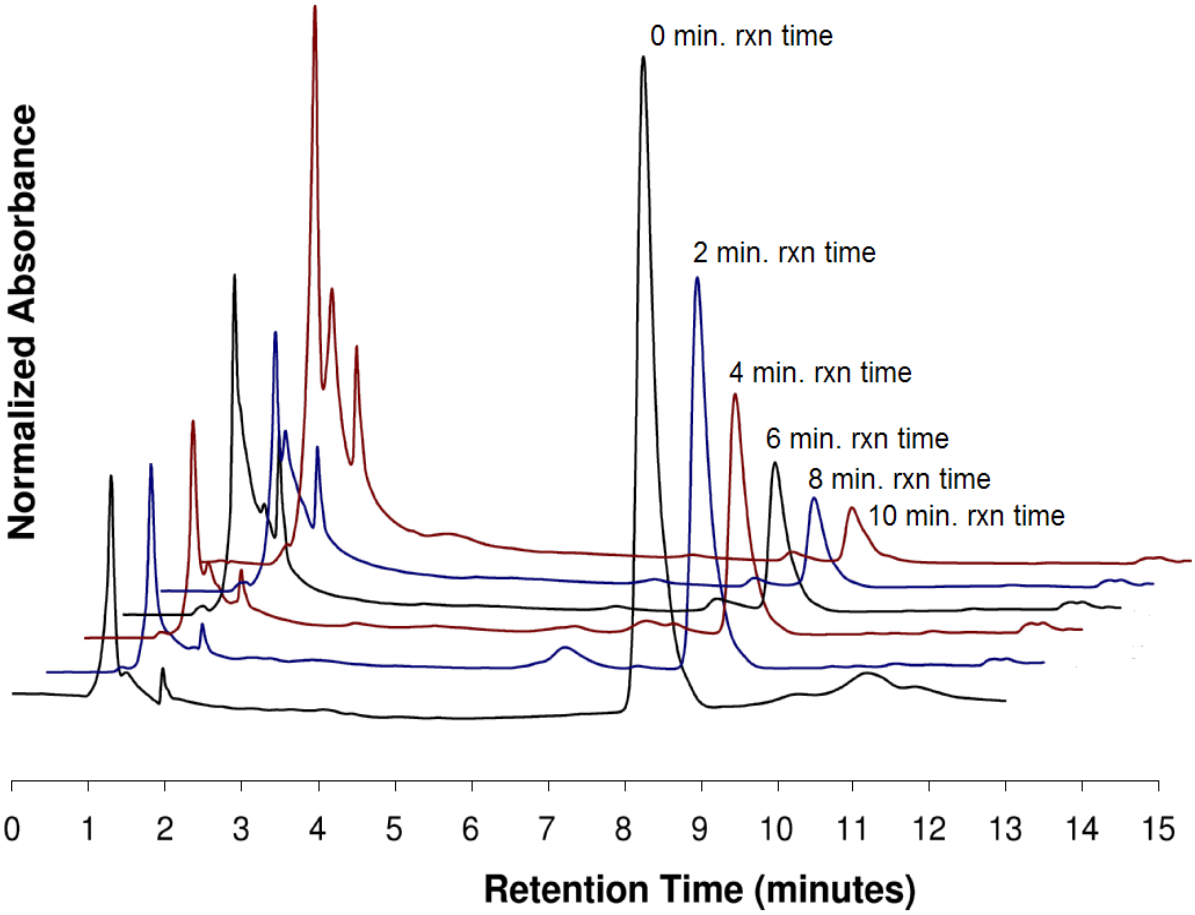

Figure 3.8. Overlay of chromatograms from 0 to 10 minute reaction times for reaction containing 1 mM 6βCDidaH_2. TNT elutes at 8.6 minutes. The product eluting at 6.7 minutes was determined to be TNB and the product eluting at 7.6 minutes is 4-ADNT.

A

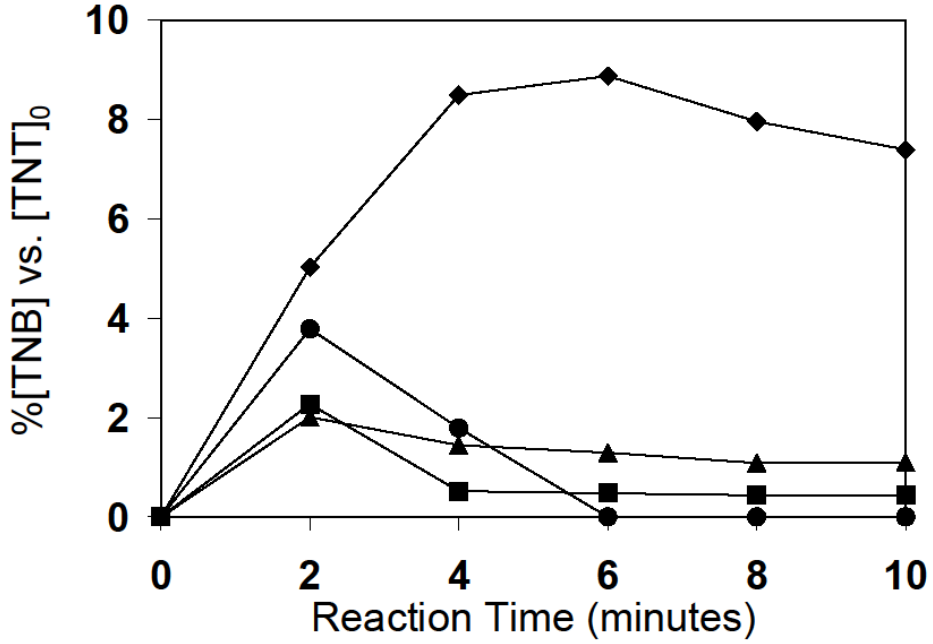

B

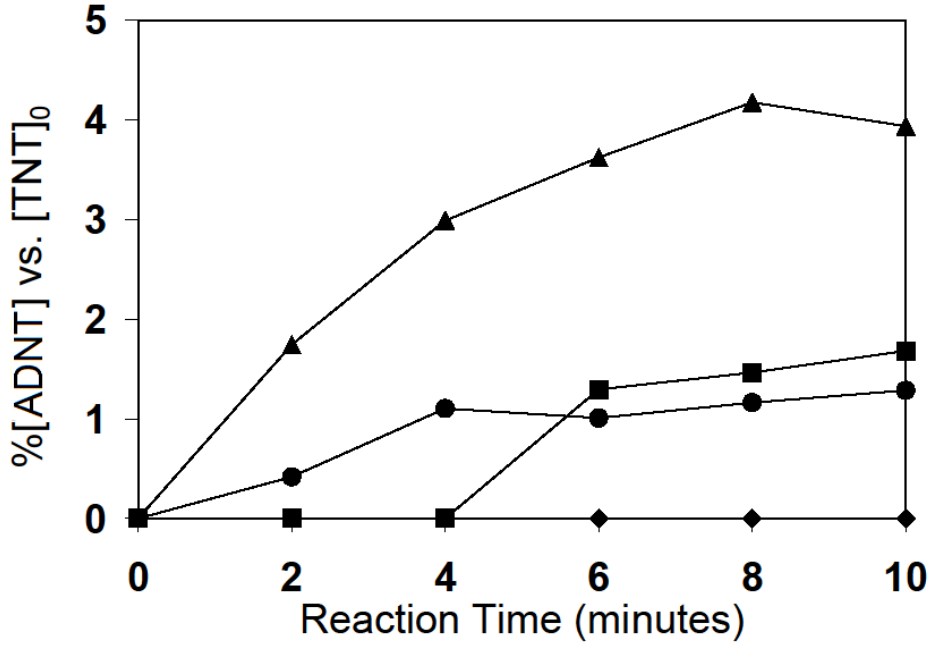

Figure 3.9. Percent concentration of TNB, (**A**), and ADNT, (**B**), relative to starting concentration of TNT in Fenton reactions conducted in the presence of 1 mM βCD (-●-), 1 mM 6βCDidaH$_2$ (-■-), 7 mM d-glucose (-▲-), water without dextrins present (-♦-).

The CD assisted Fenton reactions showed an initial build-up of TNB by 2 minutes, which then began to steadily decrease in concentration throughout the remaining time course of the reaction (Figure 3.9). For both βCD and cmβCD, the production of 4-ADNT was observed by the 2 minute time point in the reaction while βCDida and βCDedta reactions didn't show evidence of 4-ADNT production until 4 minutes. Reactions conducted with d-glucose present showed TNB and 4-ADNT being produced in nearly equal quantities at 2 minutes. After 2 minutes the TNB began to fall in concentration while 4-ADNT continued to increase in concentration until 8 minutes into the reaction.

The difference in the times in which 4-ADNT is observed in the CD assisted Fenton reactions is likely due to the increased TNT reaction rates in the presence of βCD and cmβCD relative to βCDida and βCDedta. For βCD and cmβCD reaction systems, the concentration of free Fe^{2+} in solution is higher than in the systems with the chelating CDs. This would lead to a higher initial ·OH concentration in solution. As discussed earlier in this chapter, fitting the TNT reaction rates to a pseudo-first order kinetic model showed the reaction rates for βCD and cmβCD assisted reactions to be 4-7 times faster than the control reactions, depending on pH. The βCDida and βCDedta assisted reactions were 1.5-2 times faster than controls and also showed some pH dependence. The addition of 1 mM d-glucose to the TNT Fenton reactions gave a 4-fold decrease in observed reaction rates while the 7 mM d-glucose showed a slight, though statistically significant, increase in observed rates.

While the Fenton reaction is typically considered as an oxidative process, the coexistence of both an oxidative and a reductive pathway has been demonstrated in several different studies (16, 17). In the current study, the formation of 4-ADNT in the CD and d-glucose Fenton reaction systems clearly indicates the presence of a reductive pathway. The addition of a

reductive pathway has been proposed for systems where observed rates in Fenton reactions have occurred above the expected ·OH mediated reaction rate. The increased rates have been credited to the formation of superoxide radical, $\cdot O_2^-$, and hydroperoxide anions, HO_2^-, which are both strong reducing agents capable of reacting at near diffusion controlled rates (16, 17). The formation of these reducing agents can occur when high concentrations of H_2O_2 (>0.3 M) are used according to the following steps (16):

$$H_2O_2 + \cdot OH \rightarrow \cdot O_2H + H_2O$$

$$\cdot O_2H \leftrightarrow H^+ + \cdot O_2^- \qquad pK_a = 4.8$$

$$\cdot O_2H + \cdot O_2^- \rightarrow HO_2^- + O_2$$

However, the H_2O_2 concentrations used in the current study would not be expected to produce significant amounts of these reducing agents at either of the pH values used for the Fenton reactions.

IC analysis of the reactions showed major differences between reactions run without CDs present and the CD reaction systems. In reactions without CDs present, 22.9 ± 0.8% of available nitro groups on TNT had been oxidized to nitrate by the termination of the reaction at 10 minutes. However, complete mineralization of TNT was not observed at this time point as indicated by the lack of short chain carboxylic acids in solution which would be expected from ring opening. In contrast, none of the CD reaction systems contained free nitrate at reaction termination but did have significant amounts of formate present. The βCD reaction system showed the presence of low concentrations of ammonium (10.0 ± 1.2 μM) at reaction termination. The presence of ammonium in the other CD reactions systems could not be confirmed due to chromatographic interferences. The presence of short chain carboxylic acids was also observed in reactions of βCD without TNT present. The low concentration of

ammonium coupled with the lack of free nitrate in the βCD/TNT reaction systems indicates that formate is occurring from oxidation of the CD, and not from mineralization of TNT.

Summary

The results of the kinetic and initial mechanistic studies demonstrate that the CD assisted reactions examined exhibit a significant enhancement of TNT reaction rates relative to controls without CDs. The existence of both an oxidative and reductive pathway is indicated by the presence of TNB and 4-ADNT in the CD and d-glucose containing reactions. Elucidation of a reductive pathway in CD assisted Fenton reactions of TNT have not been previously described in the literature. The presence of a reductive pathway indicates that increased reaction rates cannot be explained solely by increases in oxidative rates occurring from ternary complex formation. Pre-association of TNT with the secondary CD radicals formed during the Fenton reaction clearly play a role in the increased degradation rates of TNT relative to control reactions. This is evidenced by the higher TNT degradation rates observed in the presence of CDs, compared to d-glucose, which is likely due to pre-association of TNT with the secondary CD radicals formed during the Fenton reaction. However, the contribution to changes in the TNT degradation rates occurring from alteration in oxidative rates due to complexation of $Fe^{2+/3+}$ and TNT, reduction of TNT, and scavenging of hydroxyl radicals by CDs and secondary reaction products makes evaluation of the impact of any individual mechanism extremely difficult.

CHAPTER 4

ANALYSIS OF TNT DEGRADATION PRODUCTS IN CYCLODEXTRIN ASSISTED FENTON REACTIONS BY HPLC-UV/VIS, ESI-MS/MS AND FTICR-MS

Introduction

Nitroaromatic explosives, such as trinitrotoluene (TNT), are of particular environmental concern due to their recalcitrance in soils and their toxicity and mutagenicity to both aquatic and mammalian species (53, 59). TNT was the most widely used military explosive through the era encompassing both the First and Second World Wars and is still a major component of military explosives and munitions. As a result, contamination of soils by TNT around weapons manufacturing, testing, and disposal facilities continues to pose environmental problems (77). Current methods for remediation of TNT contaminated soils and waters consist of incineration (81), bioremediation with denitrifying bacteria (65, 75, 82), abiotic reduction processes utilizing zero-valent Fe (83, 131), Fe(II)/goethite and other Fe containing systems (22, 132), and Fenton chemistry (20, 25, 43, 111).

Numerous studies have examined reductive processes for the remediation of TNT in soils, aquatic systems and in industrial waste streams. Biotic processes in soils and aquatic systems have been shown to readily degrade TNT through reduction of the nitro groups to amines through a 6 electron process, with nitroso and hydroxylamine intermediates, as discussed in chapter 2 (Figure 2.2) (65, 75, 82). Abiotic processes utilizing zero-valent Fe, Fe(II)/goethite and Fe(II) complexes have also been examined and result in the conversion of nitro groups to amines (83, 131, 132). The amine products, while less toxic than TNT, have greater water solubility and enhanced transport mechanisms in aquatic environments (59, 78). In soil

environments with high organic content, amine products can irreversibly bind to soil humic material through condensation reactions with quinone and carboxyl moieties that are present (86). Despite the capability of these methods to efficiently reduce TNT, complete mineralization is typically not achieved and the remaining byproducts have the potential for adverse environmental effects.

Advanced oxidative processes (AOPs), such as Fenton chemistry (Fe^{2+} catalyzed generation of •OH from H_2O_2), have shown the ability to completely mineralize a wide range of environmental pollutants (133). A number of studies have examined the use of Fenton and photo-Fenton chemistry to degrade TNT in soils, soil slurries and aqueous systems. The studies demonstrated that complete destruction of TNT can be achieved and high degrees of mineralization are possible under certain conditions (25, 43, 60). However, Fenton chemistry suffers from non-specificity of the oxidant and the need for acidic conditions to prevent loss of iron as iron hydroxides (133).

Past studies by our research group and others have demonstrated the ability of cyclodextrins (CDs) to increase the efficiency of Fenton degradation of small aromatic pollutant species (20, 21). Increased degradation rates observed in the CD Fenton reaction systems are likely due to one or more of the following mechanisms: 1) the formation of a pollutant/CD/Fe^{2+} ternary complexes (20, 115); 2) the formation of secondary radicals that effectively attack the pollutant; 3) an increase in the effective solubility of hydrophobic pollutants in the presence of the cyclodextrin. However, despite evidence that CDs accelerate Fenton reaction systems for some pollutants, no systematic studies of products or degradation pathways have been conducted.

The oxidation products of TNT in a Fenton reaction system have been studied and described by Hess and coworkers (130). The initial oxidative pathway they proposed consisted of either direct oxidation of TNT to trinitrobenzene (TNB) followed by subsequent conversion to a TNB-hydroperoxyl radical intermediate or conversion of TNT to TNT-hydroperoxyl radical intermediate. The proposed TNB-hydroperoxyl and TNT-hydroperoxyl radical intermediates then undergo denitration to form 3,5-dinitrophenol (3,5-DNP) or 4,6-dinitro-*o*-cresol (4,6-DNC) and 3,5-dinitrophenyl-methylene-1-one (3,5-DNPMO), respectively. Following these steps, a series of successive denitrations leads to 1,3,5-trihydroxybenzene and eventual mineralization. In the case of CD assisted Fenton reactions, the addition of CDs to the reaction mixture is expected to alter the reaction pathways and may yield different products and relative concentrations of these products during the course of the Fenton reaction. In order to assess the viability of CD assisted Fenton reactions for the remediation of TNT, a thorough knowledge of these degradation products is required to understand their potential environmental impact.

In this study we have examined the products of CD assisted Fenton reactions of TNT using high performance liquid chromatography with UV-Vis detection (HPLC-UV/Vis), electrospray tandem mass spectrometry (ESI-MS/MS) and Fourier transform ion cyclotron resonance mass spectrometry (FTICR-MS). The CDs used in the study include two commercially available CDs, β-cyclodextrin (βCD) and carboxymethyl-β-cyclodextrin (cmβCD), and two synthetic CDs containing a metal chelating group, 6^A-[bis(carboxymethyl)amino]-6^A-β-cyclodextrin (βCDida) and 6^A-[tri(carboxymethyl)(2-aminoethyl)amino]-6^A-deoxy-β-cyclodextrin (βCDedta) (will be in a figure in prior chapter) (114). The observed products are described and proposed pathways are given.

Experimental Section

TNT (98%, min 30% H_2O), TNB (99%, min 30% H_2O), nitrobenzene (NB, 99.5%, neat), and 2,4,6-trinitrobenzoic acid (TNBA, 99%, min 30% H_2O) were obtained from Chem Service. 2,6-dinitrotoluene (2,6-DNT, 97%, min 30% H_2O), 2,4-dinitrotoluene (2,4-DNT, 97%, min 30% H_2O), and 1,3-dinitrobenzene (1,3-DNB, 98%, min 30% H_2O) were obtained from Alfa Aesar. 2- and 3-nitrotoluene (3-NT, 99%, neat) and 4-nitrotoluene (4-NT, 99%, min 30% H_2O) were obtained from TCI. Picric acid (1.2% w/v aqueous solution) was obtained from Ricca. 2-amino-4,6-dinitrotoluene (2-ADNT) and 4-amino-2,6-dinitrotoluene (4-ADNT) (analytical standard in 1:1 methanol:acetonitrile) were obtained from Accustandard. $FeSO_4 \cdot 7H_2O$ (A.C.S. grade) was obtained from Fisher Scientific. D-glucose (A.C.S. grade) was obtained from Aldrich. Acetonitrile (ACN, HPLC grade) was obtained from EMD. Solutions and reactions were prepared using deionized water (18.2 mΩ) from a Barnstead Nanopure UV system. βCD and cmβCD were donated by Cerestar, and βCDida and βCDedta were synthesized as previously reported (114).

Fenton reactions of TNT were conducted by preparing 10 mL aqueous solutions of 0.1 mM TNT, 1 mM CD, and 5 mM $FeSO_4 \cdot 7H_2O$, pH adjusted by addition of H_2SO_4 for reactions run under acidic conditions. Control experiments were conducted without CD present. Reaction solutions were added to a round bottom flask with continuous magnetic stirring. Addition of H_2O_2 was accomplished via syringe pump using a 150 mM aqueous solution added at a flow rate of 2 mL/h for all reactions. Sampling was accomplished by removing a 300 µL aliquot of the reaction mixture and adding it to a sample vial containing 300 µL of 1% v:v 1-propanol in water (HPLC studies) or 300 µL of methanol (ESI-MS/MS and FTICR-MS studies) to quench the Fenton reaction through hydroxyl radical scavenging by the alcohol. Aliquots were removed at 2

minute intervals for a total of 10 minutes for each reaction. Samples were centrifuged and filtered through 0.22 μm PTFE syringe filters to remove precipitated iron hydroxides prior to analysis.

The concentration of TNT in the reaction mixtures was measured by HPLC on an Agilent 1100 HPLC with a diode array absorbance detector. An Alltech Econosphere C18, 150 x 4.6 mm i.d., (5 μm particle size) reversed phase column was used for analysis of concentration. The mobile phase gradient for TNT analysis consisted of 30:70 ACN:water, isocratic from 0 to 3 minutes followed by a linear gradient from 3 to 13 minutes to 100% ACN and holding at 100% ACN until all analytes had eluted. Quantitation of TNT was carried out based on absorbance at 230 nm.

Preliminary analysis of TNT degradation products was conducted by HPLC using a comparison of retention times and UV absorbance spectra of known compounds. A searchable spectral library of potential degradation products was constructed in Hewlett-Packard Chemstation Software through injection of single component standards with full spectral data collection from 200-400 nm. Mass spectrometric analyses of the products was done using an Applied Biosystems 3200 Q-Trap ESI-MS/MS and by FTICR-MS using a Bruker Apex II 7.0 T Fourier transform ion cyclotron resonance mass spectrometer with an ESI source and direct sample introduction. Samples were diluted 3-5 fold in 1:1 water:methanol with 0.1% formic acid to optimize signal response and introduced to the electrospray source at 10 μL/min flow rate by syringe pump. Data were collected on the 3200 Q-Trap instrument using enhanced product ion (EPI) mode. Ionization was conducted in negative ion mode for detection of nitroaromatic TNT oxidation products by ESI-MS/MS and FTICR-MS. Positive mode ionization was used also used for confirmation of potential amine reduction products by ESI-MS/MS.

Results and Discussion

The preliminary analysis of the Fenton reaction products by HPLC demonstrated differences in the products observed between Fenton reactions conducted with and without the presence of CDs, as previously described in chapter 3. For the water control reactions conducted without CDs, the only identified product was TNB, as previously described, eluting at 6.5 minutes (Figure 4.1).

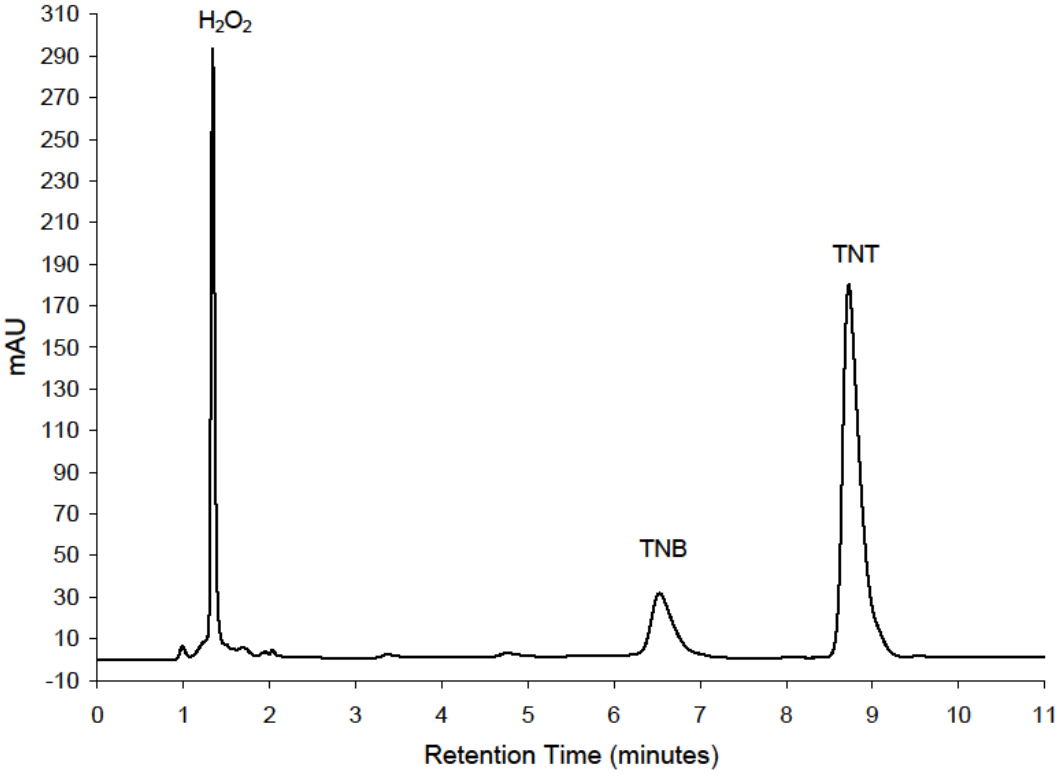

Figure 4.1. HPLC chromatogram of the Fenton reaction without CDs. The labeled peaks were identified through matching of retention time and absorbance spectra from 200-400 nm.

Reactions conducted in the presence of CDs or d-glucose showed several additional peaks which were not observed in the water control. Of these additional observed peaks, a peak eluting at 7.6

minutes was identified as 4-ADNT, a reductive product, and was observed in all reaction systems containing CDs or d-glucose (Figure 4.2).

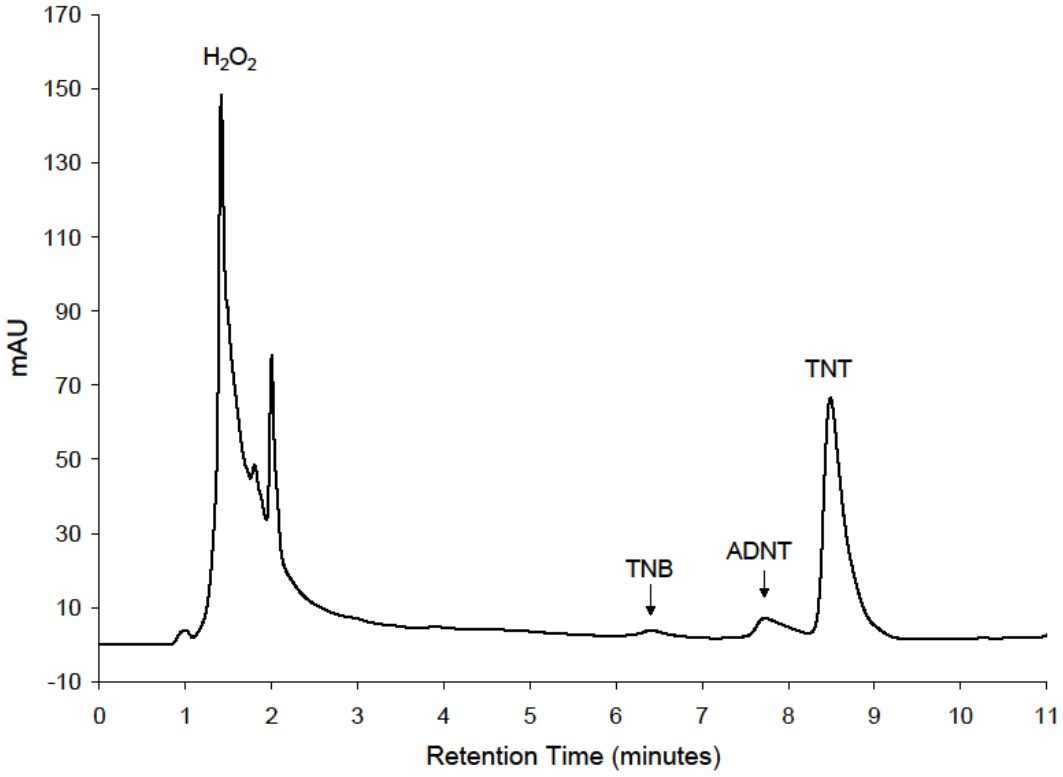

Figure 4.2. HPLC chromatogram of the Fenton reaction with βCDida at 6 minute reaction time. The labeled peaks were identified through matching of retention time and absorbance spectra from 200-400 nm.

The spectral search matches used to identify TNB and 4-ADNT are shown in the previous chapter as Figures 3.x. Excess H_2O_2 in the sampled reaction aliquots elutes near 1.5 minutes. A number of unresolved peaks co-elute with H_2O_2 from 1.5-2 minutes and this type of behavior was observed in all of the CD containing reaction systems. These early eluting compounds would be expected to be polar and hydrophilic, and as such, are not likely products of initial TNT degradation and likely arise secondary reactions involving CDs in the reaction medium. A number of other small peaks were observed to elute between 4 and 8 minutes in the

chromatograms of the reaction systems containing CDs at various sampling intervals (data not shown), but none of the observed peaks yielded a retention time or spectral match to known standards listed in the experimental section.

ESI-MS/MS Analysis

Following the initial HPLC identification of products in the Fenton reactions, ESI-MS/MS analysis of the same reaction systems was conducted to confirm the initial identification of TNB and 4-ADNT and to elucidate the identity of the unknown products. The reaction conducted without the presence of CDs gave similar results to an earlier study examining the Fenton reaction of TNT in water by Hess *et al.* (130). Figure 4.3 shows negative mode ESI-MS data of the reaction without CDs present without pH adjustment at zero and 8 minute reaction times. The zero minute (unreacted) TNT showed a peak at m/z 226, corresponding to $[TNT-H]^-$ and a small peak at m/z 212 which was determined to be $[TNB-H]^-$ and is assumed to be a minor contaminant from TNT manufacture. The 8 minute reaction showed a marked increase in the concentration of TNB relative to TNT as well as the formation of identified products 4,6-dinitro-*o*-cresol, $[4,6-DNC-H]^-$, at m/z 197, 3,5-dinitrophenyl-6-methylene-1-one, $[3,5-DNPMO-H]^-$, at m/z 195 and 3,5-dinitrophenol, $[3,5-DNP-H]^-$, at m/z 183. A number of other ions were also observed between m/z 200-220 but were not identified.

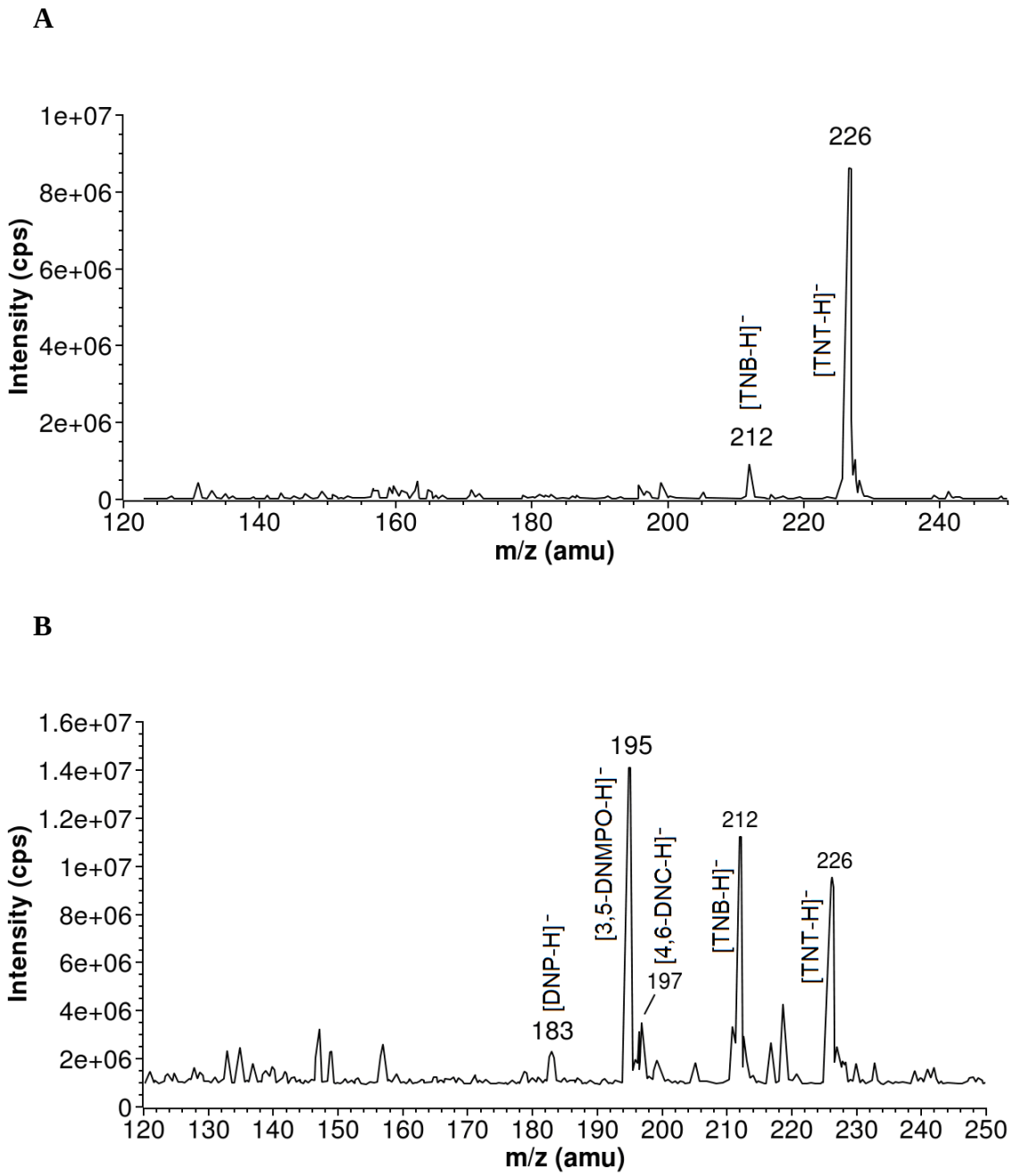

Figure 4.3. Negative mode ESI-MS analysis of the Fenton reaction without CDs present at 0 minutes (A) and 8 minutes (B). Peaks at m/z values of identified degradation products are labeled.

In contrast to the study by Hess *et al.*, the proposed complex of TNT and hydroperoxide anion $[TNT+HO_2^-\text{-}H]^-$ at m/z 260 was not observed (data not shown). Since this study used a much

lower peroxide dose than that used by Hess *et al.*, it is reasonable that the hydroperoxide adduct was not observed in these reaction systems. In addition, TNBA was not found, but dinitrobenzoic acid, $[DNBA-H]^-$, was identified at m/z 211. Both negative and positive mode ionization showed no evidence of amino-dinitrotoluene products for the reactions without CDs.

ESI-MS/MS analysis of the reactions conducted in the presence of CDs yielded many of the same oxidative products as those observed in the control reactions in water without the presence of CDs. Figure 4.4 and 4.5 show the negative mode ESI-MS of the Fenton reaction containing 1 mM βCD or 1 mM βCDida, respectively at 8 minutes reaction time. All of the CDs examined showed the formation of $[4,6-DNC-H]^-$, $[3,5-DNPMO-H]^-$, and $[TNB-H]^-$ as evidenced by peaks at m/z 197, 195, and 212, respectively. A number of additional products were observed in the CD systems that were not seen in the control reactions without CDs present.

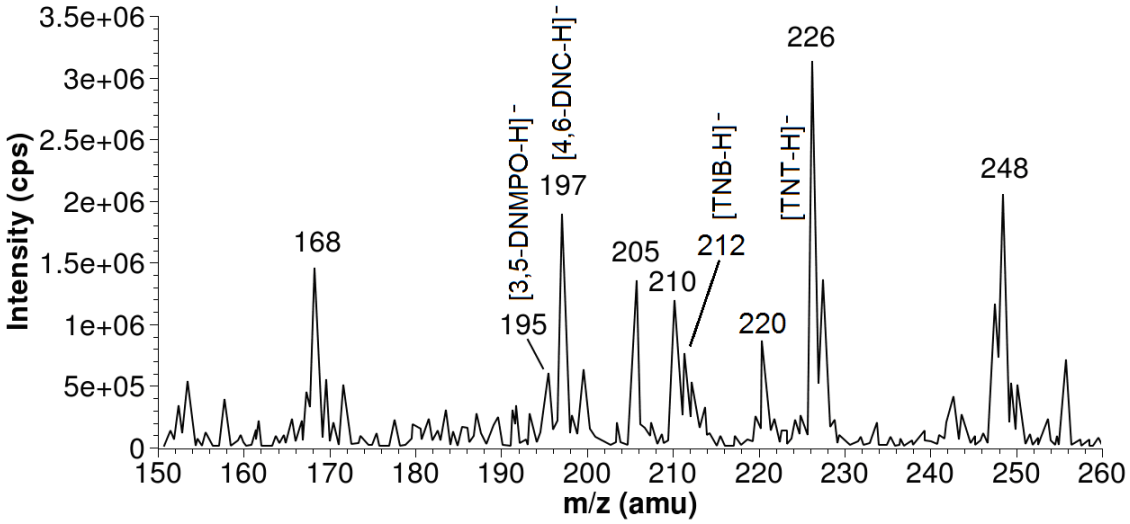

Figure 4.4. Negative mode ESI-MS of Fenton reaction at 8 minutes with 1 mM βCD.

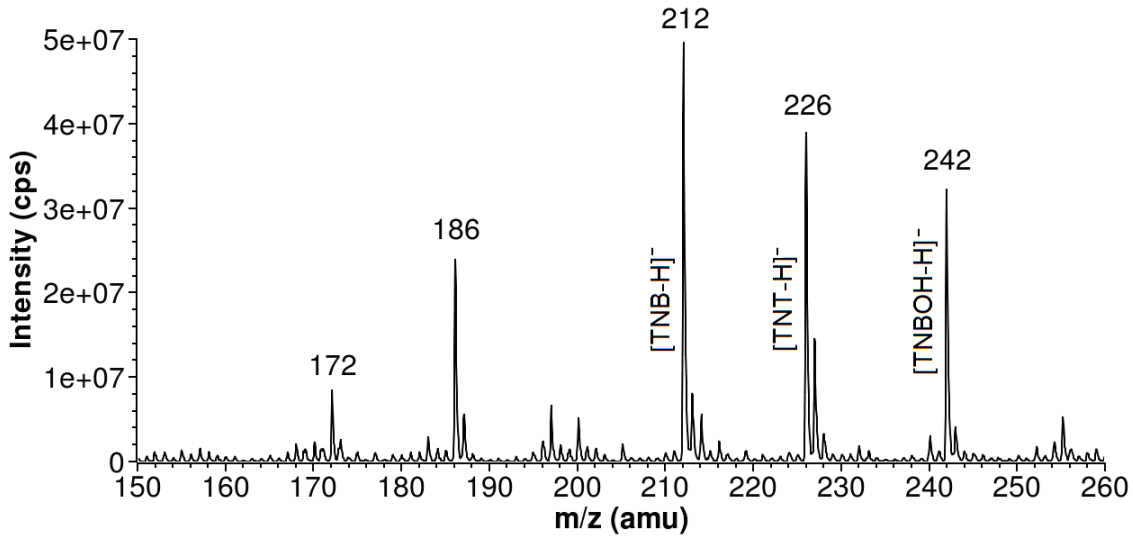

Figure 4.5. Negative mode ESI-MS of Fenton reaction at 8 minutes with 1 mM βCDida.

A notable difference between the CD assisted Fenton reactions systems and the control reactions is the relative intensity of the peaks at m/z 197 and 195, corresponding to [4,6-DNC-H]$^-$ and [3,5-DNPMO-H]$^-$, respectively. In the control reactions (Figure 4.3b), the m/z 195 peak is the dominant product of the pair while the CD assisted reactions show the opposite behavior (Figure 4.4). In the mechanism proposed by Hess *et al.*, the TNT-hydroperoxyl radical formed in the initial stage of the Fenton treatment decomposes to give 4,6-DNC and an oxidation product of 4,6-DNC, 3,5-DNPMO (130). The dominance of the less oxidized form of these products in the CD assisted Fenton reactions are indicative that the CDs provide a reaction environment with a lower oxidizing potential than control reactions without the CDs present.

The presence of a significant peak at m/z 212 during the end of the reaction in the presence of βCDida (Figure 4.5) was unexpected based on the earlier HPLC analysis of TNB concentration (Figure 3.9a). However, MS/MS analysis of the m/z 212 peak demonstrated that the identity of the product yielding the m/z 212 peak changed through the course of the reaction. In the initial phase of the reaction, the MS/MS spectrum corresponded to that of TNB (Figure

4.6a). By the 8 minute time point of the reaction, the m/z 212 peak no longer showed neutral losses typical of nitroaromatics, and was not positively identified (Figure 4.6b).

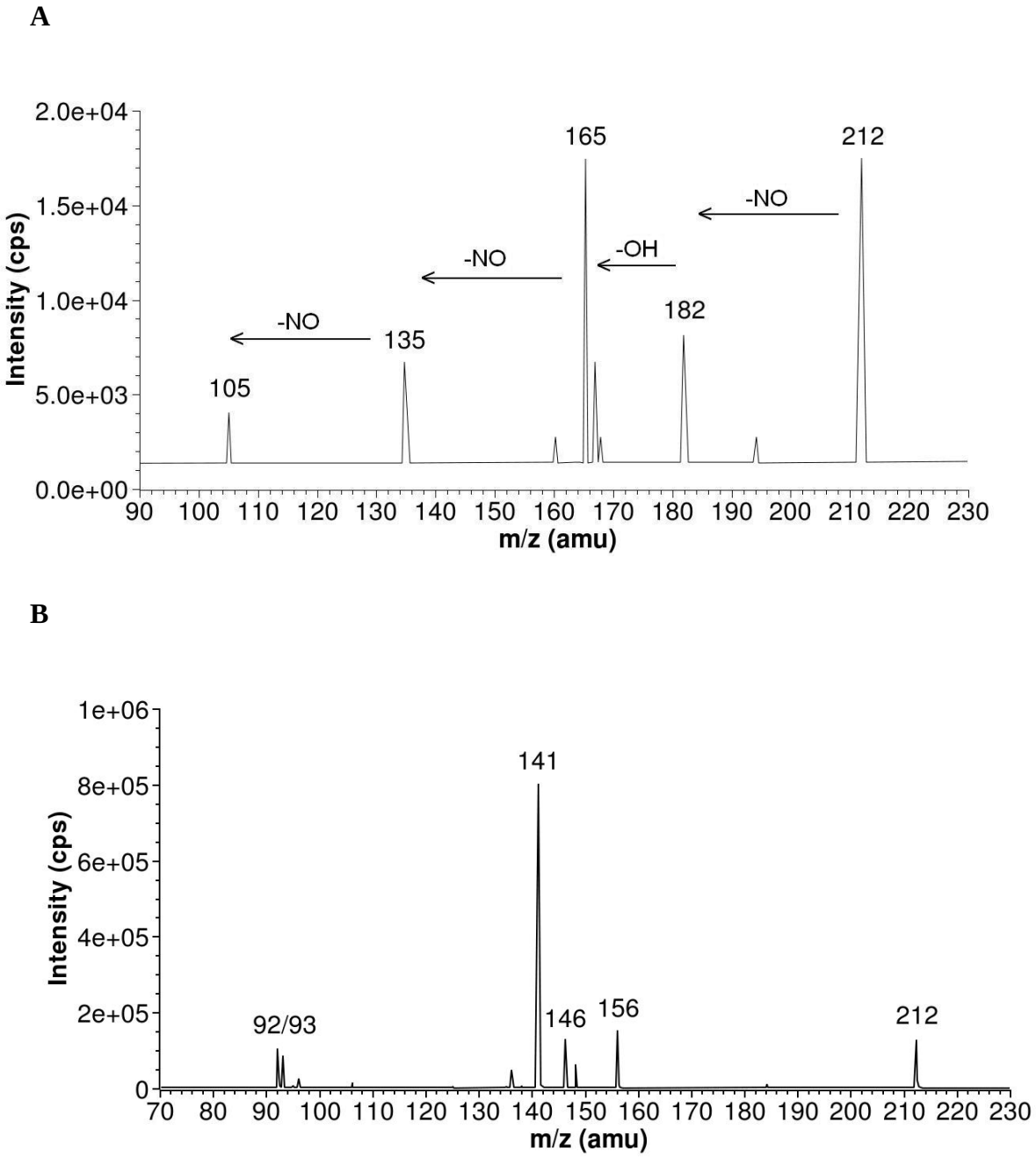

Figure 4.6. Negative mode ESI-MS/MS of m/z 212 during initial phase (A) and end of the Fenton reaction (B) in the presence of 1 mM βCDida.

A number of additional products were observed by negative mode ESI-MS in the Fenton reactions containing CDs. Peaks at m/z 248, 186, and 168 were observed in all CD containing systems and were determined by MS/MS to have a common origin in the m/z 248 peak (Figure 4.7). The common occurrence of the 248 m/z ion in all of the CD reaction systems could indicate that the ion is a cyclodextrin fragment. However, the MS/MS spectra failed to yield enough information to positively identify the product and the neutral losses observed don't correlate with what would be expected of the fragmentation of saccharides.

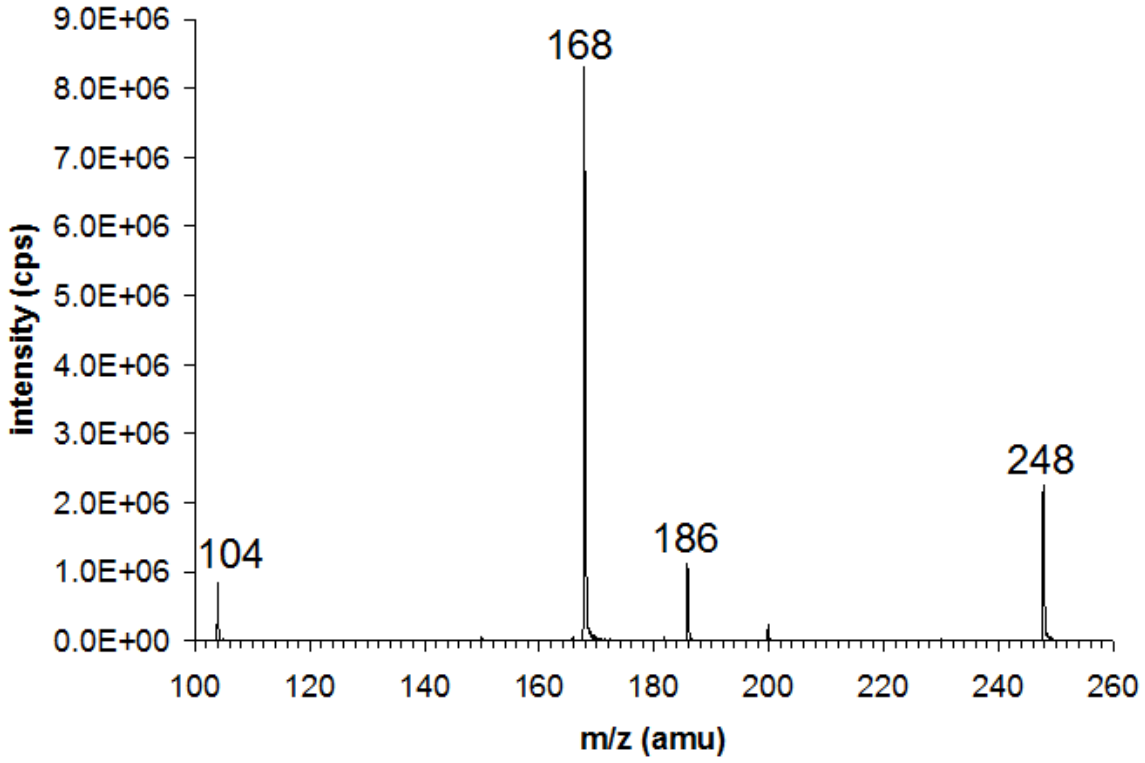

Figure 4.7. ESI-MS/MS of m/z 248 in Fenton reaction at 6 minutes with 1 mM βCD.

Fenton reactions containing 1 mM βCDida or 1 mM βCDedta showed a product at m/z 242 (Figure 4.5) which was determined by MS/MS to be 2,4,6-trinitrobenzyl alcohol-H^- [2,4,6-TNBOH-H]$^-$ (Figure 4.8). The neutral loss of 16 from m/z 242 to m/z 226 likely occurs through a loss of oxygen from the alcohol group and rearrangement to yield a trinitrotropylium ion at m/z

226. TNBOH was not observed in Fenton reactions conducted in the presence of βCD or cmβCD. MS/MS of the m/z 220 peak observed in the βCD Fenton reaction (Figure 4.7) yields a neutral loss of 15 to give a major fragment at m/z 205 and is likely a product of cyclodextrin decomposition. Both m/z 220 and 205 are observed in the negative mode ESI-MS spectra of the βCD reaction.

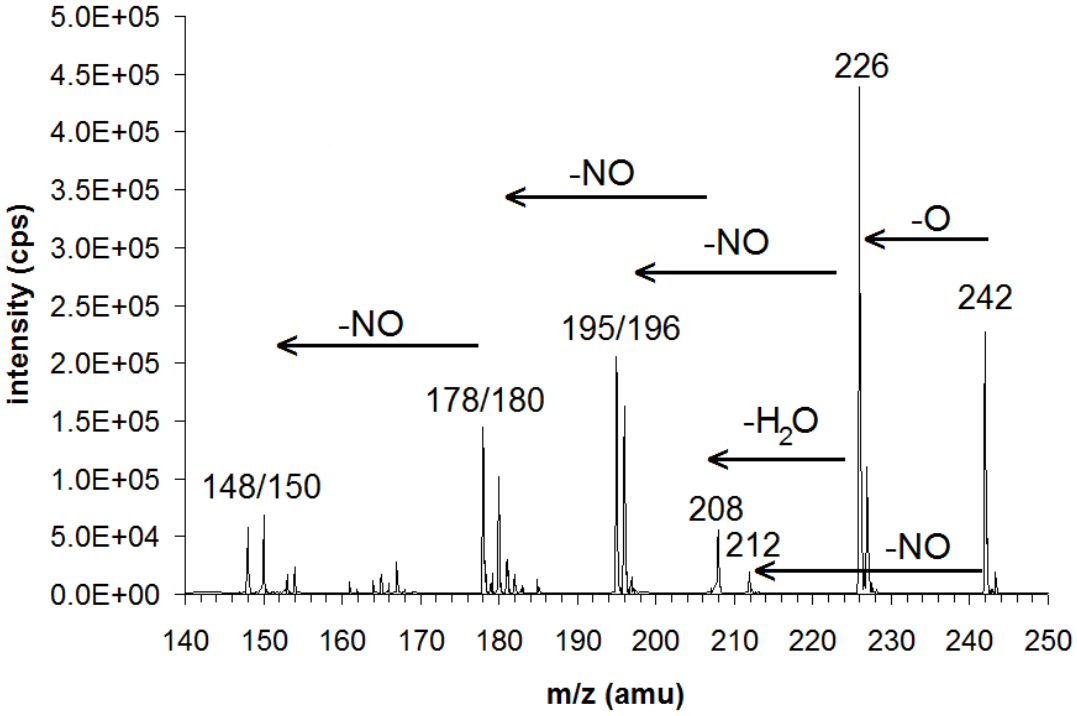

Figure 4.8. ESI-MS/MS of m/z 242 in Fenton reaction at 8 minutes with 1 mM βCDedta.

The presence of amino-dinitrotoluene reductive products was typically troublesome to confirm by ESI-MS/MS in negative ionization mode due to poor ionization efficiency. However, amino-dinitrotoluene was observed at some of the later reaction times in the CD containing reactions systems. Figure 4.9 shows the negative mode MS/MS of a 196 m/z ion in a βCD reaction system at 8 minutes reaction time, corresponding to $[ADNT\text{-}H]^-$. Positive mode ionization showed the presence of a peak at m/z 198 in a number of the CD assisted Fenton

reaction samples which also corresponded to $[ADNT+H]^+$. Both negative and positive mode ionization of the products of the control reaction showed no evidence of aminodinitrotoluenes products.

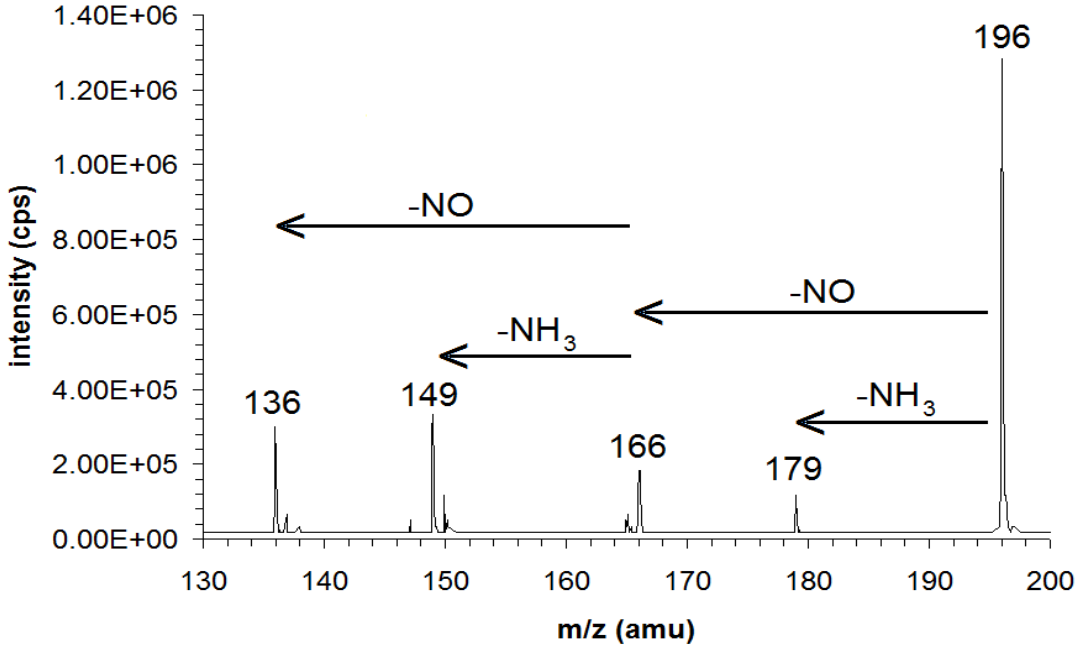

Figure 4.9. ESI-MS/MS of m/z 196 in Fenton reaction at 8 minutes with 1 mM βCD, product identified as amino-dinitrotoluene.

FTICR-MS Analysis

FTICR-MS was used to gain accurate mass information to help identify several products that had been observed for CD and d-glucose containing reactions in the negative mode ESI-MS/MS and were not identified due to either insufficient concentrations to yield reliable secondary MS data or resistance to fragmentation. FTICR-MS was also used as confirmatory method for products which were proposed in the ESI-MS/MS analysis.

A three point m/z calibration of the FTICR-MS was conducted using a combination of TNT and the previously identified products, TNB, 4,6-DNC, 3,5-DNMPO or 3,5-DNP,

depending on the reaction system examined. Identified products had exact mass tolerances of less than 2 mDa, and the elemental composition of the products determined using the search algorithms incorporated into the Bruker Xmass software for FTICR-MS instrument control and data collection. The search software was limited to an elemental composition of less than 8 carbon, 3 nitrogen, 10 oxygen, and 14 hydrogen atoms. No other elements were included in the exact mass search. The generated elemental compositions were then examined and potential structures were developed.

The FTICR-MS analysis of the βCD assisted Fenton reactions yielded further evidence of reductive products. Peaks observed at m/z of 210.0166 and 195.9987 correspond to molecular ion formulas of $C_7H_4N_3O_5$ and $C_6H_2N_3O_5$ with tolerances of 0.976 and -1.344 mDa, respectively. Ions at these m/z values were observed in a number of the CD assisted Fenton reaction samples analyzed by ESI-MS/MS but had not been positively identified, with exception of m/z 196 corresponding to ADNT in some reaction systems (see Figure 4.9). The likely structures for these molecular ion formulas correspond to [nitrosodinitrotoluene-H]$^-$ and [nitrosodinitrobenzene-H]$^-$, respectively. These reductive products were observed in all of the CD assisted Fenton reaction systems examined but were not observed in the control reactions. The presence of 2,4,6-TNBOH in the βCDida assisted Fenton reactions was confirmed by the presence of an ion at m/z 242.00387 corresponding to $C_7H_4N_3O_7$ with a tolerance of -1.603 mDa. A potential oxidation product of 2,4,6-TNBOH was observed at m/z 213.10643 corresponding to $C_7H_5N_2O_6$ with a tolerance of 1.120 mDa and is assumed to occur via denitration to yield [hydroxydinitrobenzyl alcohol-H]$^-$. Similar results were observed for the βCDedta assisted Fenton reactions. A number of other minor products were observed in the CD assisted Fenton

reaction systems. A summation of all products identified by HPLC, ESI-MS/MS and FTICR-MS over the time course of the Fenton reactions is given in Table 4.1.

Table 4.1. Decomposition products of the CD assisted Fenton reaction of TNT determined by HPLC, ESI-MS/MS or FTICR-MS ([1] oxidative products, [2] reductive products). [a] Peaks at m/z 211 were observed in all CD systems, but concentrations were insufficient for reliable MS/MS identification for the CDs not marked with an x. [b] Peaks at m/z 210 and 196 were observed for d-glucose by ESI-MS/MS but were not positively identified by FTICR-MS.

	H_2O control	βCD	cmβCD	βCDida	βCDedta	d-glucose
dinitrobenzene[1]	x	x	x	x	x	
dinitrobenzoic acid[1,a]	x	x				
3,5-dinitrophenyl-6-methylene-1-one[1]	x	x	x	x	x	x
3,5-dinitrophenol[1]	x	x	x	x	x	
4,6-dinitro-*o*-cresol[1]	x	x	x	x	x	x
dinitrotoluene[1]	x	x	x	x	x	
hydroxydinitrobenzyl alcohol[1]				x	x	
trinitrobenzene[1]	x	x	x	x	x	x
trinitrobenzyl alcohol[1]				x	x	
4-amino-2,6,-dinitrotoluene[2]		x	x	x	x	x
nitrosodinitrobenzene[2]		x	x	x	x	x[b]
nitrosodinitrotoluene[2]		x	x	x	x	x[b]

A proposed reaction scheme for the major observed components in the current study is shown in Figure 4.10. While the majority of the observed oxidative products have been reported in previous studies of the Fenton oxidation of TNT, the observation of the reductive pathways leading to the formation of nitroso and amine products when CDs are present have not been previously reported. These reductive products have been observed in microbiologically mediated reduction in certain soil types, but have not been observed in AOPs. Additionally, as previously noted in the prior chapter, the H_2O_2 concentration used in the current study is

insufficient to produce significant quantities of $\cdot O_2^-$, and HO_2^- which have been credited with initiation of a reductive pathway in some Fenton reaction systems(16).

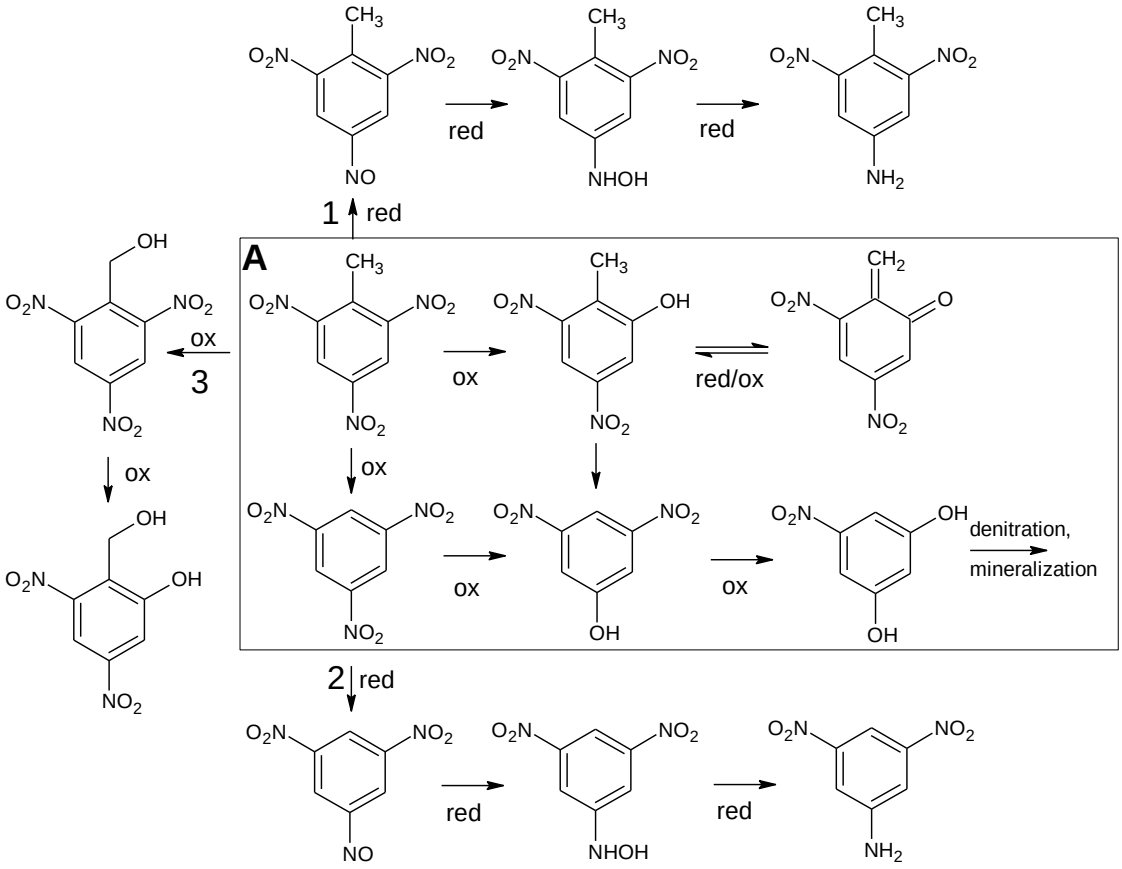

Figure 4.10. Proposed pathways TNT degradation in the presence of CDs, individual steps are labeled as oxidative (ox) or reductive (red). The pathway shown in box A is modified from Hess et al. (*20*). Pathways 1 and 2 show the reductive pathway initiated by the formation of an initial nitroso product from either TNT (1) or TNB (3). Pathway 3 was observed only for βCDida and β-CD-edta

The most likely source of the reductive pathway observed in the CD containing reactions arises from production of secondary CD radicals capable of reducing TNT. A recent study of γ-CD radicals produced through hydrogen abstraction by ·OH has shown the CD radicals to be effective reducing agents (127). Additionally, ·OH reactions with βCD demonstrate selectivity in the site of hydrogen abstraction, targeting protons on the C4, C5 and C6 carbons (129).

Complexed molecules in the CD annuli demonstrate a strong interaction with the protons on C5 carbon, since these protons reside on the interior of the annuli (Figure 4.11) (114). These prior studies involving cyclodextrin radicals in combination with the observation of reductive products in our current study yield strong evidence that cyclodextrin radicals are responsible for the reduction of TNT. The combination of selective hydrogen abstraction and TNT complexation explains the increased rates observed in the CD assisted Fenton reactions, and gives a plausible mechanism for the production of nitroso and amine reduction products observed.

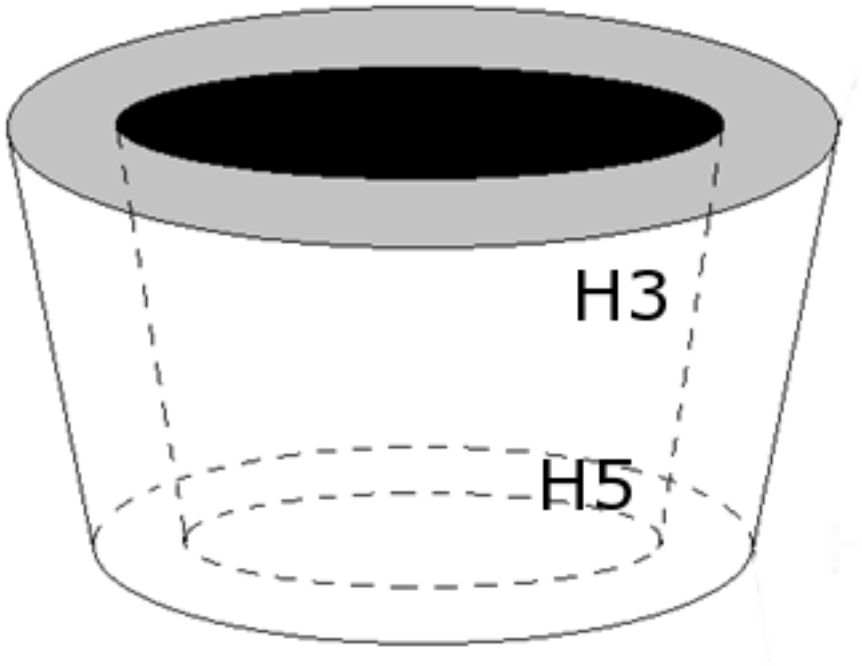

Figure 4.11. Location of protons on the C3 and C5 carbons in the annuli of a CD, labeled as H3 and H5, respectively.

The presence of TNBOH and hydroxydinitrobenzyl alcohol occurring in significant quantities only in the βCDida and βCDedta assisted Fenton reactions demonstrates mechanistic differences between these CDs and both βCD and cmβCD. Previous studies have described TNBOH as a degradation product of TNT in thermal decomposition (134), direct phototransformation (135), and catalytic oxidation by activated carbon (136). However, this

product has not been previously observed in Fenton reactions of TNT. TNBOH most likely occurs as a product due the presence of the (carboxymethyl)amino substituents of βCDida and βCDedta, though the mechanism of formation is unclear and merits further investigation.

Summary

The results of our current study show that while CD assisted Fenton reactions have shown the potential to significantly increase the kinetics of nitroaromatic degradation compared to typical Fenton systems, they also increase the complexity of the product distribution. The presence of the reductive pathways leading to the formation of nitroso and amine products for the Fenton reaction of TNT when CDs are present have not been previously reported in the literature. Additionally, the formation of trinitrobenzyl alcohol and hydroxydinitrobenzyl alcohol have not been previously found to occur in Fenton processes. The increased complexity of the product distribution, due to the presence of both an oxidative and reductive pathway, must be carefully evaluated before using CD assisted Fenton reactions as a remediation technology. The availability of multiple degradation pathways also has the potential to impact the degree of mineralization observed in the CD assisted Fenton systems as compared to typical Fenton systems.

CHAPTER 5

DETERMINATION OF ASSOCIATION CONSTANTS AND STRUCTURAL DETAILS OF CYCLODEXTRIN BINARY AND TERNARY COMPLEXES

Introduction

Complexation of TNT by CDs has been discussed in earlier chapters and the pre-association of TNT with CDs in the Fenton reaction systems described and presumed to play a significant role in the reaction pathways described. A number of studies have utilized the complexation of TNT with CDs for use in lab-scale soil flushing to desorb nitroaromatics from soil columns and for increasing the water solubility of TNT for ex-situ treatment processes (20, 23, 92). The studies have found CDs to be effective at increasing the solubility of TNT in these systems. The study by Yardin and Chiron determined the association constant of TNT with hydroxypropyl-β-cyclodextrin and methylated-β-cyclodextrin as 163 M^{-1} and 338 M^{-1}, respectively (20). These association constant values correspond to a 1.8 and 2.7 fold increase in the aqueous solubility of TNT in the presence of the CDs examined in the study.

Evidence of ternary complex formation of a guest with a CD and metal ions have been described by Wang and Brusseau in the study of cmβCD complexes with anthracene, trichlorobenzene, biphenyl and dichlorodiphenyltrichloroethane upon addition of Cd^{2+} (110). McCray and co-workers have also examined the ability of cmβCD to form ternary complexes with perchloroethylene and Pb^{2+}, Zn^{2+} and Sr^{2+} and compared their results to computational models of ternary complex formation (105). Their results found good agreement between experimental results and the computation models which proposed the existence of the ternary

complexes. Zheng and Tarr have given evidence of a ternary complex of 2-naphthol with cmβCD and Fe^{2+} through fluorescence and NMR studies (115, 116).

The association constant for a complex is analogous to an equilibrium constant for a simple reaction system as described by:

$$A + B \rightleftharpoons C \qquad 5.1$$

For complexes, it is typical to label the components as host (H), guest (G) and the host:guest complex (HG). Using this terminology, equation 5.1 becomes:

$$H + G \rightleftharpoons HG \qquad 5.2$$

And the association constant, K_a is defined as:

$$K_a = [HG] / [H][G] \qquad 5.3$$

The association constant is therefore a measure of the concentration of the host:guest complex versus the concentration of the free host and guest in solution. These calculations can be extended to more complex systems with multiple guests or hosts and equations describing these types of systems are developed later in this chapter.

A number of methods have been developed to determine K_a values for host:guest systems. Most techniques for measuring K_a utilize UV-vis, fluorescence or NMR spectroscopy, though chromatographic, mass spectrometric and calorimetric methods have also shown utility in

some applications (91, 137-141). Data analysis for host:guest systems with a 1:1 stoichiometry is frequently conducted based on a method developed by Benesi and Hildebrand in 1949, commonly referred to as the Benesi-Hildebrand method or double reciprocal plot (142). The technique was originally developed to examine the interaction of iodine with PAHs by UV spectroscopy, but the method has been refined and applied to a number of different analysis techniques.

The Benesi-Hildebrand method and variants have found wide application in the analysis of 1:1 complexes, but limiting factor in the application of these methods is that it they are unable to determine association constants for higher order complexes such as 2:1 and 1:2 (or higher) stoichiometries (138). To analyze higher order complexes, iterative computational procedures are typically used and a variety of software has been developed to perform these calculations (141). A drawback of the iterative computational techniques is that some *a priori* knowledge of the likely K_a value range for one of the complexes in solution is required for the software to converge and produce reasonable results.

The work described in this chapter details attempts at determining association constants for TNT/CD complexes by UV-vis spectroscopy using B-H calculations and a chromatographic method which used a variant of B-H calculations for determining K_a. NMR studies of ternary complex formation of CDs with 2-naphthol and Cd^{2+} as a surrogate for TNT and Fe^{2+} were also conducted. The determination of K_a values TNT/CD complexes at concentration ranges relevant to studies presented in chapters 4 and 5 has proven difficult, and the limited data collected was not in agreement with data available from an earlier study showing 1:1 TNT:CD ratios in the binary complex (20). NMR studies of ternary complex formation yielded evidence of the

existence of such systems for the CDs examined. Additionally, K_a values were determined for 2-naphthol with cmβCD, βCD and βCDida.

Benesi-Hildebrand Analysis of UV-vis Data: Introduction

Initial attempts at determining K_a for TNT:CD complexes focused on the use of UV-vis spectroscopy coupled with Benesi-Hildebrand (B-H) calculations. This approach was deemed reasonable due to the strong UV absorption characteristics of TNT and published results that binary TNT complexes with several different CDs possess a 1:1 stoichiometry (20).

The B-H method is performed by titrating one component of the host:guest complex with a large excess (typically 10-100 fold) with the other component (141). For optical spectroscopy, such as UV-vis, the component used in excess should have a negligible absorbance at the wavelength being monitored. The measured absorbance is therefore a product of the absorbance of the guest, host and guest:host complex:

$$Abs = Abs[H] + Abs[G] + Abs[H:G] \qquad 5.4$$

Under the assumption that the host has a negligible absorption at the wavelength of interest, or the absorption of the host has been accounted for by background subtraction of the host absorption at the concentrations used, Equation 5.4 reduces to:

$$Abs = Abs[G] + Abs[H:G] \qquad 5.5$$

Therefore, the change in absorbance, ΔAbs, is a function of the absorbance of the host:guest complex minus the absorbance of the guest (holding the guest concentration constant) and yields:

$$\Delta Abs = Abs[H:G] - Abs[G] \qquad 5.6$$

In order to determine association constants for methods based on absorption experiments, it is necessary to use the Beer-Lambert law (Abs = εbC, where ε is molar absorptivity, b is optical path length and C is concentration of absorbing species) (143). Using the Beer-Lambert law, and a 1 cm optical path length to simplify the equation, 5.6 becomes:

$$\Delta Abs = \varepsilon^{HG}[H:G] - \varepsilon^{G}[G] \qquad 5.7$$

Furthermore, if the guest concentration is held constant then equation 6.6 reduces to:

$$\Delta Abs = \varepsilon^{HG}[H:G] \qquad 5.8$$

Substitution of equation 5.3 into equation 5.8 yields:

$$\Delta Abs = \varepsilon^{HG}K_a[H][G] \qquad 5.9$$

Under conditions of mass balance ($[H]_0 = [H] + [HG]$, $([G]_0 = [G] + [HG])$ and rearranging, equation 5.9 becomes:

$$\Delta Abs = \varepsilon^{HG} K_a [H]_0 [G]_0 / (1 + K_a [G]_0) \qquad 5.10$$

In order to perform the Benesi-Hildebrand calculations, equation 5.10 is plotted with $1/\Delta Abs$ as a function of $1/[H]_0$ and under the conditions of $[H]_0 >> [G]_0$, equation 5.10 can be rearranged and expressed as the Benesi-Hildebrand equation (142):

$$1/\Delta Abs = 1/\varepsilon^{HG} K_a [H]_0 + 1/\varepsilon^{HG} \qquad 5.11$$

Equation 5.11 is now in the form of y = mx + b, and for complexes with a 1:1 stoichiometry a straight line will be obtained where ε^{HG} is obtained from the intercept and K_a calculated from the slope.

Benesi-Hildebrand Analysis of UV-vis Data: Experimental Section

The Benesi-Hildebrand experiments conducted to determine the K_a of the TNT:CD complexes were performed by preparing 100 μM solutions of TNT in nanopure water and adding CDs to the individual solutions at concentrations from 1 to 10 mM. The choice of varying the CD concentration was dictated by the limited solubility of TNT in water. Solutions containing only CDs were also prepared at the same concentrations for use in background subtraction of CD absorption. Experiments were performed on a Cary 500 UV-vis spectrophotometer over a wavelength range of 200-300 nm. The initial studies for TNT complexation were done using only cmβCD and βCD due to the limited amounts of βCDida and βCD-edta available.

Benesi-Hildebrand Analysis of UV-vis Data: Results and Discussion

At the wavelengths monitored, TNT shows an absorption maximum around 230 nm and both CDs examined showed minimal absorption at this wavelength (background subtraction of the CD absorption at the analyzed concentrations was still used in the data analysis). A plot of the B-H data for 100 μM TNT and 1 to 5 mM βCD is given in Figure 5.1. As figure 5.1 clearly shows, the plotted data doesn't produce a linear fit, and a Benesi-Hildebrand treatment of the data is inappropriate to determine a K_a value. As noted previously, the concentration of TNT in these experiments was held constant, therefore deviation from linearity in the B-H plots would indicate that 1:1 TNT:βCD complexation was not occurring throughout the entire CD addition range examined and that the formation of 1:2 TNT:βCD complexes appear likely. The method was also used to analyze TNT:cmβCD complexes and yielded similar results. These results for TNT:CD complexes were in contradiction to results showing a 1:1 complex of TNT with hydroxypropyl-βCD and methylated-βCD obtained by Yardin and Chiron using a chromatographic method to determine K_a (20). Based on the results of this work, and in order to compare the results to those obtained by Yardin and Chiron, a chromatographic method using HPLC for determining K_a was developed and conducted. Data to perform Benesi-Hildebrand calculations was not obtained for βCDida and βCDedta after review of the cmβCD and βCD data.

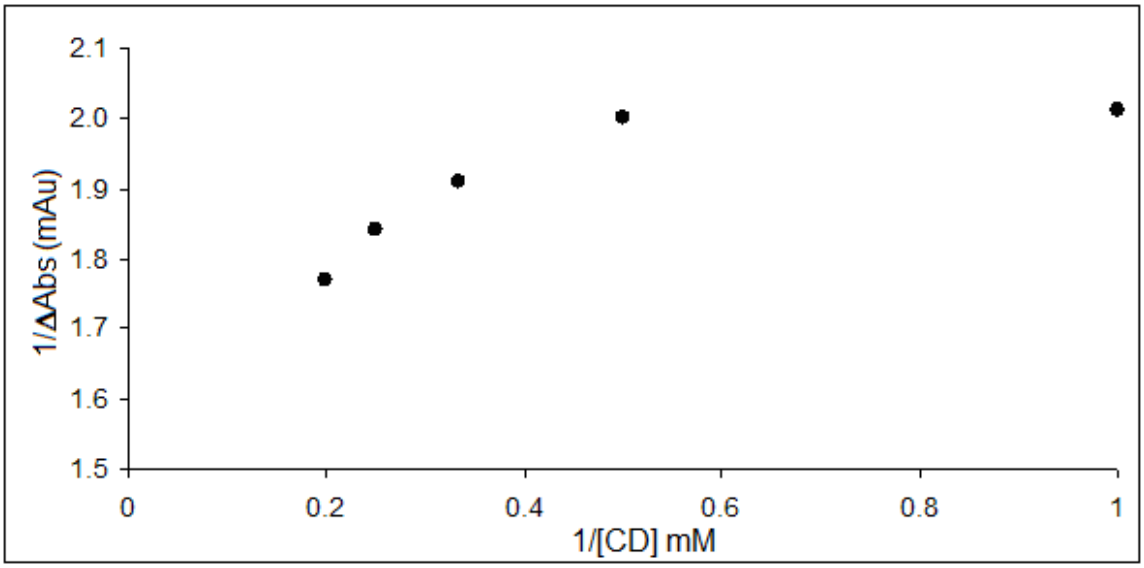

Figure 5.1. Double reciprocal plot of 1/ΔAbs vs. 1/[CD] for 100 μM TNT titrated with 1 to 5 mM βCD.

Determination of TNT:CD Association Constants by HPLC: Introduction

Several studies have examined the use of HPLC methods to determine K_a values (20, 137, 139). The K_a determinations are made by injecting the guest onto the HPLC column which contains the host compound as a component of the mobile phase. The concentration of the host compound in the mobile phase is then varied and the change in retention time of the guest compound is monitored. The method is analogous to Benesi-Hildebrand methods in optical spectroscopy, using the change in analyte retention time versus the concentration of the host in the mobile phase. The development of the initial equations is somewhat more complex than for optical spectroscopy since the interaction of the components with the stationary phase must also be taken into account and introduces terms for the partitioning of the guest and host:guest complex in the stationary phase, in addition to K_a. The three relationships can be described by equation 5.3 for K_a of the complex in the mobile phase and the following equations for guest and guest:host equilibria between the stationary (s) and mobile (m) phases (137):

$$K_g = [(G)_s] / [(G)_m] \quad 5.12$$

$$K_{h:g} = [(H:G)_s] / [(H:G)_m] \quad 5.13$$

The capacity (or retention) factor of the guest can then be determined as:

$$k' = \varphi([(G)_s] / [(G)_m] + [(H:G)_m]) \quad 5.14$$

where φ is the column phase ratio (ratio of the volume of mobile phase in the column compared to the volume of the stationary phase) . Upon rearrangement and insertion of the above equilibrium equations, equation 5.14 can be written as:

$$k' = \varphi(K_g K_a / (K_a + ([H]_t - [H:G]_m)) \quad 5.15$$

where $[H]_t$ is equal to the total amount of host in the mobile and stationary phases. $[H]_t$ is also in significant excess of $[H:G]_m$, therefore:

$$[H]_t - [(H:G)_m] \approx [H]_t \quad 5.16$$

φK_g is also equal to the capacity factor of the guest without the host in the mobile phase, k_0' (137), therefore equation 5.16 can be reduced and expressed to yield:

$$1 / k' = 1 / k_0' + (K_a[H]_t / k_0') \qquad 5.17$$

Equation 5.17 yields straight line with a slope of K_a / k_0', analogous to the Benesi-Hildebrand treatment of spectroscopic data.

The above equations also assume that that the host has little interaction with the stationary phase. This assumption is valid for systems using CDs with a reverse phase column, but TNT:CD association constants can't be determined on reverse phase columns due to the strength of the interaction of TNT with apolar stationary phases. This interaction would preclude the use of a purely aqueous mobile phase. In the study by Yardin and Chiron, a reverse phase phenyl column was used and 5% methanol was added as a modifier to the mobile phase (20). While methanol addition would reduce TNT elution times from the phenyl column, it could also impact complex formation between TNT and the CD and the results obtained using this method would not be representative of complex formation in a purely aqueous environment. Therefore, the method used for this study used a polar silica column to eliminate the need for organic solvents in the mobile phase.

Determination of TNT:CD Association Constants by HPLC: Experimental Design

The experimental design for determining the association constants by HPLC consisted of a 20 μL injection of 100 μM TNT onto a 4.6 × 150 mm, 5 μM particle size silica column. The mobile phases consisted of HPLC grade water (mobile phase A) and 2.5 mM βCD in HPLC water (mobile phase B). Mobile phases A and B were mixed at varying ratios to alter the concentration of βCD present in the mobile phase. The capacity factors were determined by first injecting a solution of iodide to determine the void volume, which was determined to be 1.080 ±

0.001 minutes for 4 replicate injections. The retention times of a single component injection of βCD was determined using HPLC grade water as the mobile phase and both βCD eluted within a few seconds of the void volume, indicating minimal interaction with the column. TNT was injected in triplicate at each concentration of CD in the mobile phase and RSDs for the retention time at each concentration was less than 1% for the three injections. The retention time of TNT was monitored at 6 different CD concentrations, ranging from 0 to 1.5 mM. The retention time for TNT with a purely aqueous mobile phase was 4.27 ± 0.02 min for triplicate injections.

Determination of TNT:CD Association Constants by HPLC: Results and Discussion

Like the B-H treatment of UV data for TNT:CD complexation, the results of this study indicate that 1:1 complexation was not occurring throughout the concentrations used. Figure 5.2 shows a plot of $1/k'$ versus the concentration of βCD in the mobile phase, and it can be clearly seen from the plot that two separate regimes exist for the change in capacity factor (determined by the retention times) for the TNT:CD complex as the CD concentration is increased. Earlier work by Yardin and Chiron had used mobile phase concentrations of CD ranging from 2.5-15 mM and the concentration of TNT was not given (20). However, the maximum aqueous solubility of TNT is approximately 200 μM at room temperature (76). Given this fact, the ratio of CD to TNT used in the study by Yardin and Chiron would have been equivalent or greater than the ratio used at the highest three CD concentrations in this study (see Figure 5.2).

The results of both the B-H treatment of UV data and HPLC analysis of K_a indicate 1:1 complexation may not be the only stoichiometry occurring at the concentration ratios of TNT:CD used in the Fenton reactions described in previous chapters. Additionally, K_a values

were not able to be determined by either method utilized, since they both require strictly a 1:1 complex in order to be evaluated.

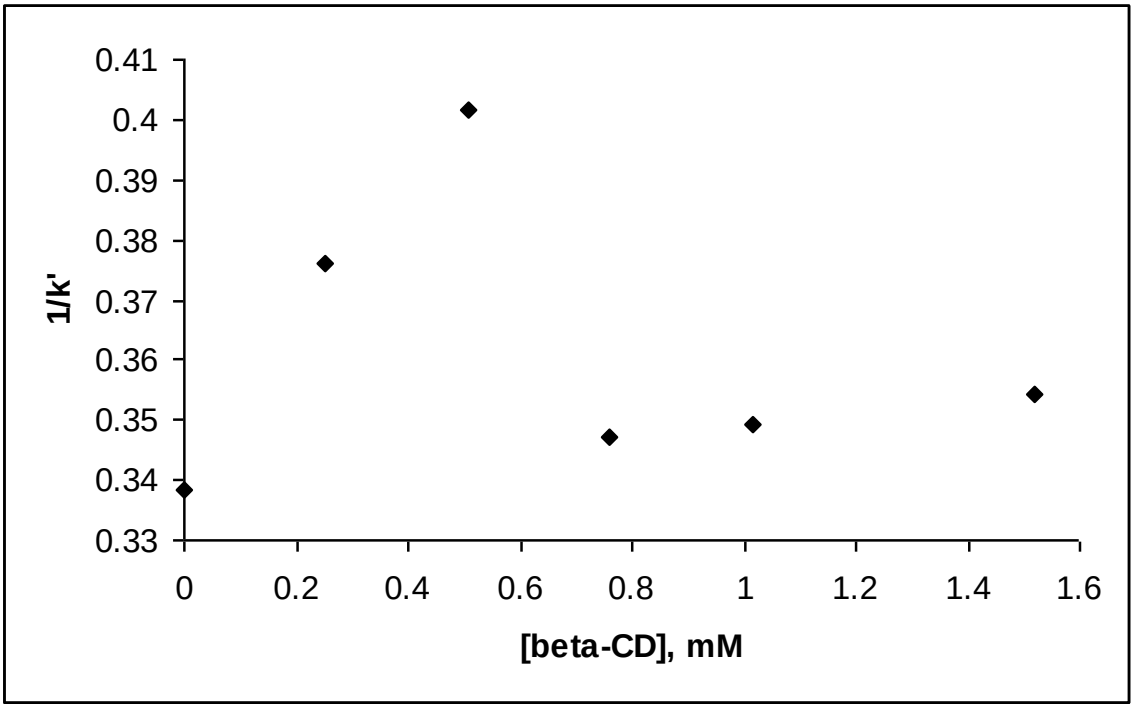

Figure 5.2. Plot of 1/*k'* versus the concentration of βCD in the mobile phase, 1/βCD not shown in order to include capacity factor of TNT without βCD in mobile phase (0 mM βCD).

Determination of Association Constants by NMR

NMR was chosen for the next attempts at K_a due to the availability of software capable of performing iterative analysis of NMR data for complexes with multiple stoichiometries (138, 144, 145). The equations to determine association constants by NMR titrations can be developed by combining the equations for determining the equilibrium constants for both the 1:1 host:guest, K_{11}, and 1:2 host:guest, K_{12}, equations and inserting those into an equation for determining the individual contributions to the observed chemical shift, δ_{obs}. The equations for 1:1 and 1:2 equilibriums are defined as:

$$H + G \xleftrightarrow{K_{11}} HG,\ K_{11} = \frac{[HG]}{[H][G]} \Rightarrow [HG] = K_{11}[H][G] \quad 5.18$$

$$HG + H \xleftrightarrow{K_{12}} H_2G,\ K_{12} = \frac{[H_2G]}{[HG][H]} \Rightarrow [H_2G] = K_{12}[HG][H] \quad 5.19$$

The value of $[H_2G]$ is solved by plugging equation 5.18 into equation 5.19:

$$[H_2G] = K_{12}K_{11}[H]^2[G] \quad 5.20$$

The mass balance of the host, guest, 1:1 and 1:2 complexes are defined as follows:

$$H_{total} = [H]_{free} + [HG] + 2[H_2G] \quad 5.20$$

$$G_{total} = [G]_{free} + [HG] + [H_2G] \quad 5.21$$

Under the conditions of fast host-guest exchange, relative to the NMR timeframe, the observed chemical shift is a concentration weighted average of the individual contributions from the free, 1:1, and 1:2 species (138):

$$\delta_{obs} = \delta_{free}f_{10} + \delta_{11}f_{11} + \delta_{12}f_{12} \quad 5.22$$

where:

$$f_{10} = \frac{[G]_{free}}{[G]_{total}};\ f_{11} = \frac{[HG]}{[G]_{total}};\ f_{12} = \frac{[H_2G]}{[G]_{total}} \quad 5.23\ a\text{-}c$$

By substituting and rearranging equations 5.19-5.22 into the expressions for the concentrations in equations 5.23 a-c, the following expressions are obtained:

$$f_{10} = \frac{[G]_{free}}{[G]_{total} + [HG] + [H_2G]} \Rightarrow \frac{1}{1 + K_{11}[H] + K_{12}K_{11}[H][G]} \quad 5.24\ a$$

$$f_{11} = \frac{K_{11}[H][G]}{[G]_{total} + [HG] + [H_2G]} \Rightarrow \frac{K_{11}[H]}{1 + K_{11}[H] + K_{12}K_{11}[H][G]} \quad 5.24\ b$$

$$f_{12} = \frac{K_{12}K_{11}[H][G]^2}{[G]_{total} + [HG] + [H_2G]} \Rightarrow \frac{K_{12}K_{11}[H][G]^2}{[G] + K_{11}[H][G] + K_{12}K_{11}[H][G]^2} \qquad 5.24\ c$$

The total concentration of the guest is a summation of the terms for f_{10}, f_{11} and f_{12} such that:

$$f_{10} + f_{11} + f_{12} = 1 \qquad 5.25$$

Equations 5.24 a-c can then be used to determine the equilibrium constants and the concentrations of the free and bound species in both the 1:1 and 1:2 binding regimes through the measurement of the chemical shifts of the species in solution. For the 1:1 binding regime, the observed chemical shift is:

$$\delta_{obs} = \frac{[HG]}{[H]_{total}}\delta_b + \frac{[H]}{[H]_{total}}\delta_f \qquad 5.26$$

where δ_{obs} is the observed chemical shift, $[H]_{total}$ is the initial concentration of host added, δ_b is the chemical shift of the fully bound species and δ_f is the chemical shift of the free host (reference shift). The calculation of K_a for a 1:1 complex by NMR can be calculated using a B-H technique analogous to the equations developed earlier in this chapter, by plotting $1/\Delta\delta_{obs}$ vs. $1/[H]_{total}$. The intercept corresponds to $1/\Delta\delta_{max}$ with a slope of $1/\Delta\delta_{max} K_a$ (141).

For 1:2 binding regimes, an analogous equation to 5.25 can be written where 2 hosts bind a single guest:

$$\delta_{obs} = \frac{2[H_2G]}{[H]_{total}}\delta_{b2}\frac{[HG]}{[H]_{total}}\delta_{b1} + \frac{[H]}{[H]_{total}}\delta_f \qquad 5.26$$

where δ_{b1} and δ_{b2} are the chemical shifts of the 1:1 and 1:2 species, respectively.

The equations for the desired parameters of K_{11}, K_{12}, [H], [HG] and $[H_2G]$, can then be solved by an iterative computational process. The iterative process uses a non-linear least squares fitting procedure that fits to a plot of observed chemical shift versus the varying

concentration of one of the species which is used to titrate a fixed concentration of the other species in solution (144, 145).

Despite the ability of software available to calculate K_a values of higher order complexes expected for TNT:CD complexes as a results of the initial studies, limitations in this method became apparent for several reasons. First, the limited solubility of TNT in H_2O/D_2O gave a very weak signal intensity, even for a saturated TNT solution in D_2O analysed by proton NMR on a high field (500 MHz) instrument (Figure 5.3).

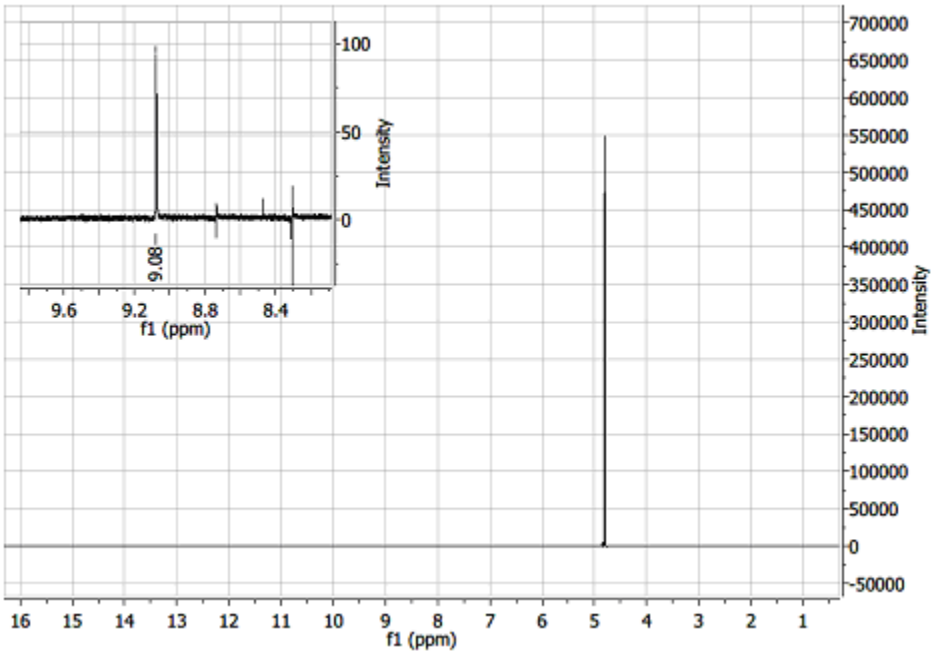

Figure 5.3. 500 MHz ^{1}H NMR spectra of 200 μM TNT in D_2O. The D_2O (HDO) reference peak is shown at 4.8 ppm and the inset shows a singlet peak for the aromatic protons of TNT at 9.08 ppm. Protons on the methyl group of TNT yield a singlet at 3.37 ppm of similar intensity (not shown).

Secondly, in the presence of βCDida and βCDedta, significant deviations in the chemical shifts are observed over the time course of analysis. A recent study by Ponnu and co-workers examining pattern identification for the detection of TNT found that in the presence of N,N,N′,N′-tetramethyl-p-phenylenediamine or tetrakis(dimethylamino)ethylene, TNT slowly formed a charge-transfer complex, with TNT acting as the electron acceptor (146). This study

also examined the interaction of the charge transfer complexes with several different CDs and found that the CDs helped to stabilize the complexes. In the NMR data collected for TNT and βCDida and βCDedta, formation of a charge transfer complex between TNT and the amine containing ligands of βCDida and βCDedta could explain chemical shift deviations observed. However, further work to examine this potential mechanism was not conducted and attempts to determine K_a values for TNT:CD complexes were not pursued further.

NMR Analysis of Binary and Ternary CD Complexes with 2-naphthol and Cd^{2+}

Further NMR studies of binary and ternary CD complexes utilized 2-naphthol as a surrogate for TNT since it had been previously shown to form complexes with cmβCD, with a K_a of 224 M^{-1}, determined by proton NMR (116). The interaction of metal ions chelated by the CDs in ternary complexes was examined using Cd^{2+} as a surrogate for Fe^{2+} to avoid the paramagnetic line broadening observed with Fe^{2+} in NMR experiments (116, 147). Initial studies focused on the determination of K_a values for 2-naphthol:CD complexes and βCD, cmβCD and βCDida were examined. The 1D proton NMR spectra and 2D correlation spectroscopy (COSY) data for βCD are shown in figure 5.4. The COSY method utilizes intramolecular proton coupling between adjacent protons to give a correlation spectrum which can be used to assign protons in a molecule to specific chemical shifts (147). The COSY spectrum contains the 1D spectrum along the diagonal and the coupling between adjacent protons is displayed off the diagonal. The chemical shift assignment is in agreement with data presented in a review of NMR studies examining CD complexation (138).

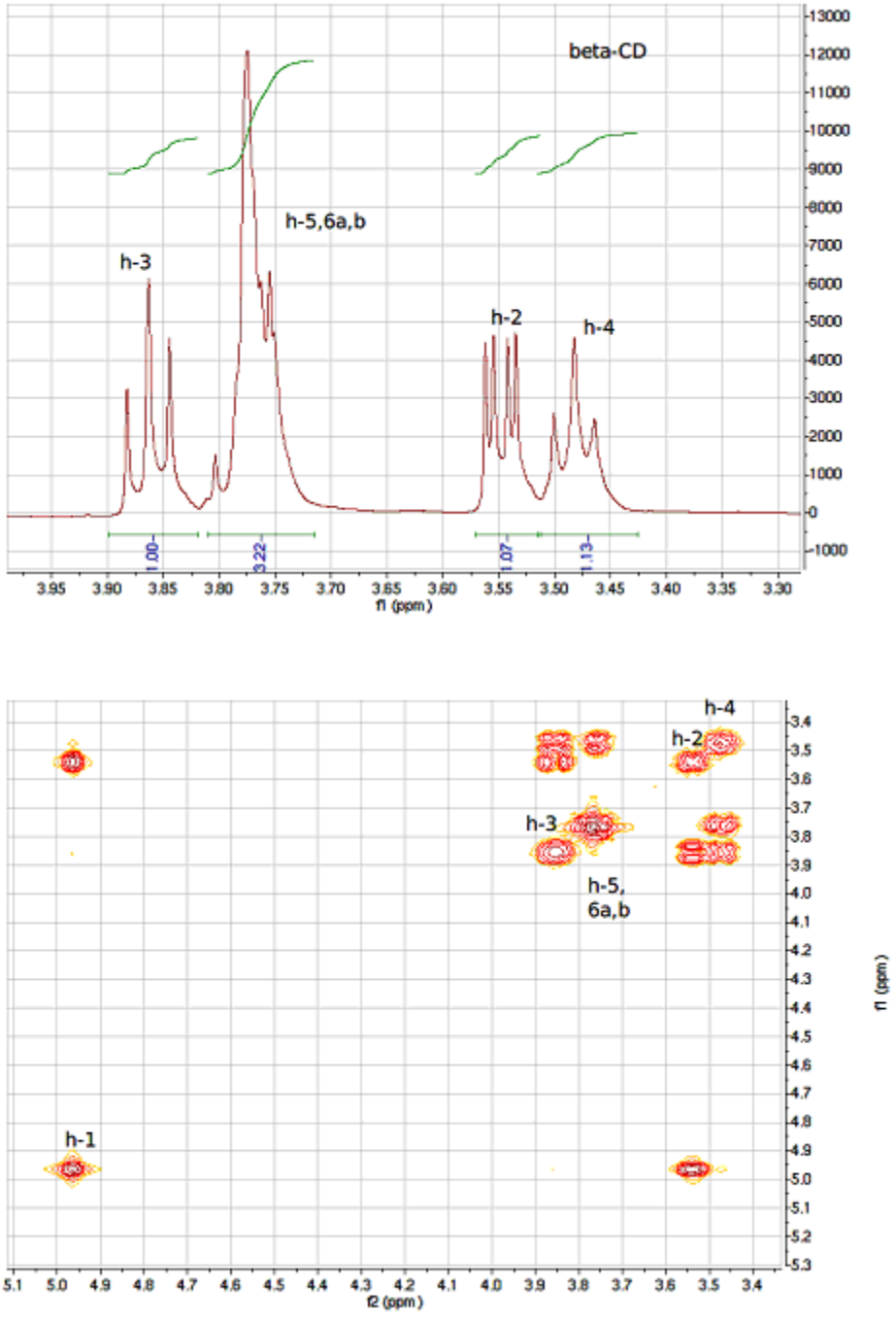

Figure 5.4. 1D proton spectra of βCD (top) and 2D COSY data used for peak assignment, integration values for the 1D spectrum are shown.

COSY experiments were also conducted for βCDida to assign the chemical shifts, and the 1D spectrum is shown in Figure 5.5, top (COSY data not shown). Chemical shift assignment

was not attempted for cmβCD due to the complexity of the proton NMR spectrum. Commercially available cmβCD is a mixture containing differing numbers of carboxymethyl groups at differing random substitution positions along the rim of the CD torus (116).

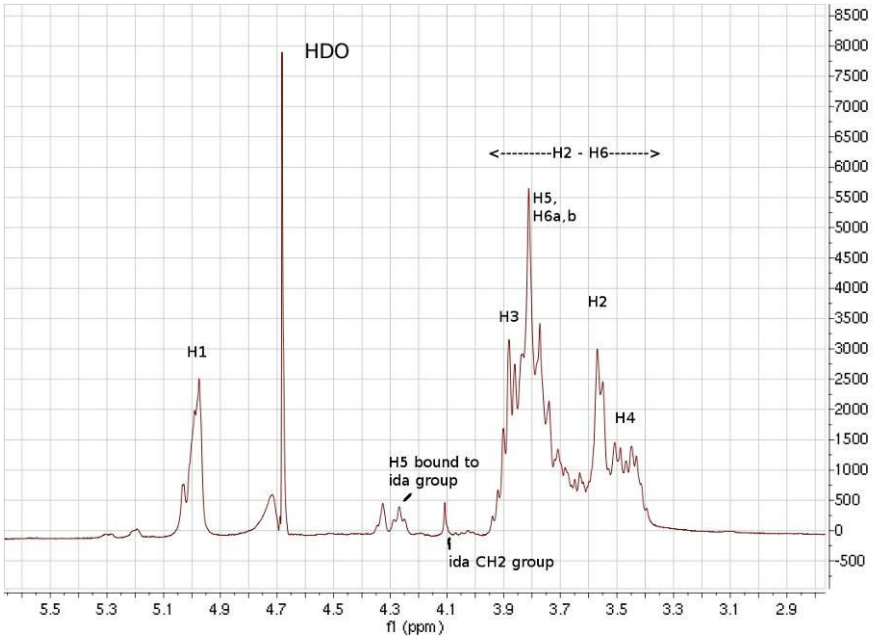

Figure 5.5. 1D proton NMR of βCDida, chemical shift assignments were made from COSY data (not shown).

As can be seen in Figures 5.4 and 5.5, the chemical shifts for protons on the C5 carbon (labeled as H5) were not resolved from the protons on the C6 carbon. As discussed in earlier chapters, complexed guests exhibit the strongest interaction with the H5 protons due to their location inside the CD torus (Figure 4.14 from previous chapter). Figure 5.5 also demonstrates that the presence of functional groups on the CD increases the complexity of the proton NMR spectra. For these reasons, the calculation of K_a values for the 2-naphthol:CD complexes utilized the changes in observed chemical shifts for 2-naphthol. Figure 5.6, top, shows the 1D proton spectrum of 2-naphthol with previously determined peak assignments (116) and 5.6, bottom,

shows the 1D proton spectrum of 2-naphthol with βCD, at a 1:1 mole ratio. Changes in the observed chemical shifts as well as significant broadening of some peaks indicate the formation of a 2-naphthol/βCD complex in solution.

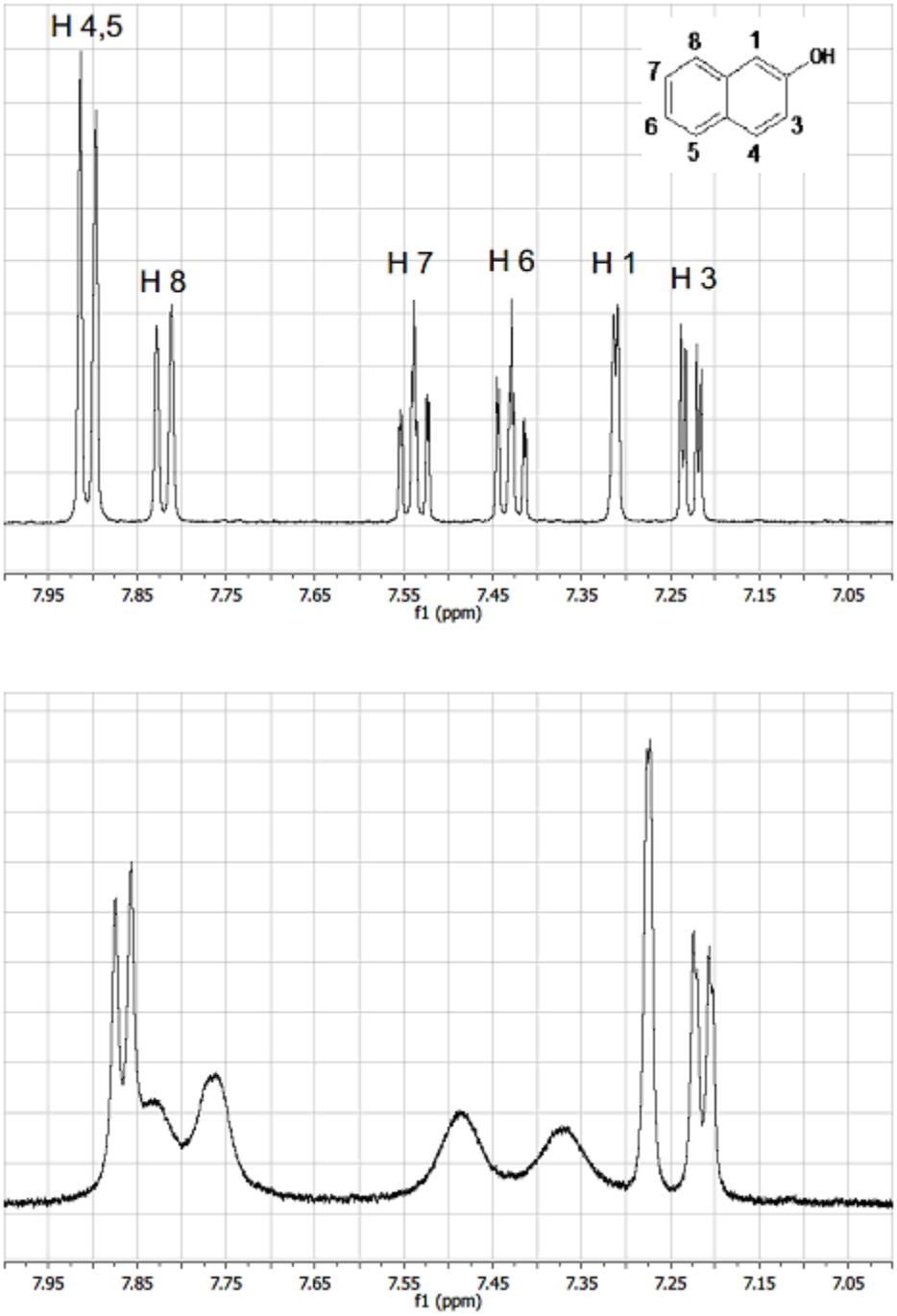

Figure 5.6. Proton NMR spectra of 2-naphthol (top) and 1:1 2-naphthol:βCD (bottom).

The results of the initial studies clearly show interaction of 2-naphthol with CDs and based on results of the earlier study of 2-naphthol with cmβCD, determination of K_a values by NMR was deemed appropriate. The association constants were determined using a fixed 2-naphthol concentration with addition of CDs at 5 different concentration ranges in a 10 to 100 fold excess. Plots of $1/\Delta\delta_{obs}$ vs. $1/[H]_{total}$ were linear for the all of the protons on 2-naphthol when titrated with βCD, cmβCD, and βCDida (βCDedta was not examined). The degree of interaction between different protons on 2-naphthol and the CDs were observed by differences in $\Delta\delta_{obs}$ between different protons, as would be expected by different local environments near the different protons, when complexed. B-H treatment of the data was used to determine K_a by averaging the values determined for each of the protons (148) and values of 231, 268 and 324 M^{-1} were found for cmβCD, βCDida, and βCD, respectively. The value for the 2-naphthol/cmβCD complex is in excellent agreement with the reported value of 224 M^{-1} (116).

The formation of ternary complexes was examined by adding varying amounts of Cd^{2+} to 1:1 mole ratio solutions of 1.25 mM 2-naphthol:CD prepared in D_2O. The CDs examined included βCD, cmβCD, and βCDida. The concentration of Cd^{2+} was varied from 0 mM (no Cd^{2+} present) to 1.25 mM, to yield equimolar concentrations of all species present. The proton spectra of 2-naphthol and the CD in solution were monitored for changes in the observed chemical shifts as the Cd^{2+} concentration was increased. Figure 5.7 shows the proton NMR spectra of 2-naphthol for 1:1:0 2-naphthol:βCDida:Cd^{2+} (top) and 1:1:1 2-naphthol: βCDida:Cd^{2+} (bottom). Figure 5.8 shows the proton NMR spectra of βCDida from 4.4 to 3.2 ppm for 1:1:0 2-naphthol:CD:Cd^{2+} (top) and 1:1:1 2-naphthol:CD:Cd^{2+} (bottom).

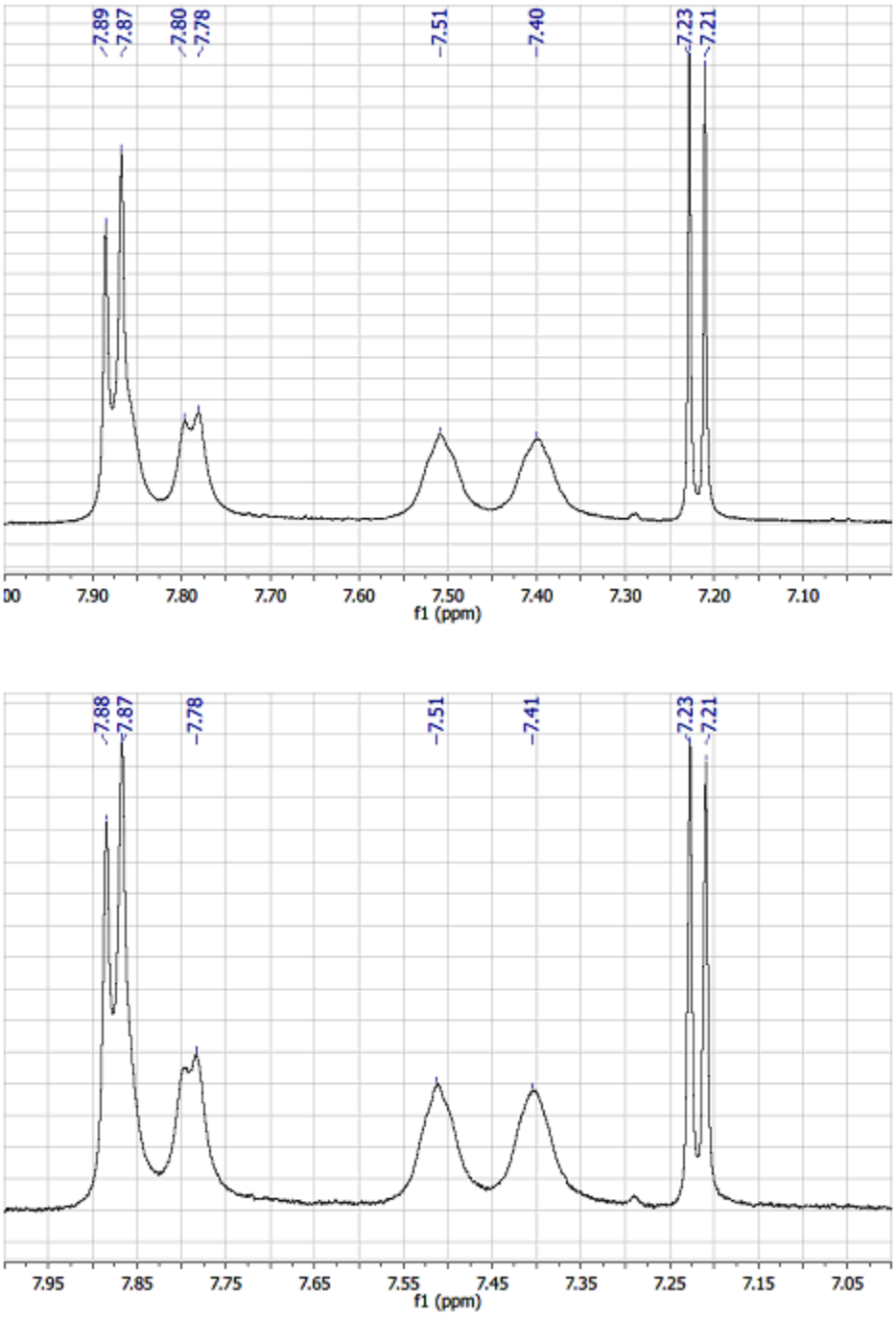

Figure 5.7. Proton NMR spectra of 2-naphthol for 1:1:0 2-naphthol:βCDida:Cd^{2+} (top) and 1:1:1 2-naphthol:CD:Cd^{2+} (bottom)

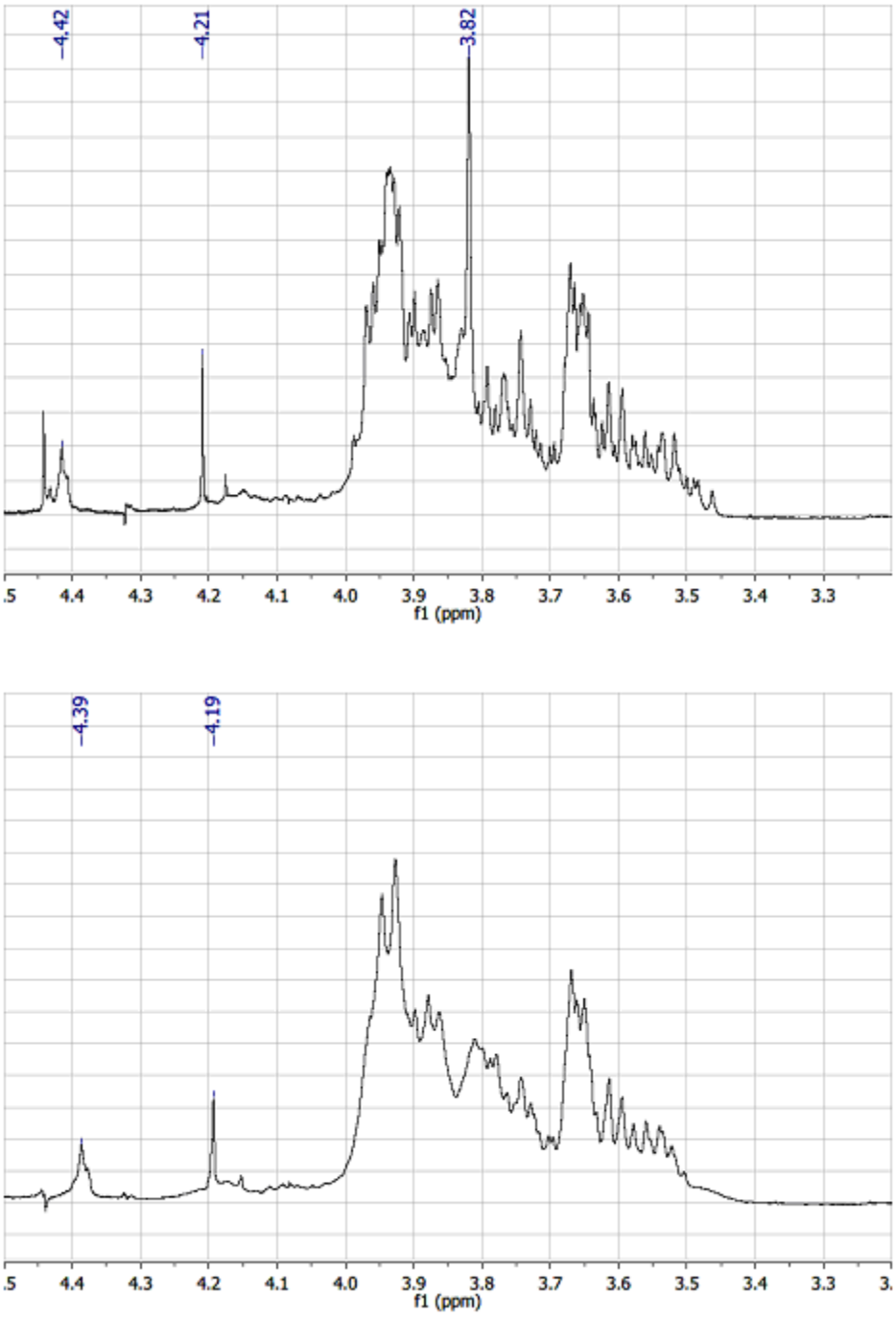

Figure 5.8. Proton NMR spectra of βCDida from 4.4 to 3.2 ppm for 1:1:0 2-naphthol:βCDida:Cd^{2+} (top) and 1:1:1 2-naphthol:CD:Cd^{2+} (bottom).

While addition of Cd^{2+} shows no effect on the chemical shifts for complexed 2-naphthol, significant changes in the proton spectra for βCDida are observed upon addition of Cd^{2+}. Loss of

the chemical shift peak at 3.82 ppm (Figure 5.8, top) as well as changes in the chemical shifts for other protons associated with the ida ligand group near 4.4 and 4.2 ppm (see Figure 5.5) are a clear indication that Cd^{2+} is coordinating to βCDida. The changes in chemical shifts demonstrate that changes in the localized structure are occurring upon chelation of Cd^{2+} by βCDida. Additionally, Cd^{2+} shows no impact upon the complexation of 2-naphthol with βCDida (Figure 5.7). Studies of ternary complexes of 2-naphthol/cmβCD/Cd^{2+} and 2-naphthol/βCD/Cd^{2+} showed similar results to the study of 2-naphthol/ βCDida /Cd^{2+} complexes, though weaker interaction between the CD and Cd^{2+} were observed, especially for βCD. While binding constants for TNT with the CDs examined in the study were not determined by NMR, the results of the 2-naphthol ternary complex studies data indicate that metal complexation does not interfere with the binding of molecules pre-associated in the CD cavity.

Summary

While attempts at the determination of K_a values for TNT/CD complexes were unsuccessful, the data collected from the UV and chromatographic methods does demonstrate that TNT forms complexes with CDs. However, the binding constants for those interactions could not be determined with the methods attempted. The NMR studies of the 2-naphthol/CD/Cd^{2+} systems, were more successful, and showed evidence of ternary complex formation. This evidence further supports conclusions presented in the earlier chapters about the importance of ternary complex formation in the Fenton reaction systems with TNT and CDs. Complexed Fe^{2+} would lead to an increase in the localized concentration of hydroxyl radicals near the bound Fe^{2+} and this clearly would have an impact on degradation rates of TNT pre-associated with the CD.

CHAPTER 6

SUMMARY AND CONCLUSIONS

The work presented in this dissertation examined the role of CDs in the Fenton oxidation of TNT, specifically: 1) the kinetics of TNT degradation in the presence of CDs for a Fenton reaction system, 2) the products of these reactions through chromatographic and mass spectrometric methods, and 3) NMR and binding studies of binary and ternary complexes. The results of these studies provided a number of new insights into the role of CDs in Fenton reactions systems. Specifically, knowledge of the impact of CDs on the kinetics and product distribution of TNT degradation was significantly expanded.

The kinetic studies conducted during the initial phase of the research presented in this dissertation clearly demonstrate that CDs play a significant role in changes in the kinetics of TNT degradation during Fenton reactions. The enhancement showed some dependence on pH, but over the time frames studied the relative rate constants versus control reactions conducted in water showed as high as a 7-fold increase for some CDs. The existence of both an oxidative and reductive pathway was indicated by the presence of TNB and 4-ADNT in the reactions containing CD and d-glucose. The presence of the reductive pathway, as indicated by the presence of 4-ADNT had not been previously described in the literature. The presence of a reductive pathway indicates that increased reaction rates cannot be explained solely by increases in oxidative rates. Pre-association of TNT with the secondary CD radicals formed during the Fenton reaction clearly play a role in the increased degradation rates of TNT relative to control reactions. This is evidenced by the higher TNT degradation rates observed in the presence of

CDs, compared to d-glucose, which is likely due to pre-association of TNT with the secondary CD radicals formed during the Fenton reaction. However, the contribution to changes in the TNT degradation rates occurring from alteration in oxidative rates due to complexation of $Fe^{2+/3+}$ and TNT, reduction of TNT, and scavenging of hydroxyl radicals by CDs and secondary reaction products makes evaluation of the impact of any individual mechanism extremely difficult.

The results of the mass spectrometric studies of reaction products show that while CD assisted Fenton reactions have shown the potential to significantly increase the kinetics of nitroaromatic degradation compared to typical Fenton systems, they also increase the complexity of the product distribution. The presence of the reductive pathways leading to the formation of nitroso and amine products for the Fenton reaction of TNT when CDs are present have not been previously reported in the literature. Additionally, the formation of trinitrobenzyl alcohol and hydroxydinitrobenzyl alcohol has not been previously found to occur in Fenton processes. The increased complexity of the product distribution, due to the presence of both an oxidative and reductive pathway, must be carefully evaluated before using CD assisted Fenton reactions as a remediation technology. The availability of multiple degradation pathways also has the potential to impact the degree of mineralization observed in the CD assisted Fenton systems as compared to typical Fenton systems.

While attempts at the determination of K_a values for TNT/CD complexes were unsuccessful, the data collected from the UV and chromatographic methods does demonstrate that TNT forms complexes with CDs. However, the binding constants for those interactions could not be determined with the methods attempted. The NMR studies of the 2-naphthol/CD/Cd^{2+} systems, were more successful, and showed evidence of ternary complex formation. These evidence further supports conclusions presented in the earlier chapters about

the importance of ternary complex formation in the Fenton reaction systems with TNT and CDs. Complexed Fe^{2+} would lead to an increase in the localized concentration of hydroxyl radicals near the bound Fe^{2+} and this clearly would have an impact on degradation rates of TNT pre-associated with the CD.

In conclusion, the role of CDs in accelerating the degradation rates of small organic compounds, and specifically TNT, is significantly more complicated than just providing a route to enhanced oxidative processes through complex formation. While it is obvious that complexes do form and do play a role in the enhancement, multiple processes along both oxidative and reductive pathways are occurring. The complexity of these systems is readily demonstrated by the numerous degradation products described. The results of these studies indicate that CDs do potentially have a role in increasing the efficiency and utility of the Fenton reaction for environmental remediation.

References

1. Pignatello, J.J., E. Oliveros, and A. MacKay, *Advanced oxidation processes for organic contaminant destruction based on the Fenton reaction and related chemistry.* Critical Reviews in Environmental Science and Technology, 2006. **36**(1): p. 1-84.
2. Goi, A., N. Kulik, and M. Trapido, *Combined chemical and biological treatment of oil contaminated soil.* Chemosphere, 2006. **63**(10): p. 1754-1763.
3. Morelli, R., et al., *Fenton-Dependent Damage to Carbohydrates: Free Radical Scavenging Activity of Some Simple Sugars.* Journal of Agricultural and Food Chemistry, 2003. **51**(25): p. 7418-7425.
4. Kavitha, V. and K. Palanivelu, *The role of ferrous ion in Fenton and photo-Fenton processes for the degradation of phenol.* Chemosphere, 2004. **55**(9): p. 1235-1243.
5. Fenton, H.J.H., *Oxidation of tartaric acid in the presence of iron.* Journal of the Chemical Society 1894. **65**: p. 899-910.
6. Haber, F. and J. Weiss, *The catalytic decomposition of of hydrogen peroxide by iron salts.* Proceedings of the Royal Society, A., 1934. **134**: p. 332-351.
7. Barb, W.G., J.H. Baxendale, and P. George, *Reactions of ferrous and ferric ions with hydrogen peroxide.* Nature, 1949. **163**: p. 692-694.
8. Barb, W.G., et al., *Reactions of ferrous and ferric ions with hydrogen peroxide. Part I.- The ferrous reaction.* Transactions of the Faraday Society, 1951. **47**: p. 462-500.
9. Barb, W.G., et al., *Reaction of ferrous and ferric ions with hydrogen peroxide. Part II.- The ferric ion reaction.* Transactions of the Faraday Society, 1951. **47**: p. 591-616.
10. Chen, R. and J.J. Pignatello, *Role of Quinone Intermediates as Electron Shuttles in Fenton and Photoassisted Fenton Oxidations of Aromatic Compounds.* Environmental Science & Technology, 1997. **31**(8): p. 2399-2406.
11. Sawyer, D.T., A. Sobkowiak, and T. Matsushita, *Metal (MLx=Fe, Cu, Co, Mn]/hydroperoxide induced activation of dioxygen for the oxygenation of hydrocarbons: oxygenated Fenton chemistry.* Accounts of Chemical Research, 1996. **29**: p. 409-416.
12. Bossmann, S.H., et al., *New Evidence against Hydroxyl Radicals as Reactive Intermediates in the Thermal and Photochemically Enhanced Fenton Reactions.* The Journal of Physical Chemistry A, 1998. **102**(28): p. 5542-5550.
13. Ayoub, K., et al., *Application of advanced oxidation processes for TNT removal: A review.* Journal of Hazardous Materials, 2010. **178**(13): p. 10-28.
14. Lundstedt, S., Y. Persson, and L. Öberg, *Transformation of PAHs during ethanol-Fenton treatment of an aged gasworks' soil.* Chemosphere, 2006. **65**(8): p. 1288-1294.
15. Von Sonntag, C. and H.P. Schuchmann, *Peroxyl radicals in aqueous solutions*, in *Peroxyl Radicals*, Z.B. Alfassi, Editor. 1997, John Wiley and Sons: New York. p. 173-234.
16. Watts, R.J., et al., *Role of Reductants in the Enhanced Desorption and Transformation of Chloroaliphatic Compounds by Modified Fenton's Reactions.* Environmental Science & Technology, 1999. **33**: p. 3432-3437.
17. Peyton, G.R., et al., *Reductive Destruction of Water Contaminants during Treatment with Hydroxyl Radical Processes.* Environmental Science & Technology, 1995. **29**(6): p. 1710-1712.

18. Buxton, G.V., et al., *Critical Review of rate constants for reactions of hydrated electrons, hydrogen atoms and hydroxyl radicals ([center-dot]OH/[center-dot]O[sup -] in Aqueous Solution.* Journal of Physical and Chemical Reference Data, 1988. **17**(2): p. 513-886.
19. Tarr, M., *Fenton and modified Fenton methods for pollutant degradation*, in *Chemical Degradation Methods for Wastes and Pollutants: Environmental and Industrial Applications*, M. Tarr, Editor. 2003, Marcel Dekker, Inc. p. 484.
20. Yardin, G. and S. Chiron, *Photo-Fenton treatment of TNT contaminated soil extract solutions obtained by soil flushing with cyclodextrin.* Chemosphere, 2006. **62**: p. 1395-1402.
21. Lindsey, M.E., et al., *Enhanced Fenton degradation of hydrophobic organics by simultaneous iron and pollutent complexation with cyclodextrins.* The Science of the Total Environment, 2002.
22. Matta, R., K. Hanna, and S. Chiron, *Fenton-like oxidation of 2,4,6-trinitrotoluene using different iron minerals.* Science of the Total Environment, 2007. **385**(1-3): p. 242-251.
23. Murati, M., et al., *Electro-Fenton Treatment of TNT in Aqueous Media in Presence of Cyclodextrin. Application to Ex-situ Treatment of Contaminated Soil.* Journal of Advanced Oxidation Technologies, 2009. **12**(1): p. 29-36.
24. Zazo, J.A., et al., *Chemical Pathway and Kinetics of Phenol Oxidation by Fenton's Reagent.* Environmental Science & Technology, 2005. **39**(23): p. 9295-9302.
25. Li, Z.M., S.D. Comfort, and P.J. Shea, *Destruction of 2,4,6-Trinitrotoluene by Fenton Oxidation.* Journal of Environmental Quality, 1997. **26**(2): p. 480-487.
26. Pignatello, J.J., *Dark and photoassisted iron(3+)-catalyzed degradation of chlorophenoxy herbicides by hydrogen peroxide.* Environmental Science & Technology, 1992. **26**(5): p. 944-951.
27. Sun, Y. and J.J. Pignatello, *Chemical treatment of pesticide wastes. Evaluation of iron(III) chelates for catalytic hydrogen peroxide oxidation of 2,4-D at circumneutral pH.* Journal of Agricultural and Food Chemistry, 1992. **40**(2): p. 322-327.
28. Pignatello, J.J. and Y. Sun, *Photo-Assisted Mineralization of Herbicide Wastes by Ferric Ion Catalyzed Hydrogen Peroxide*, in *Emerging Technologies in Hazardous Waste Management III*. 1993, American Chemical Society. p. 77-84.
29. Sun, Y. and J.J. Pignatello, *Photochemical reactions involved in the total mineralization of 2,4-D by iron(3+)/hydrogen peroxide/UV.* Environmental Science & Technology, 1993. **27**(2): p. 304-310.
30. Sun, Y. and J.J. Pignatello, *Organic intermediates in the degradation of 2,4-dichlorophenoxyacetic acid by iron(3+)/hydrogen peroxide and iron(3+)/hydrogen peroxide/UV.* Journal of Agricultural and Food Chemistry, 1993. **41**(7): p. 1139-1142.
31. Sato, C., et al., *Decomposition of Perchloroethylene and Polychlorinated Biphenyls with Fenton's Reagent*, in *Emerging Technologies in Hazardous Waste Management III*. 1993, American Chemical Society. p. 343-356.
32. Lin, S.H. and C.C. Lo, *Fenton process for treatment of desizing wastewater.* Water Research, 1997. **31**(8): p. 2050-2056.
33. Tang, W.Z. and S. Tassos, *Oxidation kinetics and mechanisms of trihalomethanes by Fenton's reagent.* Water Research, 1997. **31**(5): p. 1117-1125.
34. Murray, C.A. and S.A. Parsons, *Removal of NOM from drinking water: Fenton's and photo-Fenton's processes.* Chemosphere, 2004. **54**(7): p. 1017-1023.

35. Pignatello, J.J., D. Liu, and P. Huston, *Evidence for an Additional Oxidant in the Photoassisted Fenton Reaction.* Environmental Science & Technology, 1999. **33**(11): p. 1832-1839.
36. Arienzo, M., J. Chiarenzelli, and R. Scrudato, *Remediation of metal-contaminated aqueous systems by electrochemical peroxidation: an experimental investigation.* Journal of Hazardous Materials, 2001. **87**(1-3): p. 187-198.
37. Kuo, W.G., *Decolorizing dye wastewater with Fenton's reagent.* Water Research, 1992. **26**(7): p. 881-886.
38. Mosteo, R., et al., *Sequential Solar Photo-Fenton-Biological System for the Treatment of Winery Wastewaters.* Journal of Agricultural and Food Chemistry, 2008. **56**(16): p. 7333-7338.
39. Mosteo, R., et al., *Factorial experimental design of winery wastewaters treatment by heterogeneous photo-Fenton process.* Water Research, 2006. **40**(8): p. 1561-1568.
40. Khoufi, S., F. Aloui, and S. Sayadi, *Treatment of olive oil mill wastewater by combined process electro-Fenton reaction and anaerobic digestion.* Water Research, 2006. **40**(10): p. 2007-2016.
41. Pérez, M., et al., *Removal of organic contaminants in paper pulp treatment effluents under Fenton and photo-Fenton conditions.* Applied Catalysis B: Environmental, 2002. **36**(1): p. 63-74.
42. Sevimli, M.F., *Post-Treatment of Pulp and Paper Industry Wastewater by Advanced Oxidation Processes.* Ozone: Science & Engineering: The Journal of the International Ozone Association, 2005. **27**(1): p. 37 - 43.
43. Chen, W.-S., C.-N. Juan, and K.-M. Wei, *Mineralization of dinitrotoluenes and trinitrotoluene of spent acid in toluene nitration process by Fenton oxidation.* Chemosphere, 2005. **60**(8): p. 1072-1079.
44. Watts, R., M. Udell, and R. Monsen, *Use of Iron Minerals in Optimizing the Peroxide Treatment of Contaminated Soils.* Water Environment Research, 1993. **65**(7): p. 839-844.
45. Martens, D. and W. Frankenberger, *Enhanced Degradation of Polycyclic Aromatic Hydrocarbons in Soil Treated with an Advanced Oxidative Process - Fenton's Reagent.* Journal of Soil Contamination, 1995. **4**(2): p. 175-190.
46. Lu, M., et al., *Removal of residual contaminants in petroleum-contaminated soil by Fenton-like oxidation.* Journal of Hazardous Materials, 2010. **179**(1-3): p. 604-611.
47. Peters, S.M., T.T. Wong, and J.G. Agar. *A Laboratory Study on the Degradation of Gasoline Contamination Using Fenton's Reagent*. in *54th Canadian Geotechnical Conference*. 2001. Calgary, Alberta Canada: The Canadian Geotechnical Society.
48. Watts, R.J. and S.E. Dilly, *Evaluation of iron catalysts for the Fenton-like remediation of diesel-contaminated soils.* Journal of Hazardous Materials, 1996. **51**(1-3): p. 209-224.
49. Baehr, K. and J.J. Pignatello, *Ferric complexes as catalysts for "Fenton" degradation of 2,4-D and metolachlor in soil.* Journal of Environmental Quality, 1994. **23**: p. 365-370.
50. Pignatello, J.J. and M. Day, *Mineralization of methyl parathion insecticide in soil by hydrogen peroxide activated with iron(III)-NTA or HEIDA complexes.* Hazardous Waste and Hazardous Materials, 1996. **13**: p. 237-244.
51. Anipsitakis, G.P. and D.D. Dionysiou, *Radical Generation by the Interaction of Transition Metals with Common Oxidants.* Environmental Science & Technology, 2004. **38**(13): p. 3705-3712.

52. Wilbrand, J., *Notiz über Trinitrotoluol.* Annalen der Chemie und Pharmacie, 1863. **128**: p. 178-179.
53. Hathaway, J.A., *Toxicity of Nitroaromatic Compounds*. Chemical Industry Institute of Toxicology Series, ed. D.E. Rickert. 1985, New York: Hemisphere Publishing Corporation.
54. Schmelling, D.C., K.A. Gray, and P.V. Kamat, *Role of Reduction in the Photocatalytic Degradation of TNT.* Environmental Science & Technology, 1996. **30**(8): p. 2547-2555.
55. ATSDR, *Toxicological Profile of 2,4,6-Trinitrotoluene*, ATSDR, Editor. 1995, U.S. Department of Health and Human Services.
56. Bordeleau, G., et al., *Environmental Impacts of Training Activities at an Air Weapons Range.* Journal of Environmental Quality, 2008. **37**(2): p. 308-317.
57. Hathaway, J.A., *Trinitrotoluene: A Review of Reported Dose-Related Effects Providing Documentation for a Workplace Standard.* Journal of Occupational Medicine, Vol. 19, No. 5, pages 341-345, 1977.
58. Dilley, J.V., et al., *Short-term oral toxicity of a 2,4,6-trinltrotoluene and hexahydro-1,3,5-trinitro-1,3,5-triazine mixture in mice, rats, and dogs.* Journal of Toxicology and Environmental Health, 1982. **9**(4): p. 587 - 610.
59. Neuwoehner, J., et al., *Toxicological Characterization of 2,4,6-Trinitrotoluene, its Transformation Products, And Two Nitramine Explosives.* Environmental Toxicology and Chemistry, 2007. **26**(6): p. 1090-1099.
60. Liou, M.J., M.C. Lu, and J.N. Chen, *Oxidation of TNT by photo-Fenton process.* Chemosphere, 2004. **57**(9): p. 1107-1114.
61. Grummt, T., et al., *Genotoxicity of nitrosulfonic acids, nitrobenzoic acids, and nitrobenzylalcohols, pollutants commonly found in ground water near ammunition facilities.* Environmental and Molecular Mutagenesis, 2006. **47**: p. 95-106.
62. Dodard, S.G., et al., *Ecotoxicity characterization of dinitrotoluenes and some of their reduced metabolites.* Chemosphere, 1999. **38**: p. 2071-2079.
63. Dryzga, O., et al., *Toxicity of explosives and related compounds to the luminescent bacterium Vibrio fischeri NRRL-B-11177.* Archives of Environmental Contamination and Toxicology, 1995. **51**(229-235).
64. Maeda, T., et al., *Relationship Between Mutagenicity and Reactivity or Biodegradability for Nitroaromatic Compounds.* Environmental Toxicology and Chemistry, 2007. **26**(2): p. 237-241.
65. Achtnich, C., et al., *Stability of Immobilized TNT Derivatives in Soil as a Function of Nitro Group Reduction.* Environmental Science & Technology, 2000. **34**(17): p. 3698-3704.
66. Lewis, T., D. Newcombe, and R. Crawfold, *Bioremediation of soils contaminated with explosives.* Journal of Environmental Management, 2004. **70**: p. 291-307.
67. USEPA. *Former Nebraska Ordnance Plant*. 2009 [cited; Available from: http://www.epa.gov/region7/cleanup/npl_files/ne6211890011.pdf.
68. Walsh, M.E., C.A. Ramsey, and T.F. Jenkins, *The effect of particle size reduction by grinding on subsampling variance for explosives residues in soil.* Chemosphere, 2002. **49**(10): p. 1267-1273.
69. Jenkins, T.F., et al., *Identity and distribution of residues of energetic compounds at army live-fire training ranges.* Chemosphere, 2006. **63**(8): p. 1280-1290.

70. Hawari, J., et al., *Microbial degradation of explosives: biotransformation versus mineralization.* Applied Microbiology and Technology, 2000. **54**: p. 605-618.
71. Travis, E.R., et al., *Impact of Transgenic Tobacco on Trinitrotoluene (TNT) Contaminated Soil Community.* Environmental Science & Technology, 2007. **41**(16): p. 5854-5861.
72. USEPA. *Integrated Risk Information System (IRIS) - 2,4,6-Trinitrotoluene*. 2002 [cited; Available from: http://www.epa.gov/iris/subst/0269.htm.
73. Wollin, K.M. and H.H. Dieter, *Toxicological Guidelines for Monocyclic Nitro-, Amino- and Aminonitroaromatics, Nitramines, and Nitrate Esters in Drinking Water.* Archives of Environmental Contamination and Toxicology, 2005. **49**(1): p. 18-26.
74. Rogers, J.D. and N.J. Bunce, *Treatment methods for the remediation of nitro aromatic explosives (Review).* Water Research, 2001. **35**: p. 2101-2111.
75. Achtnich, C., et al., *Reductive Transformation of Bound Trinitrophenyl Residues and Free TNT during a Bioremediation Process Analyzed by Immunoassay.* Environmental Science & Technology, 1999. **33**(19): p. 3421-3426.
76. Ro, K.S., et al., *Solubility of 2,4,6-Trinitrotoluene (TNT) in Water.* Journal of Chemical Engineering Data, 1996. **41**: p. 758-761.
77. Weis, M., et al., *Fate and Metabolism of [15N]2,4,6-Trinitrotoluene In Soil.* Environmental Toxicology and Chemistry, 2004. **23**(8): p. 1852-1860.
78. Eriksson, J., et al., *Binding of 2,4,6-Trinitrotoluene, Aniline, and Nitrobenzene to Dissolved and Particulate Soil Organic Matter.* Environmental Science & Technology, 2004. **38**(11): p. 3074-3080.
79. Douglas, T.A., et al., *A time series investigation of the stability of nitramine and nitroaromatic explosives in surface water samples at ambient temperature.* Chemosphere, 2009. **76**(1): p. 1-8.
80. Bandstra, J.Z., et al., *Reduction of 2,4,6-Trinitrotoluene by Iron Metal: Kinetic Controls on Product Distributions in Batch Experiments.* Environmental Science & Technology, 2005. **39**(1): p. 230-238.
81. Bradley, P.M. and F.H. Chapelle, *Factors Affecting Microbial 2,4,6-Trinitrotoluene Mineralization in Contaminated Soil.* Environmental Science & Technology, 1995. **29**(3): p. 802-806.
82. Daun, G., et al., *Biological Treatment of TNT-Contaminated Soil. 1. Anaerobic Cometabolic Reduction and Interaction of TNT and Metabolites with Soil Components.* Environmental Science & Technology, 1998. **32**(13): p. 1956-1963.
83. Hofstetter, T.B., et al., *Complete Reduction of TNT and Other (Poly)nitroaromatic Compounds under Iron-Reducing Subsurface Conditions.* Environmental Science & Technology, 1999. **33**(9): p. 1479-1487.
84. Dunnivant, F.M., R.P. Schwarzenbach, and D.L. Macalady, *Reduction of substituted nitrobenzenes in aqueous solutions containing natural organic matter.* Environmental Science & Technology, 1992. **26**(11): p. 2133-2141.
85. Thorn, K.A., J.C. Pennington, and C.A. Hayes, *^{15}N NMR Investigation of the Reduction and Binding of TNT in an Aerobic Bench Scale Reactor Simulating Windrow Composting.* Environmental Science & Technology, 2002. **36**(17): p. 3797-3805.
86. Thorn, K.A., et al., *N-15 NMR Study of the Immobilization of 2,4- and 2,6-Dinitrotoluene in Aerobic Compost.* Environmental Science & Technology, 2008. **42**(7): p. 2542-2550.

87. Thorn, K.A. and K.R. Kennedy, *15N NMR Investigation of the Covalent Binding of Reduced TNT Amines to Soil Humic Acid, Model Compounds, and Lignocellulose.* Environmental Science & Technology, 2002. **36**(17): p. 3787-3796.
88. Weiß, M., et al., *Fate and Metabolism of [15N]2,4,6-Trinitrotoluene In Soil.* Environmental Toxicology and Chemistry, 2004. **23**(8): p. 1852-1860.
89. Szejtli, J., *Introduction and General Overview of Cyclodextrin Chemistry.* Chemical Reviews, 1998. **98**(5): p. 1743-1754.
90. Szente, L. and J. Szejtli, *Non-chromatographic analytical uses of cyclodextrins.* Analyst, 1998. **123**: p. 735-741.
91. Connors, K.A., *The Stability of Cyclodextrin Complexes in Solution.* Chemical Reviews, 1997. **97**(5): p. 1325-1358.
92. Sheremata, T. and J. Hawari, *Cyclodextrins for Desorption and Solubilization of 2,4,6-Trinitrotoluene and Its Metabolites from Soil.* Environmental Science and Technology, 2000. **34**: p. 3462-3468.
93. Villiers, A., *Sur la transformation de la fécule en dextrine par le ferment butyrique.* Les Comptes Rendus de l'Académie des sciences, 1891: p. 435-438.
94. Schardinger, F., Wiener Klinische Wochenschrift, 1904. **17**: p. 207.
95. Schardinger, F., *Bacillus macerans.* Zentralbl. Bakteriol. Parasintenk. Abt. 2, 1905. **14**: p. 772.
96. Schardinger, F., *Bildung kristallisierter Polysaccharide (Dextrine) aus Starke kleister durch Mikrobien.* Zentralbl. Bakteriol. Parasintenk. Abt. 2, 1911. **29**: p. 188-197.
97. Freudenberg, K., H. Boppel, and M. Meyer-Delius, Naturwissenschaften, 1938. **26**: p. 123.
98. Freudenberg, K. and F. Cramer, Zeitschrift fur Naturforschung 3b, 1948: p. 464.
99. Freudenberg, K. and M. Meyer-Delius, Berichte der Deutschen Chemischen Gesellschaft, 1938. **71**: p. 1596.
100. Freudenberg, K. and W. Rapp, Berichte der Deutschen Chemischen Gesellschaft, 1936. **69**: p. 2041.
101. Freudenberg, K. and R. Jacobi, *Über Schardinger Dextrine aus Stärke.* Liebigs Annalen der Chemie, 1935. **518**: p. 102-108.
102. French, D., *The Schardinger Dextrins.* Advances in Carbohydrate Chemistry, 1957(12): p. 189-260.
103. Cramer, F., *Einschlussverbindungen*. 1954, Berlin: Springer-Verlag.
104. Loftsson, T. and D. Duchêne, *Cyclodextrins and their pharmaceutical applications.* International Journal of Pharmaceutics, 2007. **329**(1-2): p. 1-11.
105. McCray, J.E. and M.L. Brusseau, *Cyclodextrin-Enhanced In Situ Flushing of Multiple-Component Immiscible Organic Liquid Contamination at the Field Scale: Analysis of Dissolution Behavior.* Environmental Science & Technology, 1999. **33**(1): p. 89-95.
106. Brusseau, M.L., X. Wang, and Q. Hu, *Enhanced Transport of Low-Polarity Organic Compounds through Soil by Cyclodextrin.* Environmental Science & Technology, 1994. **28**(5): p. 952-956.
107. McCray, J.E. and M.L. Brusseau, *Cyclodextrin-Enhanced in Situ Flushing of Multiple-Component Immiscible Organic Liquid Contamination at the Field Scale: Mass Removal Effectiveness.* Environmental Science & Technology, 1998. **32**(9): p. 1285-1293.
108. Wang, J.M., et al., *Cyclodextrin-Enhanced Biodegradation of Phenanthrene.* Environmental Science & Technology, 1998. **32**(13): p. 1907-1912.

109. Skold, M.E., et al., *Enhanced Solubilization of a Metal and Organic Contaminant Mixture (Pb, Sr, Zn, and Perchloroethylene) by Cyclodextrin.* Environmental Science & Technology, 2008. **42**(23): p. 8930-8934.
110. Wang, X. and M.L. Brusseau, *Simultaneous Complexation of Organic Compounds and Heavy Metals by a Modified Cyclodextrin.* Environmental Science & Technology, 1995. **29**(10): p. 2632-2635.
111. Wei, B. and M. Tarr, *Role of cyclodextrins in Fenton remediation of TNT (2,4,6-trinitrotoluene).* in *225th ACS National Meeting*. 2003, American Chemical society: New Orleans, LA.
112. Boving, T.B., X. Wang, and M.L. Brusseau, *Cyclodextrin-Enhanced Solubilization and Removal of Residual-Phase Chlorinated Solvents from Porous Media.* Environmental Science & Technology, 1999. **33**(5): p. 764-770.
113. Donnelly, K.C., et al., *Mutagenic interactions of model chemical mixtures.* Chemosphere, 1998. **37**(7): p. 1253-61.
114. Sandow, M., et al., *Complexes of 6^A-(2-Aminomethylamino)-6^A-deoxy-B-cyclodextrin and 6^A-[Bis(carboxylatomethyl)amino]-6^A-deoxy-B-cyclodextrin with (R)- and (S)-Tryptophanate and (R)- and (S)-Phenylalaninate in Aqueous Solution. A pH Titrimetric and N.M.R. Spectroscopic Study.* Australian Journal of Chemistry, 1999. **42**: p. 1143-1150.
115. Zheng, W. and M.A. Tarr, *Evidence for the Existence of Ternary Complexes of Iron, Cyclodextrin, and Hydrophobic Guests in Aqueous Solution.* Journal of Physical Chemistry B, 2004. **108**: p. 10172-10176.
116. Zheng, W. and M. Tarr, *Assessment of ternary iron-cyclodextrin-2-naphthol complexes using NMR and fluorescence spectroscopies.* Spectrochimica Acta, Part A: Molecular and Biomolecular Spectroscopy, 2006. **65A**(5): p. 1098-1103.
117. Sandow, M., et al., *Binary and ternary metallo-β-cyclodextrins of 6^A-[Bis(carboxylatomethyl)amino]-6^A-deoxy-β-cyclodextrin.* Australian Journal of Chemistry, 2000. **53**: p. 149-153.
118. Pham, D.-T., et al., *1H NMR studies of enantioselective host-guest complexation by modified .beta.-cyclodextrins and their europium(III) complexes.* Tetrahedron Asymmetry, 2008. **19**(2): p. 165-175.
119. *Hyperquad 2003*, Protonic Software: 2, Templegate Avenue, Leeds LS15 OHD, UK.
120. Alderighi, L., et al., Coordination Chemistry Reviews, 1999. **184**: p. 311.
121. Martel, A. and R. Smith, *Critical Stability Constants, Volume 1: Amino Acids*. 1974, New York and London: Plenum Press.
122. May, B.L., et al., Journal of the Chemical Society, Perkins Transactions, 1997. **1**: p. 3157.
123. Lindsey, M. and M. Tarr, *Inhibition of hydroxyl radical reaction with aromatics by dissolved organic matter.* Environmental Science & Technology, 2000. **34**(3): p. 6.
124. Emmrich, M., *Kinetics of the Alkaline Hydrolysis of Important Nitroaromatic Co-contaminants of 2,4,6-Trinitrotoluene in Highly Contaminated Soils.* Environmental Science & Technology, 2001. **35**(5): p. 874-877.
125. Ussher, S.J., et al., *Effect of Model Ligands on Iron Redox Speciation in Natural Waters Using Flow Injection with Luminol Chemiluminescence Detection.* Analytical Chemistry, 2005. **77**(7): p. 1971-1978.

126. Marangon, K., et al., *Comaprison of the effect of alpha-lipoic acid and alpha-tocopherol supplementation on meaures of oxidative stress.* Free Radical Biology and Medicine, 1999. **27**(9/10): p. 1114-1121.
127. Quaranta, A., et al., *Single and double reduction of C60 in 2:1 [gamma]-cyclodextrin/[60]fullerene inclusion complexes by cyclodextrin radicals.* Chemical Physics, 2008. **354**(1-3): p. 174-179.
128. Deeble, D.J., B.J. Parsons, and G.O. Phillips, *Medical, Biochemical and Chemical Aspects of Free Radicals*, in *Medical, Biochemical and Chemical Aspects of Free Radicals*, O. Hayaishi, et al., Editors. 1989, Elsevier: Amsterdam, The Netherlands. p. 505-510.
129. Gilbert, B.C., et al., *Free-radical reactions of carbohydrate moieties in macromolecular structures. EPR evidence for the importance of steric and stereoelectronic effects and for the influence of inclusion in cyclodextrins.* Journal of the Chemical Society, Perkins Transactions 2, 2000. **2**: p. 2001-2007.
130. Hess, T., et al., *Studies on nitroaromatic compound degradation in modified Fenton reactions by electrospray ionization tandem mass spectrometry (ESI-MS-MS).* The Analyst, 2003. **128**: p. 156-160.
131. Arienzo, M., *Use of abiotic oxidative-reductive technologies for remediation of munition contaminated soil in a bioslurry reactor.* Chemosphere, 2000. **40**(4): p. 441-448.
132. Hundal, L.S., et al., *Removal of TNT and RDX from water and soil using iron metal.* Environmental Pollution, 1997. **97**(1-2): p. 55-64.
133. Pignatello, J.J., E. Oliveros, and A. MacKay, *Advanced Oxidation Processes for Organic Contaminant Destruction Based on the Fenton Reaction and Related Chemistry.* Critical Reviews in Environmental Science and Technology, 2006. **36**: p. 1-84.
134. Dacons, J.C., H.G. Adolph, and M.J. Kamlet, *Novel observations concerning the thermal decomposition of 2,4,6-trinitrotoluene.* The Journal of Physical Chemistry, 1970. **74**(16): p. 3035-3040.
135. Godejohann, M., et al., *Application of Continuous-Flow HPLC-Proton-Nuclear Magnetic Resonance Spectroscopy and HPLC-Thermospray-Mass Spectroscopy for the Structural Elucidation of Phototransformation Products of 2,4,6-Trinitrotoluene.* Analytical Chemistry, 1998. **70**(19): p. 4104-4110.
136. Vasilyeva, G.K., V.D. Kreslavski, and P.J. Shea, *Catalytic oxidation of TNT by activated carbon.* Chemosphere, 2002. **47**(3): p. 311-317.
137. Ravelet, C., et al., *Stoichiometry and Formation Constants of Six PAHs with γ-Cyclodextrin, Determined by HPLC Using a Cyano Stationary Phase.* Journal of Liquid Chromatography & Related Technologies, 2002. **25**(3): p. 421.
138. Schneider, H.J., et al., *NMR Studies of Cyclodextrins and Cyclodextrin Complexes.* Chemical Reviews, 1998. **98**(5): p. 1755-1786.
139. Fujimura, K., et al., *Reversed-phase retention behavior of aromatic compounds involving .beta.-cyclodextrin inclusion complex formation in the mobile phase.* Analytical Chemistry, 1986. **58**(13): p. 2668-2674.
140. Dotsikas, Y. and Y.L. Loukas, *Efficient determination and evaluation of model cyclodextrin complex binding constants by electrospray mass spectrometry.* Journal of the American Society for Mass Spectrometry, 2003. **14**(10): p. 1123-1129.
141. Fielding, L., *Determination of Association Constants (Ka) from Solution NMR Data.* Tetrahedron, 2000. **56**(34): p. 6151-6170.

142. Benesi, H.A. and J.H. Hildebrand, *A Spectrophotometric Investigation of the Interaction of Iodine with Aromatic Hydrocarbons.* 1949. **71**(8): p. 2703-2707.
143. Harris, D., *Quantitative Chemical Analysis*. 4th ed. 1995, New York: W.H. Freeman and Company.
144. Hynes, M.J., *WinEQNMR2 A Program for the calculation of equilibrium constants from NMR chemical shift data*. 2008.
145. Hynes, M.J., *EQNMR: A Computer Program for the Calculation of Stability Constants from Nuclear Magnetic Resonance Chemical Shift Data.* Journal of the Chemical Society, Dalton Transactions, 1993: p. 311-312.
146. Ponnu, A., N. Edwards, and E. Anslyn, *Pattern recognition based identification of nitrated explosives.* New Journal of Chemistry, 2008. **32**: p. 848-855.
147. Jacobsen, N.E., *NMR Spectroscopy Explained, Simplified Theory, Applications and Examples for Organic Chemistry and Structural Biology*. 2007, Hoboken, New Jersey: John Wiley & Sons, Inc.
148. Salvatierra, D., et al., *Determination of the Inclusion Geometry for the Î²-Cyclodextrin/Benzoic Acid Complex by NMR and Molecular Modeling.* The Journal of Organic Chemistry, 1996. **61**(26): p. 9578-9581.

VITA

The author was born in Charleston, Illinois. He obtained his Bachelor's degree in chemistry from Southern Illinois University at Carbondale in 1995. He obtained a Master's degree in chemistry with a graduate minor in toxicology from New Mexico State University in 2000. After obtaining the Master's degree, the author worked for a consulting firm in Redmond, Washington. In 2005 the author joined the University of New Orleans chemistry graduate program to obtain a Ph.D. in analytical chemistry and joined Professor Matthew Tarr's research group.